Evaluation of Cancellous Screw Pullout Strength at Varying Levels of Torque in the Human Trabecular Bone of Femoral Heads
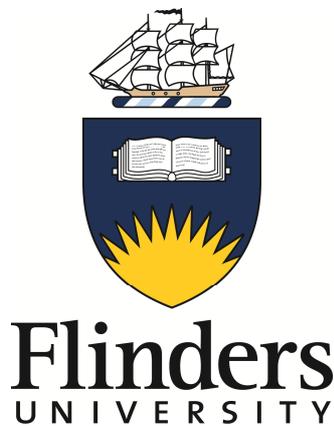
Rosidah Ab. Lazid

B.Sc. Biomedical Engineering, Marquette University, Milwaukee, Wisconsin.
M.Sc. Biomedical Engineering, University of Malaya, Kuala Lumpur.

School of Computer Science, Engineering and Mathematics,
Faculty of Science and Engineering, Flinders University

Thesis submitted November 2016
in fulfilment of the requirements for
the degree of Doctor of Philosophy

Principal Supervisor: Professor Karen Reynolds
Associate Supervisors: A/Prof John Costi and Dr. Egon Perilli

Contents

Summary

In orthopaedic surgery, implants such as cancellous screws are used in bone fracture treatment to stabilise the fractured bone to assist bone healing. The screws are implanted into the bone with the aid of torque. The bone as a host material provides site for the anchorage of the screw threads. Most mechanical failures experienced in screw fixation occur at the bone-screw construct anchorage due to the collapse of bone structures. The host bone quality therefore plays a pivotal role in determining the success of screw fixation.

In clinics, a patient's bone quality is assessed by measuring areal bone mineral density (aBMD) using dual-energy x-ray absorptiometry (DXA) technology, and aBMD is widely used in the assessment of bone fracture risk. The assessment of bone micro-architecture in clinics is still however limited to peripheral anatomical sites, such as the wrist or ankle using peripheral Quantitative Computed Tomography (pQCT). However, with the current rate of technological developments, it may be possible in the future to assess micro-architecture at other anatomical sites, such as the hip.

During fracture fixation using screws, surgeons rely on their judgement to determine the point at which to stop screw tightening. However, it has been shown that inconsistencies exist among surgeons, leading to overtightening and stripping of the bone around the screw threads. This might be linked to variations in the quality of the host bone among patients.

The overall objective of this thesis was to investigate the respective roles of aBMD and micro-architecture of trabecular bone of human femoral heads on $F_{Pullout}$ and T_{Insert} (including plateau torque or $T_{Plateau}$ — torque at screw head

contact) in a laboratory environment. $F_{Pullout}$ is defined as the maximum uniaxial tensile force (Newton) needed to produce failure in the bone and T_{Insert} refers to the torque applied during cancellous screw insertion.

Fifty-two excised human femoral heads obtained from hip replacement surgery and cadavers were used. Femoral heads were chosen because of their rich trabecular content and the common clinical occurrence of hip fractures particularly in osteoporosis. The aBMD and micro-architecture of each specimen were evaluated using DXA and micro-computed tomography (micro-CT). A partially threaded cancellous screw was inserted in each femoral head specimen using an automated micro-mechanical test device to the point at which the screw head contacted the bone, and the torque at this point was recorded ($T_{Plateau}$). Screw insertion was then continued to a point between screw head contact and failure, after which a pullout test was performed and $F_{Pullout}$ recorded. Micro-CT images were obtained both at head contact and just prior to pullout.

These experiments were used to address three aims:

Aim #1: To determine the relationships between $T_{Plateau}$ and aBMD and micro-architecture. The results indicate that $T_{Plateau}$ exhibited the strongest correlation with the structure model index (SMI, R = - 0.82, p < 0.001), followed by bone volume fraction (BV/TV, R = 0.80, p < 0.01) and aBMD (R = 0.76, p < 0.01). Stepwise forward regression analysis showed an increase for the prediction of $T_{Plateau}$ when aBMD was combined with microarchitectural parameters, i.e., aBMD combined with SMI (R^2 increased from 0.58 to 0.72) and aBMD combined with BV/TV and bone surface density (BS/TV) (R^2 increased from 0.58 to 0.74).

Aim #2: To determine the relationships between the $F_{Pullout}$ and insertion torque prior to pullout (T_{Insert}), aBMD and micro-architecture. Results showed that $F_{Pullout}$ exhibited strongest correlations with T_{Insert} ($R = 0.88$, $p < 0.001$), followed by SMI ($R = -0.81$, $p < 0.001$), BV/TV ($R = 0.73$, $p < 0.001$) and aBMD ($R = 0.606$, $p < 0.01$). Combinations of T_{Insert} with microarchitectural parameters and/or aBMD did not improve the prediction of $F_{Pullout}$.

Aim #3: To determine the effect of three different insertion torque levels after head contact on the holding strength of the trabecular bone surrounding the cancellous screw. $F_{Pullout}$ for screws tightened to an average of 80% T_{Max} was significantly greater than for screws tightened to an average of 90% T_{Max} ($F_{Pullout}$ = 2.07 ± 0.28 kN vs. 1.48 ± 0.40 kN, $p = 0.019$), but was not significantly different to screws tighten to an average of 70% T_{Max} ($F_{Pullout}$ = 1.79 ± 0.31 kN, $p = 0.33$). $F_{Pullout}$ at 70% T_{Max} was greater than $F_{Pullout}$ at 90% T_{Max} ($p = 0.019$), but not significantly different ($p = 0.27$), which could be due to sample size.

In conclusion, $T_{Plateau}$, which has previously been shown to be a strong predictor for insertion failure torque is significantly dependent on bone micro-architecture, particularly SMI and BV/TV, followed by aBMD. Bone with low SMI or that contains a more plate-like trabecular structure, high BV/TV and aBMD, is likely to offer a structural environmental in which the screw threads cut into more material, leading to an increase in $T_{Plateau}$. $F_{Pullout}$ of cancellous screws depends most strongly on the applied T_{Insert}, followed by micro-architecture and aBMD of the host bone. This indicates that for a bone specimen with a given trabecular bone micro-architecture and density, increases in applied T_{Insert} beyond screw head contact within the linear range will increase $F_{Pullout}$ of the screw. However

the strength of the construct reduces as insertion levels approach failure torque, probably due to yielding of the bone around the screw threads.

Declaration

I certify that this thesis does not incorporate without acknowledgement any material previously submitted for a degree or diploma in any university; and that to the best of my knowledge and belief it does not contain any material previously published or written by another person except where due reference is made in the text.

Rosidah Ab. Lazid

Acknowledgements

Many people have contributed in a variety of ways in my journey to complete this PhD. I am grateful for all of the invaluable assistance I received with this work. First and foremost, I would like to thank Professor Karen Reynolds, my principal supervisor, for her support, guidance, and patience throughout my postgraduate tenure. Her knowledge and expertise in the field are impressive and have given me something for which to strive. I would also like to thank A/Prof. John Costi and Dr. Egon Perilli, my associate supervisors. Their guidance whether in biomechanics, bone biology, micro-CT scanning and processing, statistics, or the ethical conduct of research, has been invaluable.

Special thanks to the National Health and Medical Research Council (NHMRC) for the grant that made this project possible; Dr. Julia Kuliwaba and Dr. Ian Parkinson of the Bone and Joint Research Laboratory in the Surgical Pathology at the SA Pathology, for providing me with femoral heads bone specimens; Chris Schultz of the Nuclear Medicine and Bone Densitometry, at the Royal Adelaide Hospital and Ruth Williams of the Adelaide Microscopy at the University of Adelaide for their assistance during DXA and micro-CT scans when needed; and Pawel Skuza of the Flinders University for his advice on statistics.

Preparing and testing the human bone specimens was time- and labour-intensive, and I depended on the help of many people, including Richard Stanley, Dr. Aaron Mohtar and Dr. Melissa Ryan. Thanks to them all for their time and help. I also thank Kelly Knight and Debbie Cocks for their kind assistance in administrative

matters, and my sis-in-law, Faridah Hanim and friend, Kathy Steven for their initial help in English. My ex-colleague and dearest friend, Samantha Cardimon, thank you for helping out with the English sentence construction and grammar.

I owe thanks to Ans and Peter Bakker, Dr. Anne-Louise Smith, Dr. Tony Carlisle, and John Robson and family for their kindness in helping my family and I to settle well in Adelaide. Last, but certainly not least, I would like to thank my wonderful parents, brothers and sisters for their unconditional support throughout my journey up to now. To my beloved husband, Waleed Jaseem and wonderful children, Saif J. and Fahad J., my gratitude beyond words for your love, understanding, and patience throughout these years. THANK YOU ALL!!!

Abbreviations

aBMD	Areal Bone Mineral Density
AO	Arbeitsgemeinshaft für Osteosynthesefragen
ASIF	Association for the Study of Internal Fixation
BS/TV	Bone Surface Fraction
BV/TV	Bone Volume Fraction
CT	Computed Tomography
DXA	Dual-Energy X-ray Absorptiometry
E	Elastic Modulus
FE	Finite Element
FEA	Finite Element Analysis
$F_{Pullout}$	Pullout or fixation strength of bone screw
ID	Inner Diameter
Micro-CT	Micro Computed Tomography
MRI	Magnetic Resonance Imaging
pQCT	Peripheral Quantitative Computed Tomography
QCT	Quantitative Computed Tomography
R	Coefficient of Correlation
R^2	Regression Coefficient

SMI	Structure Model Index
OD	Outer Diameter
SS	Stainless Steel
Tb.N	Trabecular Number
Tb.Sp	Trabecular Separation
Tb.Th	Trabecular Thickness
Ti	Titanium
T_{Insert}	Insertion or tightening torque
T_{Max}	Maximum or stripping torque
$T_{Plateau}$	Plateau Torque
T-Score	The unit of reporting aBMD
WHO	World Health Organisation

Chapter I

Introduction

1.0   About the Thesis

This PhD research is part of a larger research project supported by a National Health and Medical Research Council (NHMRC) grant entitled "The Development and Validation of a Finite Element Model for Orthopaedic Screw Insertion into Trabecular Bone" (Grant ID 595933).

The overall aim of this research was to understand the role of insertion torque (T_{Insert}) and the cofounding factors of bone quality — bone mineral density and micro-architecture measured by dual-energy x-ray absorptiometry (DXA) and micro-computed tomography (micro-CT) on the screw fixation or pullout strength ($F_{Pullout}$) in trabecular bone of femoral head specimens, harvested from patients who had undergone total hip arthroplasty surgery.

Data for the research study were obtained through biomechanical testing of screw insertion and pullout tests, which were conducted in the Biomechanics Laboratory, Flinders University. Screw insertion and pullout tests were performed with the aid of a micro-mechanical test device and an Instron mechanical testing machine respectively. DXA and micro-CT scans of the femoral head specimen to obtain aBMD and bone morphology data were performed at the Royal Adelaide Hospital and Adelaide Microscopy of the University of Adelaide, respectively.

It is hoped that the outcome of this research will be to provide further insight into the bone-screw construct, which will in the future help in the design of surgical tools for orthopaedic surgery (e.g., screws and surgical drills), improve screw fixation techniques, and allow the overall management of the orthopaedic treatment to cater to the different bone qualities of incoming patients.

2.0 Thesis Structure

The thesis is comprised of eight chapters and a brief summary of those chapters is provided below.

Chapter I - Introduction

The chapter presents the introduction to the thesis and the overall thesis structure.

Chapter II – Bone Biology, Structure and Disease

Chapter II provides an overview of bone biology and the structure of the human skeletal system. The unique hierarchical structure, biological and chemical compositions of bone materials define a bone's mechanical strength. Through life, bone undergoes modeling and remodeling to maintain its functions and health. However, bone loss can occur, whether due to age or to disease, which can deteriorate bone quality, compromise its strength, and can lead to the risk of bone fracture. For this thesis, knowledge of bone micro-architecture and its biomechanical properties that contribute to bone quality and strength is considered fundamental in understanding the mechanisms that affect the pullout strength of a bone screw in trabecular bone during fracture fixation.

Chapter III – Biomechanical Study of Screw Fixation

Chapter III reviews previous studies performed by other researchers with respect to screw fixation in bone. The topics include bone screw, the effect of screw design, insertion technique, insertion torque, and cofounding factors of bone quality (such as bone mineral density and micro-architecture) on the pullout strength of a bone screw in human, animal, and synthetic bone models.

Chapter IV – Research Aim

The current challenges experienced by clinicians during screw fixation in orthopaedic surgery and the shortcoming of previous studies that have led to the research aims of the thesis are described in chapter IV.

Chapter V to VII detail the three studies performed to answer the three main questions addressed by this thesis, namely:

Chapter V – Study 1: Does Cancellous Screw Plateau Torque Depend on Bone Mineral Density and/or Micro-architecture?

Chapter VI – Study 2: Does the Pullout Strength of Cancellous Screws in Human Femoral Heads Depend on Applied Insertion Torque, Trabecular Bone Micro-architecture and Areal Bone Mineral Density?

Chapter VII – Study 3: Comparison between the Pullout Strength of Cancellous Screws at Three Levels of Tightening Torque in Human Femoral Head.

Chapter VIII – Conclusion and Future Work

This chapter contains the conclusions that synthesise the overall key findings and suggestions for potential future research directions.

Chapter II

Bone Biology, Structure and Disease

2.0 The Human Skeletal System

Bone is a living tissue that can perform highly complex and diverse functions, including biological, chemical, and mechanical functions. In a human adult, there are 206 bones which form the skeletal system (Figure 2.0), providing support and shape for the body, protection for the internal organs, and sites for muscles attachments, storage for minerals (calcium and potassium) and for producing blood cells for body functions (Ortner and Turner-Walker, 2003; Starr and McMillan, 2013; Steele and Bramblett, 1988).

2.1 Bone Function and Composition

Bone acts as a primary load-bearing structure for the skeletal system and as a lever for movements. Therefore, the bone's structure needs to be; stiff (e.g., long bone), exhibiting resistance to deformation, flexible (e.g., end part of long bone and vertebra), having the capability to absorb energy by deforming, and light in weight for facilitating movements (Bartl and Frisch, 2009).

Bone is an inhomogeneous material, composed of 50% to 70% mineral, 20% to 40% organic matrix, 5% to 10% water and < 3% lipids (Clarke, 2008). The

mineral content of bone is mostly hydroxyapatite [Ca_{10} $(PO_2)_6$ $(OH)_2$], with small amounts of carbonate, magnesium, and acid phosphate (Clarke, 2008; Cowin, 2001). The organic matrix consists of 90% collagen type I and about 10% non-collagenous proteins (Cowin, 2001).
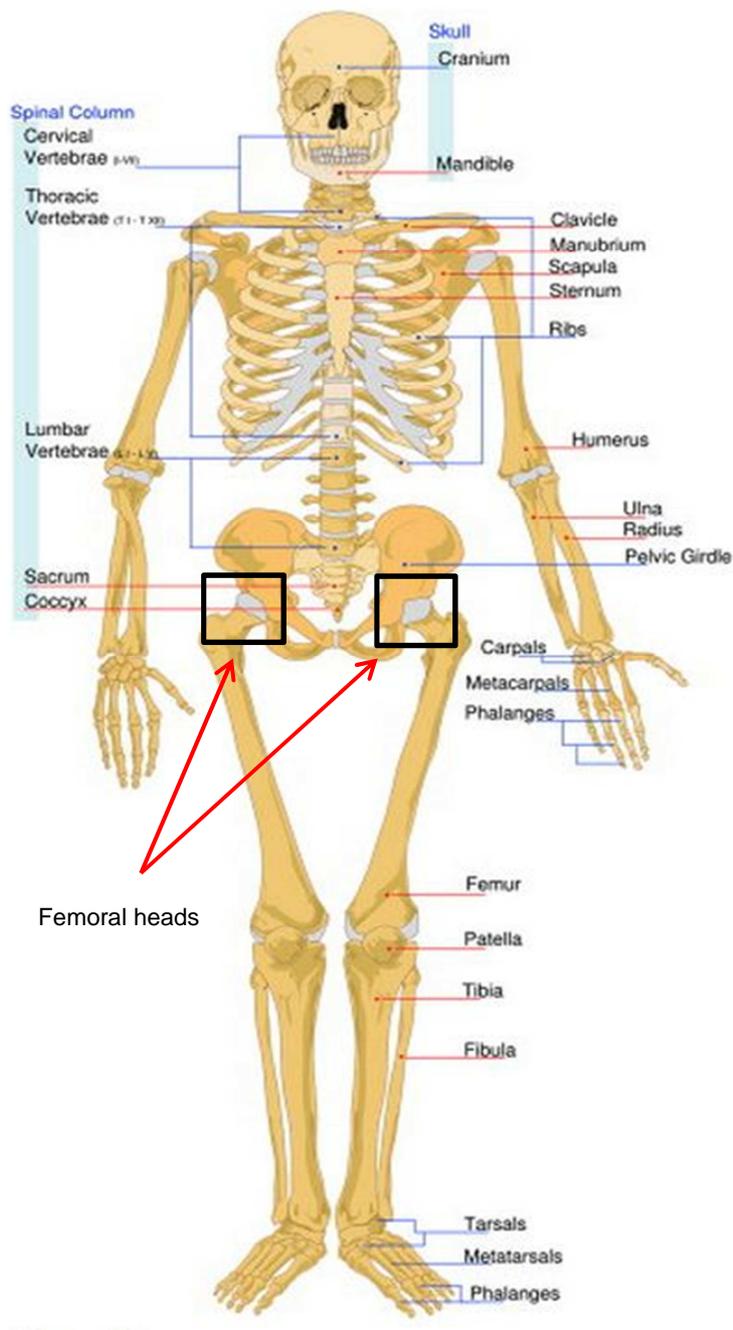
Figure 2.0:   An overview of a major human skeleton, (Rhodes, 2014). Reproduced with permission from Elsevier.

2.2 Bone Structure and Hierarchy

The structure of bone can be divided into six hierarchical levels, spanning from whole bone to the molecular structures, at different length scales, from macroscopic (whole organ) to sub-nanostructure (Figure 2.1). This thesis focuses on the bone structure at the micro-architectural level, particularly for trabecular bone.
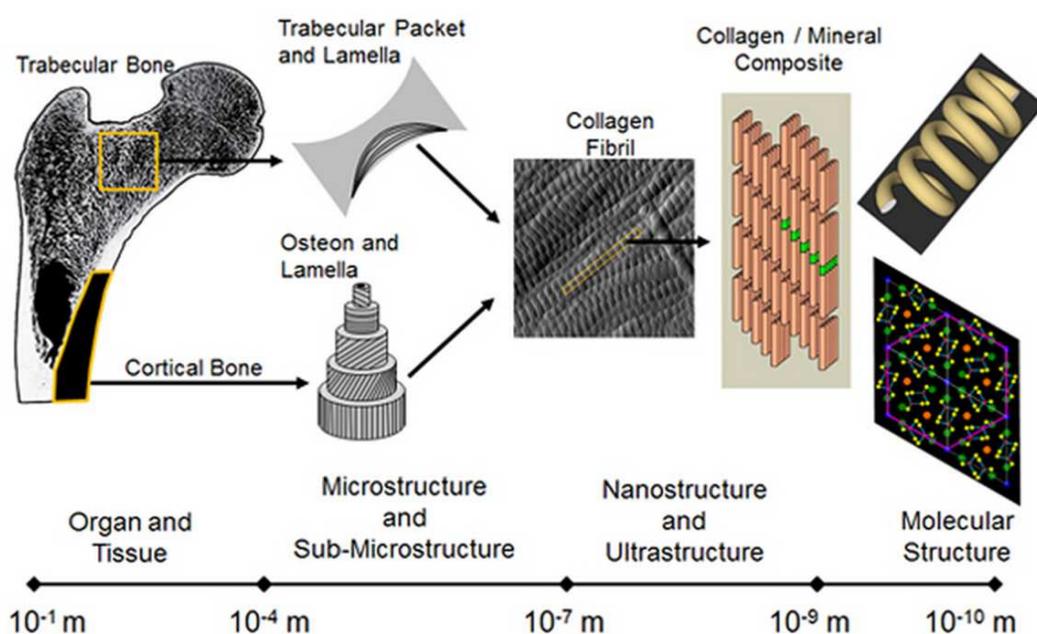
Figure 2.1: The hierarchical structure of different length of scales, from whole bone structure at macroscopic level to the molecular structure at sub-nanostructure, (Burr and Allen, 2013). Reproduced with permission from Elsevier.

2.2.1 Whole Bone Organ

Bone as an organ (e.g., whole vertebra, femur, tibia), represents the largest scale of bone structure in the hierarchy, at the macro-structure level, encompassing both cortical and trabecular types of bone. The biomechanical characteristics of a whole bone depend on its geometry, size and composition.

2.2.2 Bone Micro-architecture

At the next hierarchical level, that is the micro-structure level, bone organ is distinguished into trabecular bone and cortical bone. The structural unit that presents in both trabecular and cortical bones is known as lamellar bone. Lamellar bone is composed of 3 to 70 µm thick unit layers of lamellae that contain collagen fibres parallel to each other. Osteons on the other are present only in cortical bone (Cowin, 2001).

Different bones and skeletal sites within bones have different compositions of trabecular and cortical bones. In healthy bone, the adult human skeleton is composed of 20% trabecular bone and 80% cortical bone (Clarke, 2008; Eriksen et al., 1994). Biologically, the proximal femur comprises the majority of trabecular bone, particularly in the neck and femoral head, while cortical bone forms a thin layer surrounds the neck and becomes thicker as the bone progress distally.

2.2.3 Bone Cellular Mechanism

Bone Modeling

Bone modeling occurs during birth to adulthood. In bone modeling, bone formation and resorption take place on different surfaces (not coupled). During the phase of bone modeling, skeletal mass is gained and changed to the overall skeletal form (Cowin, 2001).

Bone Remodeling

Bone remodeling mainly occurs in the adult skeleton to maintain bone mass by replacing old bone tissues with new bone tissues. Unlike bone modeling, bone remodeling involves coupling of bone formation and bone resorption (Cowin, 2001).

2.3 Trabecular Bone

Trabecular bone ("trabecula" from Latin "small beam") (Figure 2.2), also known as spongy or cancellous bone, is formed in the interior of vertebral bodies, the epiphysis and metaphysis of long bones (such as the femoral head), and flat bones (such as the skull, pelvis and scapula) (Gibson, 2005). Trabecular bone is made of interconnecting trabeculae resembling a honeycomb-network of trabecular rods and plates, ranging from 50 to 400 µm in thickness with interconnected bone marrow compartments interspersed (Clarke, 2008; Gibson, 2005). At low density, the trabecular network is primarily comprised of rod-like structures while at high density trabecular bone is mostly comprised of plate-like structures (Gibson, 2005). Trabecular bone has a greater range of porosity (30% to 95%) compared to cortical bone (5% to 20%) (Hayes & Bouxsein 1997).

Bone grows and remodels in response to load, and thus the density of trabecular bone adapts to the magnitude of the loads and the orientation of the trabeculae adapts to the direction of the loading to which it is subjected. The orientations of the trabecular struts at different anatomical sites (such as in the proximal femoral and in the vertebral) can vary considerably. Because of the variations in trabecular

architecture, there is more variation in the stiffness and strength of trabecular bone than in many other types of cellular materials (Gibson 2005).
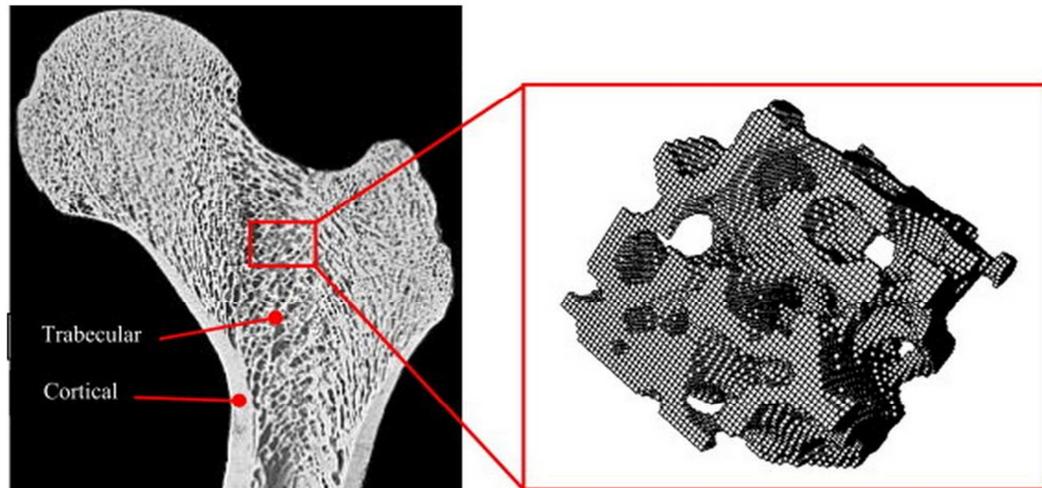
Figure 2.2: Section of human proximal femur revealing trabecular bone and cortical bone. Reprinted from Numerical Procedure from the Multiscale Bone Adaptation Prediction based on Neural Networks and Finite Element Simulation, (Hambli, 2011). Reproduced with permission from Elsevier.

2.3.1   Trabecular Bone Morphology (Micro-architecture Parameters)

The quantification of trabecular bone morphology can be performed by several methods such as using the traditional two dimensional (2D) histomorphometric methods or based on three dimensional (3D) reconstructions of x-ray images obtained from micro-computed tomography or other imaging modalities with 3D capabilities such as peripheral quantitative computed tomography (pQCT) (Hildebrand et al., 1999; Parkinson et al., 2008; Perilli et al., 2007; Perilli et al., 2012b):

Among the 3D-morphometric parameters of trabecular bone micro-architecture that can be calculated are:

- Bone volume fraction (BV/TV, %) is the ratio of bone volume to total volume by dividing the sum of voxels marked as bone by the sum of voxels composing the volume of interest and multiplied by 100.

- Structure model index (SMI) is a topological parameter indicating a ratio of rod-like to plate-like trabecular structures, with typical values ranging from 0 (ideal plate-like) to 3 (ideal rod-like), and values in between representing a mixture of plate- and rod-like structures. Negative values of SMI can be found in bone with high bone volume fraction as SMI is very strongly confounded by BV/TV through the fraction of the surface that is concave, and the magnitude of the concavity (Salmon et al., 2015).

- Trabecular thickness (Tb.Th, µm) is the average thickness of individual trabeculae, calculated using the sphere-fitting method. The sphere-fitting method is realised by means of distance transform.

- Trabecular separation (Tb.Sp, µm) is the average distance between the edges of two trabeculae.

- Trabecular number (Tb.N, mm^{-1}) is a measure of trabecular plates per unit length.

- Bone surface fraction (BS/TV, mm^{-1}) is the ratio of bone surface area to total volume measured within the volume of interest.

2.4   Cortical Bone

Cortical bone, also known as compact bone (although it is not really completely "compact"), forms the outer layer of the bone, particularly of the shaft of long

bones in the skeleton. Cortical bone is dense and surrounds the marrow space. The cortical bone is the main structure responsible for the mechanical strength of the skeleton. It can withstand a greater stress, but less strain before failure, than trabecular bone. Cortical osteons are called Haversian systems. Haversian systems are cylindrical in shape, approximately 400 mm long and 200 mm wide at their base, and their canals form a branching network within the cortical bone (Figure 2.3). The mineralised tissue of the cortical bone makes up 80% of the human skeleton (Clarke, 2008).
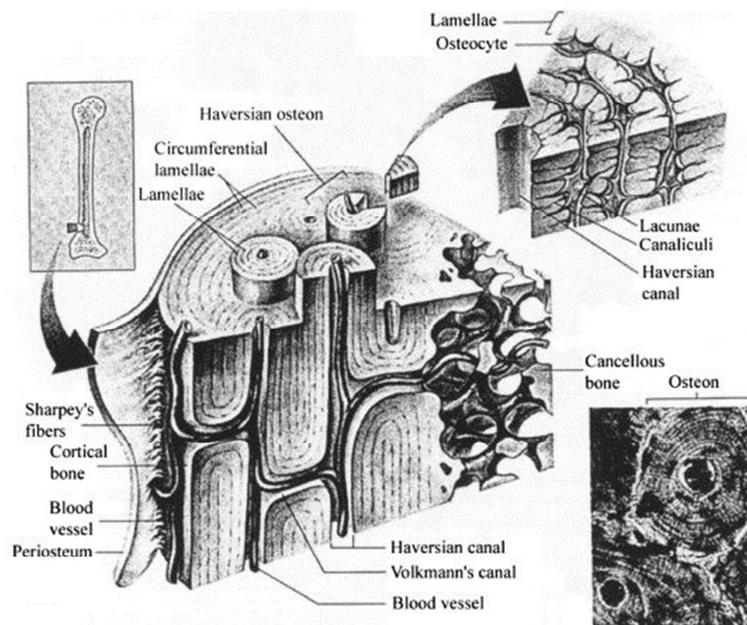
Figure 2.3: The micro-architecture of cortical bone, which consists of Haversian systems and osteons. The arrangement of circular-shaped osteons provides the compact nature of cortical bone, (Doblaré et al., 2004). Reproduced with permission from Elsevier.

A possible distinction between cortical and trabecular bone can be made based on porosity. Cortical bone can be defined as bone tissue that has a porosity P of less than 30 percent or, equivalently, a volume fraction V_f of greater than about 0.70

$(V_{f=} 1 - P)$. Volume fraction is the ratio of the volume of actual bone tissue to the bulk volume of the specimen (Keaveny et al., 2003).

2.5   Bone Quality

Bone quality is a composite of multiple properties — bone mass, geometry and tissue material that defines the bone strength, the ability to resist fracture. The geometric properties of the bone that contribute to the quality of bone include the whole bone macroscopic geometry and the trabeculae microscopic architecture or micro-architecture. The tissue material properties include the constituent tissues emerging from the composition and arrangement of the primary microstructural constituents, collagen and mineral as described in Section 2.1 as well as micro-damaged and microstructural discontinuities such as micro-porosity and lamellar boundaries (Donnelly, 2010; Gordon et al 1998; Gourion-Arsiquaud et al., 2009; Van der Meulen et al., 2001).

Despite the multiple properties contributing to bone quality, bone mass is the primary property that can be measured in clinics presently to assess patient's bone strength or fracture risk. Bone mass measurement is generally categorised by the bone mineral density (BMD) or the areal bone mineral density (aBMD) if assessed by dual-energy x-ray absorptiometry. The inclusion of other bone quality properties such as bone micro-architecture and material properties in addition to BMD (or aBMD) may improve the assessment of bone strength and fracture risk, as well as the evaluation of screw fixation performance relative to that from BMD alone.

Therefore, the interest among researchers has increased in the complementary measures of bone quality properties, particularly micro-architecture that may improve the assessment of bone strength and screw fixation strength at the bone-screw construct. From herein, the working term of bone quality throughout this thesis implies to its composite properties, aBMD (or BMD) and/or micro-architecture.

2.6   Biomechanical Properties of the Bone

From a biomechanical perspective, the composition of bone comprising bone mineral and an organic matrix is comparable to that of a composite material — the bone mineral provides mechanical rigidity and load-bearing strength, whereas the organic matrix provides elasticity and flexibility (Clarke, 2008; Cowin, 2001). The composition of bone material varies with age, sex, type of bone, anatomical location, and presence of bone disease. A heterogeneous porous cellular solid built of trabecular bone has anisotropic biomechanical properties that depend on the porosity of the bone as well as the architectural arrangement in space and connectivity of the individual trabeculae (Keaveny et al., 2003).

Like any engineering material, the mechanical properties of bone are measured experimentally by performing mechanical tests under various loading (such as compression, tension, or torsion) and environmental (temperature and hydration) conditions. Force versus Deformation (structural properties) (Figure 2.4[a]) and/or Stress versus Strain curves (material properties) (Figure 2.4 [b]) are

typically derived from the mechanical tests in which important parameters that characterise some of the biomechanical properties of the bone can be calculated.
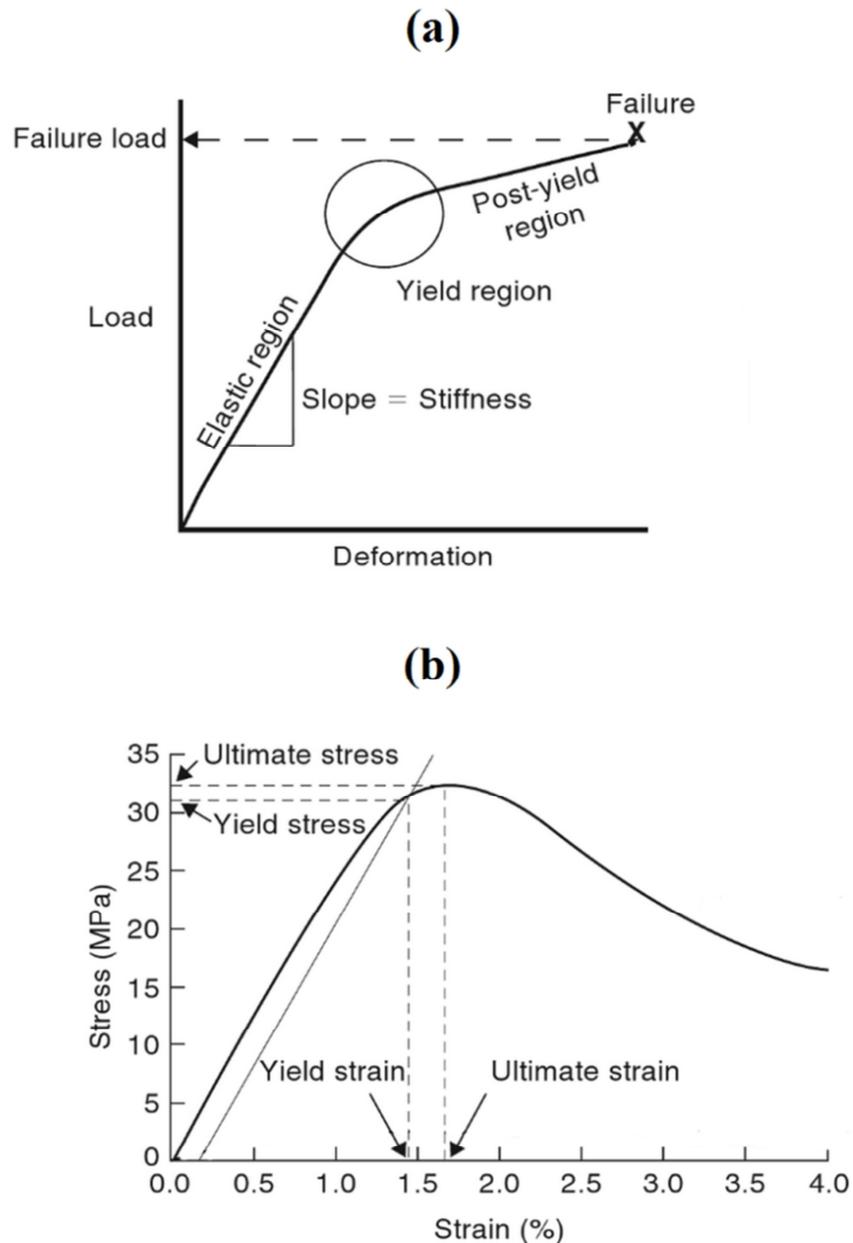
Figure 2.4:
(a) The load versus deformation (structural) curve obtained from compressive tests on whole bone. The curve exhibits three distinct regimes, classified as elastic deformation, plastic deformation (within the post-yield region), and failure.
(b) The stress versus strain (material) curve resembles the load versus deformation curve, but provides insight into the biomechanical properties of bone material, (Morgan and Bouxsein, 2008). Young's Modulus is defined by the slope of the stress-strain curve in the linear region prior to yield. Reproduced with permission from Elsevier.

Stiffness

Bone stiffness refers to a structural property influenced by the geometry (cross-sectional area and length) of the bone as well as the materials of which it is comprised. It is a measure of resistance to deformation (rigidity) during loading. Bone stiffness is derived by calculating the slope in the elastic region (linear region) of the load-displacement curve, i.e., by the ratio between load and deformation (Figure 2.4[a]). Typically, the mean values of the femoral head trabecular bone stiffness measured in compression are around 15-20 GPa (Cowin, 2004; Mente and Lewis, 1987; Rho et al., 1993).

Elasticity

Bone elasticity is described by the Young's modulus (E), which refers to a material property that is intrinsic to the material and is not influenced by the bone's geometry. It is a measure of intrinsic stiffness (Turner, 2006). The Young's modulus is defined by the slope in the elastic region of the stress-strain curve (Figure 2.4[b]), i.e., the ratio between stress (force/area) and strain (elongation/initial length). In general, the value of the femoral head trabecular bone E measured in compression is 17 GPa (Bayraktar et al., 2004).

Yield Point

The yield point of the load-displacement or stress-strain curve indicates the point at which the material (bone structure or tissue) begins to undergo permanent (plastic) deformation. Typically, the yield point is identified based on the observation of the point where the curves become non-linear (Figure 2.4[a]) or by an offset method (Figure 2.4 [b]), where a line parallel with the linear portion of

the curve is offset by 0.03% to 0.2% strain and drawn to intersect with the load-displacement or stress-strain curve. The point at the intersection is defined as the yield point (Turner, 1989).

Strength

The strength of bone is defined by the point at which failure (or fracture) occurs (maximum failure load in Figure 2.4 [a]).

Toughness

The structural toughness of bone is the work/energy required to produce failure and is defined as the area under the curve (Figure 2.4[a]) up to the failure load, and therefore depends on both the failure load and ultimate displacement. Meanwhile, the material toughness of bone is defined as the area under the curve (Figure 2.4[b]) up to the ultimate stress, and therefore depends on both the ultimate stress and ultimate strain.

Bone is also viscoelastic, which means the biomechanical response is time dependent, i.e., the bone response depends on the strain rate at which the loads are applied. At higher strain rates, bone exhibits increased strength and stiffness compared to slower strain rates.

2.7   Bone Disease, Associated Risk and Treatment

Ageing and Osteoporosis

As people age, bone loss generally occurs in all parts of their skeleton, and this can affect bone strength. In the human life cycle, bone development undergoes several phases; bone mass increases during growth, reaches a plateau in young adulthood, and declines after an average age of 30 years. According to the World Health Organisation (WHO), men's bone mass tends to decline at a rate of approximately 4% per decade, while women's bone mass tends to decline at the higher rate of approximately 15% per decade, especially after menopause (WHO, 2003). Additional bone loss takes place in both men and women due to other factors such as vitamin D and calcium deficiency, unhealthy lifestyles and natural causes.

Osteoporosis originates from the Latin words "*osteon*" and "*porosis,*" which literally mean '"hole" and '"passage" in a bone. By definition, "osteoporosis is a progressive systemic bone disease characterised by low bone mass and deterioration of bone micro-architectural tissue that compromises bone strength and increases susceptibility to fragility fracture" (WHO, 2003). Bone loss affects the bone micro-architecture. In trabecular bone, thinning of trabecular struts occurs, with fenestration of trabecular bone plates in which a plate-like structure is transformed into a rod-like structure. These perforations cause diminishing of the bone volume fraction (BV/TV) and can cause loss of trabecular bone connectivity.

The diagnosis of osteoporosis is performed with the aid of medical imaging technology such as dual-energy x-ray absorptiometry (DXA), computed tomography (CT), quantitative computed tomography (QCT), magnetic resonance imaging (MRI), and ultrasound. The most widely used technology is DXA, accepted as the "gold standard" technology by the World Health Organisation (WHO) for the assessment of bone mineral density (WHO, 2003).

DXA is a non-invasive procedure performed in clinic. DXA measures a patient's aBMD and then compares it to the average aBMD of a young healthy reference population, as per WHO guidelines. The DXA results for clinical interpretation are presented as a T-score, expressed in multiples of statistical standard deviation (SD) values from the normal reference value. T-scores provide a quantitative measure for the diagnosis of osteoporosis, defined as follows: T-score > -1 indicative of normal; -1 > T-score > -2.5 indicative of osteopaenia; and T-score < 2.5 indicating osteoporosis, and increased fracture risk. If measurements are taken at various time points, these T-scores can assist clinicians in estimating the severity of bone loss and the patient's responsiveness to bone therapy.

Risk of Osteoporosis

The main complication of osteoporosis is an increased risk of fragility fractures due to loss of bone mass, deterioration of trabecular micro-architecture, and loss of bone strength. Fragility fractures can occur even due to low impact trauma, e.g., in a normal fall, which is a common cause of bone fracture in elderly populations (Compston, 2010; Giangregorio et al., 2006). Skeletal sites that are

prone to fragility fractures are the bones of the wrist, spine, and hip (Cummings and Melton, 2002).

According to the Australian Institute of Health and Welfare (AIHW), in 2011-12, an estimated 652,000 Australians over the age of 50 (9% of this age group; 3% among men and 15% among women) were diagnosed with osteoporosis. Out of 652,000, 19,000 people were hospitalised due to hip fracture (AIHW, 2014). In 2015, about 25,396 Australians over the age of 50 years had experienced hip fractures (women: 17,648 and men: 7,748). Meanwhile in 2016, it is estimated this number to increase to 26,322 (4% increase) (Watts et al., 2014). Globally, by 2025, it is estimated the incidence of fragility fractures as a whole will increase to 3 million or higher worldwide.

In summary, bone modeling (which occurs during birth to adulthood) and remodeling (which occurs throughout life) are responsible for maintaining bone health — quality, micro-architecture and strength — while allowing significant flexibility without compromising its mechanical strength. Bone's material composition varies with age, sex, type of bone, anatomical sites and disease (e.g., osteoporosis), with associated alterations to its quality, aBMD, micro-architecture and strength.

Chapter III

Biomechanical Studies of Screw Fixation

This chapter provides a background to fracture treatment, an overview of the biomechanics of screw fixation and describes previous studies in the literature investigating the fixation strength or pullout strength of bone screws.

3.0   Background - Bone Fracture Treatment

Bone fracture can be treated by both operative and non-operative procedures, depending on the criticality of the fracture, degree of fracture fragmentation, site of fracture, and condition of the patient (Giannoudis and Schneider, 2006). Regardless of the treatment choices, the primary goal of fracture treatment is to restore the functional anatomy, allow for early mobilisation and rehabilitation, and reinstate the patient's health to the level prior to fracture with minimal risk of complications.

Before the introduction of orthopaedic implants in clinics, bone fracture was treated conservatively by non-operative procedures. A cast, splint and/or traction were used externally to stabilise the bone fracture. This mode of treatment usually prolonged bed rest and could be a high risk for certain patients, resulting in mal- and non-union of the fractured bones. This condition could escalate over time and result in high rates of morbidity and mortality (Koval and Zuckerman, 2000). The non-operative treatments of casting and/or splinting are still in practice today, but

selective for certain types of fracture cases as well as for patients who are medically unfit for surgical procedures.

Today, surgical treatments of bone fracture are aided by better medical technology and wide ranges of implant choices, resulting in improved clinical outcomes. Fragility fractures, such as in osteoporotic long bones at the femoral neck, are either stabilised mechanically by internal screw fixation or by arthroplasty which makes use of a prosthesis to replace the damaged/weakened bone that is beyond repair. With respect to bone screws, despite better access to wider ranges of implant choices, little is yet known about the performance of those implants used in different environments, including in different bone qualities, and using different insertion techniques, and tightening to different levels of insertion torque.

3.1   An Overview: Biomechanics of Screw Fixation and Pullout Strength of Screw

For decades (dating back to the 1880s) (Peltier, 1990), fractured bones in orthopaedic surgery were stabilised with the use of implants, the most common type being the screw. There are so many different applications for bone screws in orthopaedic and trauma surgery. Consequently, there are just as many different screw designs, dependent on application and anatomical location and size of the bone being fixed. Bone screws are manufactured to high quality and precision. Brief detail of bone screw design, profiles, types and designs are highlighted in the next section.

3.2   Bone Screw

The physical attributes or profile of the screws as shown in Figure 3.1[a] are designed specifically to gain purchase in bones of different types and sizes. In order to use bone screws effectively, the surgeons must be familiar with the screw's design.

3.2.1   Screw Characteristic

A bone screw typically consists of the head, core, thread and tip constructs. Each of these constructs provides an important function in the overall performance of the screw to gain purchase. Each of these constructs is briefly described below.

Head

The head is the top part of the screw construct. Its profile provides the means to turn the screw. The main functions of the head are to transmit the applied torque to the bone-screw construct, act as a stop to prevent the screw from sinking in the bone and stop the insertion. Screw heads also could be threaded such as in locking screws to allow locking into plates for angular stability.

Core

The core is the solid segment of the screw from which the thread profiles form outwards. The diameter of the core is the smallest (or narrowest) diameter of the screw, which is measured across the base of the threads. The core diameter is also known as the *minor diameter, inner diameter* or *root diameter*, which influences the size of the pilot hole required to accommodate the screw in the bone.
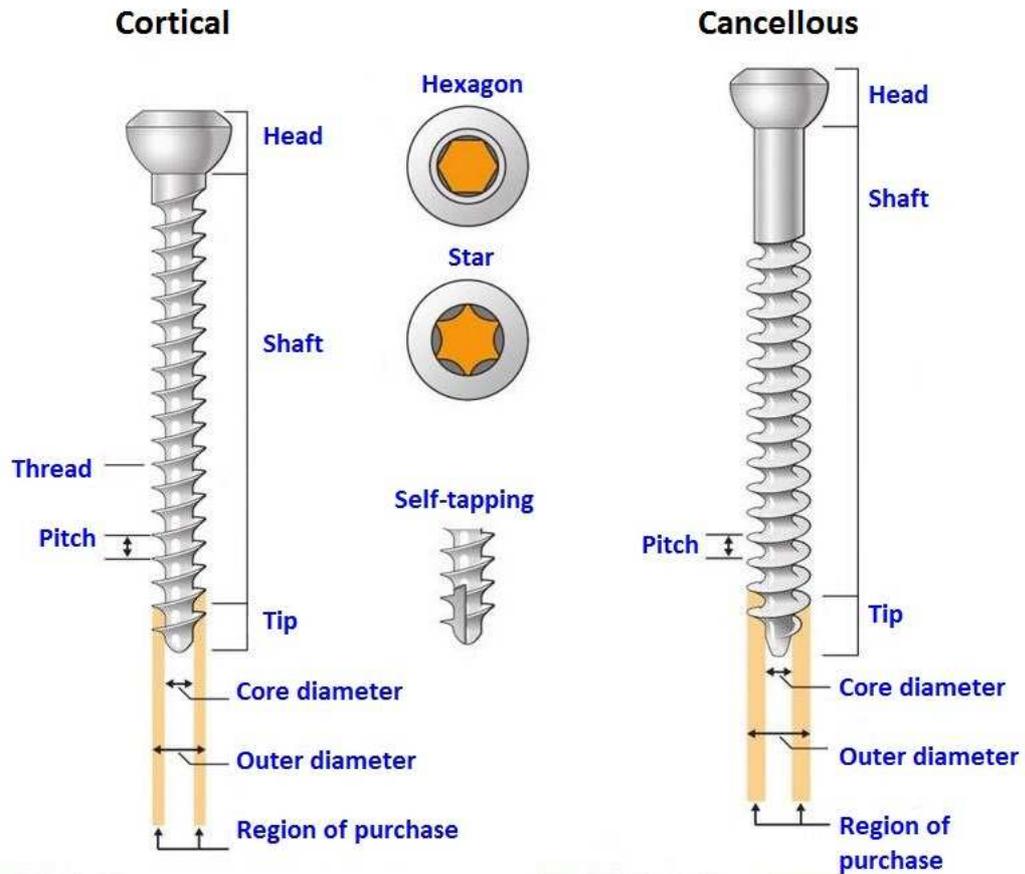
Figure 3.1: Bone screws, cortical and cancellous screws with their respective design parameters (White et al., 2016). Reproduced with permission from Elsevier.

Thread

A screw thread is a ridge of uniform section in the form of a helix wrapped around the screw core. The diameter of the thread is also known as *outer diameter* or *major diameter*. One of the functions of the outer diameter is to maximise resistance to pullout failure.

Pitch

The thread geometry includes the pitch profile. The pitch is the linear distance travelled by a screw for a complete revolution (360°) of the screw. In each complete revolution, the screw travels by a distance equal to the distance between the threads.

Tip

The tips of the bone screws have three common designs — smooth conical shape (non-tapping screw), cutting flutes (self-tapping) and self-tapping and self-drilling tipped. The tip designs determine the need for bone preparation. The non-tapping screw needs pre-drilling of a pilot hole and then tapping (the creation of a thread in the bone by the use of a separate thread-cutting tool – a tap). The self-tapping screw needs pre-drilling of pilot hole, but creates its own thread in the bone. The self-tapping and self-drilling-tip screw is able to self-drill and create a thread in the bone.

Length

The nominal length of a screw is measured from the top of the screw head to the bottom of the screw tip. The length of screw needs to be carefully chosen depending on its intended use. If the screw length is too short for the intended use, it may not achieve full purchase in the bone, hence, could lead to loose fixation; and if the screw is too long, it may irritate the surrounding soft tissues or protrude subcutaneously.

3.2.2   Screw Type and Design

Although bone screws have various designs and sizes, they are crafted to two basic types, i.e., cancellous screws and cortical screws. Both cancellous and cortical screws are used for different functions in trabecular and cortical bones respectively, depending on the fractures and anatomical locations. The screws either be used on their own or paired with other implants such as plates, rods or nails to support and stabilise a fracture.

3.2.3   Type of Bone Screw

Cancellous Screw

As name implies, a cancellous screw is intended for better purchase in the cancellous (or trabecular) bones. The cancellous screw generally has greater thread depth and threads are more widely spaced (i.e., larger pitch) compared to cortical screws (Figure 3.1). The cancellous screws can be fully threaded or partially threaded. The partially threaded cancellous screws can either be solid or cannulated.

Cortical Screw

The cortical screw is intended for better purchase in the cortical bones. The cortical screw has shallow thread depth and threads are closely spaced (i.e., smaller pitch) (Figure 3.1). The cortical screw also can be fully threaded or partially threaded.

3.2.4   Uses of Bone Screw

Lag Screw

The lag screw is commonly used to provide inter-fragmentary compression between the bone fragments at the fracture (Figure 3.2). The screw can be fully threaded or partially threaded. The fully threaded lag screw is commonly used in cortical bones, while the partially threaded lag screw is used in trabecular bones.
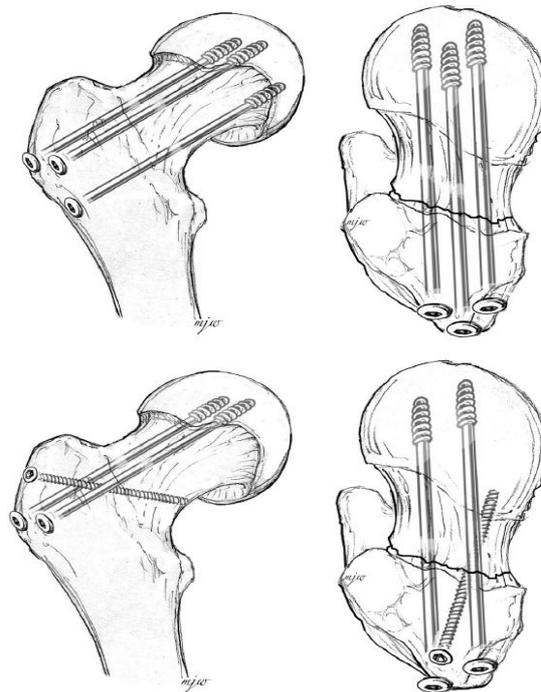
Figure 3.2: Illustrations of the two views of surgical technique for partial and full threaded cancellous screws fixation of the femoral neck fracture. The upper panel view shows the inverted traingle configuration of the lag screw fixations and lower panel shows the trochanteric lag screw configuration (Hawks et al., 2013). Reproduced with permission from Elsevier.

Despite the widespread use of the lag screws, failure rates in the range of 8 – 17% remain common (Mainds and Newman, 1989; Davis et al., 1990; Baumgaertner et al., 1995; Madsen et al., 1998; Nordin et al., 2001; Ehmke et al., 2005). The dominant failure mode is due to migration of the lag screw, which leads to varus

collapse and cut-out of the lag screw from the bone (Baumgaertner et al., 1995; Baumgaertner et al., 1997; Haynes et al., 1997; Ehmke et al., 2005).

Pedicle screw

The pedicle screw is one of the most commonly used and rapidly growing forms of stabilisation for correcting deformity and/or treating trauma of the vertebral pedicle bones (Figure 3.3) The screw can either be used on its own or with rod and plate instrumentation, and has various designs and shapes (cylindrical and conical). The main failure modes associated with pedicle screw are screw fatigue and bending failure with rates ranging from 3 to 7.1% (Cotler and Star, 1990; Matsuzake et al., 1990; Dickman et al., 1992; Niu et al., 1996; Chen-Sheng et al., 2004) and back-out which could lead to loss of fixation.
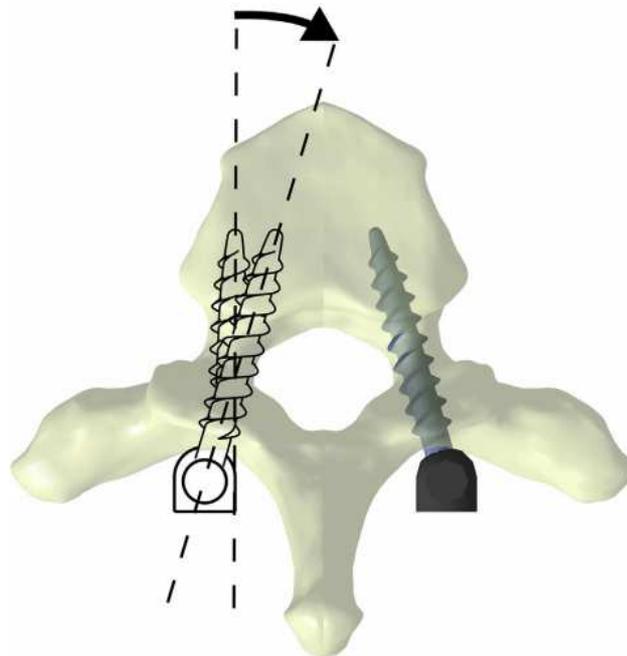
Figure 3.3: Placement of a pedicle screw into the vertebral pedicle and the direction of the imposed insertion angles in the transverse plane (Amirouche et al., 2016). Reproduced with permission from Elsevier.

Anchor Screw

The anchor screw is also called bone anchor or suture anchor. It is used as an anchor to wire or suture soft tissues to bone (Figure 3.4). It is made of absorbable or metallic materials. Suture anchors were introduced in 1991 for clinical application in open surgeries, and later for arthroscopic repair techniques, commonly in the shoulder and knee regions for reattaching ligaments and tendons.
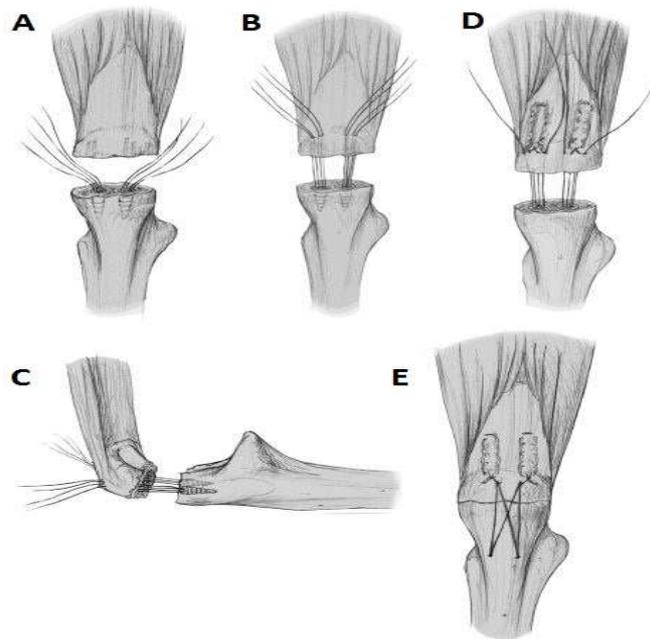
Figure 3.4: (A to E) Illustrations of surgical technique for suture anchor fixation of an olecranon (elbow) fracture (Bateman et al., 2015). Reproduced with permission from Elsevier.

Different failure modes were reported depending on the material of the anchor screws. The absorbable anchor screw may fail due to pullout from bone, eyelet failure (cut-out) and degradation (Hecker et al., 1993; Meyer et al., 2003; Demirhan et al., 2000; Meyer and Gerber, 2004), while the metallic anchor screw may fail due to pullout of the anchor or cutting of the suture at the eyelet (Rossouw et al., 1997; Meyer et al., 2003; Meyer and Gerber, 2004).

Locking screw

The locking screw is used in combination with a 'locking' plate that has reciprocal grooves or screw thread around the plate holes (Figure 3.5). The screw has threads around the head that meshes with the screw threads within the plate hole to allow the transfer of forces from the bone to the plate without compressing the bone, thus enhancing the vascular supply to the fracture site. It is typically used to treat fractures in osteoporotic bones and short metaphyseal bone segments.
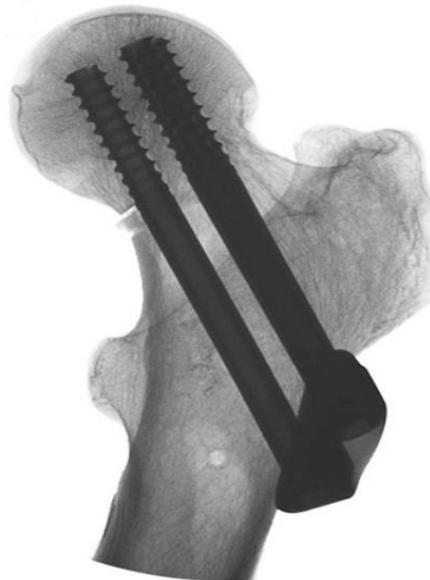
Figure 3.5: The image illustrates cannulated bone screws in an inverted triangle configuration with a locking plate (Basso et al., 2014). Reproduced with permission from Elsevier.

The main failure modes commonly associated with the locking screws are screw loosening and disengagement, leading to screw back-out and migration, which can have major consequences that lead to surgical re-intervention (Shah et al., 2002; Cho and Youm, 2009; Rapuri et al., 2011; Thienpont et al., 2013; Sanders and Raeymaekers, 2014).

3.3 Fixation of Bone Screw

The screw is a mechanical device and its insertion into bone is made possible with the use of rotational moment or torque. Traditionally, torque is generated manually by hand via a screwdriver, but in recent years it has been generated by electric or pneumatic powered drills. It has been clinically established that the use of powered drills provides improved coaxial alignment and precision of screw insertion (Thomas et al., 2008).

The torque that is produced during screw insertion is converted into a linear movement, which can be observed through the advancement of the screw into the bone until it attains screw head contact with the bone surface. During the screw insertion (prior to screw head contact), cutting or shredding of the bone is involved. A study from our laboratory found the insertion torque at plateau level prior to head contact was a strong predictor for the bone failure torque (Reynolds et al., 2013).

If torque is continued to be applied after the screw reached head contact, this creates what is known as a "tightening effect" in which torque is converted to compression (or clamping action) under the screw head and between bone fragments. No further advancement of the screw into the bone is possible at this stage, as it has already reached screw head contact.

The aim of the screw fixation is to achieve the optimum fixation strength at the bone-screw construct. However, complications may develop in the screw fixation

during the intraoperative and/or postoperative periods. Among the complications of screw fixation are screw loosening, cut-out, migration, breakage, protrusion through the femoral head and detachment.

Although pure pullout is not a common mode of screw failure seen in clinical situations, quasi-static methods of testing that include pullout are commonly carried out to measure the screw fixation strength due to the simplicity of the experiment setup and testing protocol. In this mode of testing, the strength of the bone-screw construct is generally defined by its resistance to screw pullout in a laboratory setting. Screw pullout is thought to be a good predictor of bone screw fixation strength (Poukalova et al., 2010; Ramaswamy et al., 2010; Yakacki et al., 2010; Batulla et al., 2013; Mueller et al., 2013).

According to Bechtol et al. (1959), the pullout strength is defined as the maximum uniaxial tensile force (Newton) needed to produce failure in the bone. It is measured by a pullout test, where tensile force at a predetermined pullout rate is applied along the longitudinal axis of the screw until the screw strips off or shears out of the fixation site (Bechtol et al., 1959; Frandsen et al., 1984). An international standard development organisation, the American Society for Testing and Materials (ASTM), stated that the standard pullout rate for the test method for determining the axial pullout strength of medical bone screws is at 5 mm / min (ASTM, F 543-07). From herein, the strength of the bone-screw construct will be referred to as the pullout strength.

Numerous studies have been conducted to investigate possible factors that affect screw pullout strength, such as screw design and dimension, screw material, insertion technique, bone quality (bone mineral density and aBMD), and insertion torque, in human, animal, and synthetic bones (Ansell and Scales, 1968; Bechtol et al., 1959; Charnley, 1960; Frandsen et al., 1984b; Koranyi et al., 1970; Reynolds et al., 2013; Ryken et al., 1995; Schatzker et al., 1975; Søreide et al., 1980). These will be discussed in the following sections.

3.4 Cadaveric Bone versus Animal Bone versus Synthetic Bone

In the bone-implant related research such as the evaluation of screw fixation strength (or pullout strength), it is critical to conduct the biomechanical testing on bone samples that have close resemblance with those seen clinically to allow direct comparison with the clinical scenario. In this respect, performing tests in vivo on the live bones are the most ideal choice.

The cellular mechanisms within live bones as mentioned earlier (sub-chapter 2.2.3) are still functioning to support bone life, thus, provide the actual scenario of choice for the investigation of the screw fixation strength at any phases of fixation either at the early post-operative (primary fixation strength) phase as well as at the time-dependent changes after bone remodeling and osseointegration occurred in bones surrounding the screw fixation as (secondary fixation strength). The option to use live bones, particularly from the human subject to conduct biomechanical testing however may not always be possible due to the testing regimes that are

generally invasive, destructive and irreversible, which can be life threatening to the humans.

With this constraint, cadaveric bones, animal bones and synthetic bones are the common substitutes to live bones for the biomechanical testing, which are performed in vitro. The following sections highlight the characteristics of cadaveric, animal and synthetic bones and their respective advantages and disadvantages in contributing to the findings of bone-implant studies.

Cadaveric Bone

Cadaveric bones pose the closest resemblance to live bones (in vivo) from the human subject in terms of their biological properties and structures compared to the other bone substitutes such as animal and synthetic bones. Thus, cadaveric bones are the most desirable substitutes for biomechanical testing in bone-implant research.

Unlike live bone, cadaveric bones lack the normal bone cellular functions, responsible for the remodeling of the bone tissues (sub-chapter 2.2.3); hence, time-dependent changes in bone surrounding the screw will not occur. Therefore, the biomechanical testing on the bone-implant such as the evaluation of screw fixation strength studies are limited to the immediate point (time 0) of screw fixation only; and screw fixation strength studies at the time-dependent phase cannot be accounted for.

Similar to live bones, cadaveric bones are not uniform, resulting in the use of bone samples with vastly heterogeneous bone quality and strength, which contribute to a large sample size requirement in order to obtain a satisfactory significance and power for statistical comparisons (Christifilini et al., 1996; Heiner and Brown, 2001; Sommers et al., 2007; Marti et al., 2001). Additionally, cadaveric bones are difficult to obtain, costly and require stringent protocols and ethics for handling, storage and disposing of the bone samples. These constraints have turned some researchers to opt for animal bones or synthetic bone substitutes, depending on their respective study objectives.

Animal Bone

Animal bones are the simplified representations, which they pose the same or similar biological functions and structures as of the living human subjects. Using animal bones for the biomechanical testing may offer advantages over human cadaveric bones since they are often simpler to control and manipulate, and ethical concerns may be less troublesome to address. Although the use of bones in living animal have been disputed over the last 150 years, they provide a possible option to investigate screw fixation strength either at the early stage of screw fixation or at time-dependent changes in bone surrounding the screw (Oroszlany et al., 2015).

Bones from the sheep, bovines and pigs are the common choices for the biomechanical testing, allowing them to be performed in both environments, in vivo and in vitro. In selecting the animals however their bones' phenotypes and cross-species biomechanical properties must be carefully considered for

comparability with the human subjects and clinical scenarios. The sample size for animal bones also still be large to obtain a satisfactory significance and power for statistical comparisons and reproducibly. Since there are no established standards and there is a wide variety of bone shapes and sizes, a large number of variables must be considered when establishing biomechanical testing procedures. The need for control groups and the care of animals have contributed to higher costs. Due to this, synthetic bones becoming a better option for bone substitutes.

Synthetic Bone Sample

The Synthetic materials offer a wide range of possibilities as bone materials. The main advantage of the synthetic materials is that they can be engineered to meet certain requirements, and will have constant material properties and cut into standard sizes. The structures and mechanical properties (e.g., strength and stiffness) of the synthetic materials can be made to resemble that of trabecular or cortical bones. They provide an uncontaminated, clean test environment, which makes them the ideal choice when biological processes in the human body are not part of the research. However, the uses of synthetic bones lack the biological diversity that exists in live bone of human subjects, which does not allow direct comparison to the clinical setting. Thus, key findings obtained through synthetic bone testing should be validated on cadaveric bones.

3.5   Pullout Strength: The Effect of Screw Design and Dimension

In 1984, Frandsen and colleagues explored how screw design and screw size affect the screw pullout strength. They used two different screw designs and

dimensions (cancellous screws: 15 and 30 mm in length, both with outer diameter [OD] of 6.5 mm; and hip compression screws: 19.1 and 28.6 mm in length, both with OD of 12.7 mm) and performed screw insertions into 40 human cadaveric femoral heads, followed by pullout tests for the measurement of pullout strength. The results demonstrated that the pullout strength of screws of both designs increased with the length and OD. For example, when the screw OD was increased from 6.5 mm in cancellous screws to 12.7 mm in hip compression screws, a 70% increase in pullout strength was obtained (Frandsen et al., 1984).

Asnis et al. (1996) compared the holding strength of cancellous screws of different pitch, OD and inner diameter (ID). These screws were inserted into synthetic bone models of different densities (0.15 g/ml and 0.22 g/ml), and holding strengths were measured through screw pushout tests using a servo hydraulic testing machine. The cancellous screws with wider OD (6.5 mm) demonstrated significantly higher holding strength compared to screws with thinner OD (4.5 mm) ($p < 0.001$). Similarly, a decrease in pitch (or increase in threads per inch) also significantly increased the holding strength of the cancellous screw (Asnis et al., 1996).

In another study, the pullout strengths of two different designs of bone screws (conical pedicle screw versus cylindrical pedicle screw) of similar dimensions (thread pitch, area, and contour) were compared. Using porcine lumbar vertebrae, Abshire et al. (2001) found that the conical screws provided a 17% increase in the pullout strength compared to the cylindrical screws, suggesting that conical screw designs engage more bone between the conical screw threads than cylindrical

screws (Abshire et al., 2001). Similarly, Ryken et al. (1995) determined in human vertebrae that the pullout strength of bicortical screws was significantly higher (253 N) (p = 0.008) compared to the pullout strength of unicortical screws (170 N), suggesting that fixation of bicortical screws provides stronger mechanical stability than unicortical screws.

In summary, the factors of screw design and dimension have shown to influence the pullout or holding strength of screws as demonstrated by the studies mentioned above. Screws with bigger OD and smaller pitch size (or more threads per inch) were found to provide greater pullout strength than those screws with smaller OD and fewer threads. A likely explanation is that with the varying thread designs and dimensions, the contact areas between bone and thread may vary, thus altering the distribution of forces, and generating variation in pullout strength. However, the anatomical location of insertion and the required function of use dictate to a great extent the design and dimensions of the screw chosen for the surgery.

3.6 Pullout Strength: The Effect of Screw Material

Many bone screws are constructed from stainless steel due to its biocompatibility as well as strength (Burval et al., 2007; Lin et al., 2003; Patel et al., 2010; Shea et al., 2014; Taniwaki et al., 2003). Titanium has been widely considered in newer designs of screws because it is more flexible (or ductile) and bioactive (tissue bonds to the screw), potentially improving bone ingrowth and mechanical fixation. It also offers superior compatibility when scanned with magnetic

resonance imaging (MRI) and computed tomography (CT), producing images with significantly less interference (metal artefacts) compared to stainless steel screws (Christensen et al., 2000; Shea et al., 2014; Shi et al., 2012).

To determine whether the characteristics of titanium improves the anchorage of screws within osteoporotic bone, Christensen et al. (2000) investigated the effect of titanium screws (Ti-6AL-4V) (n = 9) versus stainless steel pedicle screws (316L) (n = 9) on the pullout strength and bone in-growth in the vertebra bone of 18 skeletally mature female Göttingen mini-pigs. The screws were implanted while the animals were placed under general anaesthesia. After three months, the animals were sacrificed and pullout tests were performed on the screws. Despite a significantly different (p < 0.04) osteointegration between the bone and the titanium screw (43.8%) compared to the stainless steel pedicle screw (29.4%), there was only a 5% increase in pullout strength compared to the stainless steel screw (pullout strength: titanium screw = 2232 ± 259 N; stainless screw = 2128 ± 277 N) and this was not statistically significant (Christensen et al., 2000; Shea et al., 2014).

In a similar animal study, the pullout strength of two expandable titanium pedicle screws of different elastic modulus (E) were compared, i.e., between Ti-24Nb-4Zr-7.9Sn (E = 42 GPa) and Ti-6AL-4V (E = 110-114 GPa). These screws were implanted into the vertebra of live female sheep (n = 4) with induced osteoporosis (bone E = ~13.5 GPa) (Rho et al., 1997; Shea et al., 2014). The study's hypothesis was that the screw (Ti-24Nb-4Zr-7.9Sn) with E closer to that of bone would produce greater pullout strength than the screw of higher E. At six months post-

screw implantation, the animals were sacrificed for the pullout tests. The integration between the bone and screw with E more closely matched to bone was highly noticeable and its pullout strength was higher by 19.3% ($p < 0.05$), compared to the screw with higher E (Shea et al., 2014; Shi et al., 2012).

In summary, the use of titanium screws in osteoporotic bone generally demonstrated more bone ingrowth and increase of pullout strength compared to stainless steel screws. Titanium screws with E more closely matched to bone resulted in better osseointegration at the bone-screw construct, and hence stronger fixation.

3.7   Pullout Strength: The Effect of Pilot Holes

A pilot hole is normally drilled prior to screw insertion so that the screw can be easily guided in the direction of interest. In the process, the size of the pilot hole must be optimised to prevent undersized or oversized pilot holes. If a pilot is too small (undersize), it may increase resistance to screw insertion that could cause screw fracture or fracture of surrounding bone structures. However, if a pilot hole is too large (oversize), it may decrease contact between the screw and bone structures, thus compromising the pullout strength of the screw (Battula et al., 2008; Steeves et al., 2005).

Pilot holes in synthetic bone:

To test if different pilot hole sizes affect pullout strength, Battula et al. (2008) compared the pullout strength of bone screws inserted into pilot holes of four

different sizes: 2.45 mm (70% of the screw OD of 3.5 mm); 2.5 mm (71.5% of OD); 2.55 mm (73% of OD); and 2.8 mm (80% of OD) using osteoporotic synthetic bone models. The findings were that an increase in pilot hole size relative to 2.5 mm reduces the pullout strength as well as the amount of torque required for insertion. They suggested using a pilot hole size no larger than 71.5% of OD to maximise the pullout strength and minimise iatrogenic damage in osteoporotic bone (Battula et al., 2008).

In another similar study, the screw pullout strength from three pilot holes, smaller (2.8 mm), similar (3.8 mm) and larger (4.5 mm) than the inner diameter of the pedicle screw were compared. This experiment was performed in a Landrace breed swine vertebral bone. The results obtained in this study were consistent with the findings by Battula et al. (2008), which indicated that an increase in pilot hole size reduces the pullout strength of pedicle screws. Based on the findings, Leite and colleague suggested that the effect of bone removal during pilot hole drilling had affected the ability of the bone-screw contact to create a strong anchorage of the screw threads. With an increased pilot hole diameter, a larger amount of bone was removed and a smaller amount of bone remained to be compacted around the screw, thus reducing the insertion torque and compromising pullout strength (Leite et al., 2008).

Pilot holes in human bone:

Steeves et al. (2005) investigated the effects of pilot hole sizes on the pullout strength of bone screws in human cadaveric femurs and tibia. The femurs and tibia were cut in half through the transverse (or horizontal) plane to provide direct

access to the trabecular part of the bone for screw insertion. The study compared the pullout strength of cancellous screws (OD: 6.5 mm and ID: 3.0 mm) from two pilot hole sizes, i.e., 3.5 mm (recommended size of pilot hole specified by the AO/ASIF (Schatzker, 1991) and 2.5 mm (reduced size of pilot hole). Four pilot holes of 3.5 mm and 2.5 mm (two of each size) were randomly, but equally, assigned to be drilled at locations in a line along the metaphysis of the femurs and tibia respectively, i.e., at the extreme lateral, inner lateral, inner medial, and extreme medial metaphysis.

Predictably, cancellous screws demonstrated a significantly ($p < 0.05$) higher screw pullout strength using a smaller size pilot hole (2.5 mm) than the manufacturer's recommended size (3.5 mm) for all the locations of screw insertions except at the inner lateral site of the distal femurs and proximal tibia, which showed the reverse trend (pullout strength of 2.5 mm pilot hole = 107.4 N; pullout strength of 3.2 mm pilot hole = 163.8 N). They suggested that inserting a screw into a smaller pilot hole might create the beneficial effect of compressing the debris of the cancellous bone's trabeculae filling the hole, thereby resulting in an increased pullout strength of the cancellous screw.

In summary, the overall results from various studies indicate that, whether tested in synthetic, animal, or human bones, pullout strengths of bone screws in reduced pilot hole sizes are higher compared to pilot hole sizes similar to or larger than the screw's ID.

3.8 Pullout Strength: The Effect of Non-Tapped and Pre-Tapped Pilot Holes

Clinically in bone surgery, a non-tapping pilot hole is prepared when self-tapping screws are used with the intention to simplify the procedure, avoid additional trauma to the patient and shorten the operation time. A pre-tapped pilot hole is prepared when non-self-tapping screws are used, typically involving cortical bone and attempting to insert a screw obliquely into the bone to lag two bone fragments together (Baumgart et al., 1993; Shea et al., 2014). The decision of whether to use a non-tapping or pre-tapping pilot hole depends on the surgeon's judgement for each situation.

Thompson et al. (1997) compared the pullout strength of non-cannulated cancellous screws in pre-tapped pilot holes, and cannulated cancellous screws in non-tapped pilot holes using synthetic polyurethane bone models of apparent densities within the range reported for normal human cancellous bone. Their results indicated no demonstrable effect on the screw pullout strength when the screws were inserted with or without tapping the pilot hole. However, in porous material of density similar to osteoporotic bone, they discovered that the screw pullout strength decreased in the pre-tapped pilot hole and suggested that this was caused by the removal of materials by the tap which enlarged the hole considerably. This finding was also in agreement with the other pullout strength studies involving pedicle screws in a synthetic bone model with a density similar to osteoporotic bone (Chen et al., 2009; Pfeiffer and Abernathie, 2006).

In a similar study, but performed in seven pairs of femora from immature (1 – 7 months) foals, Johnson et al. (2004) compared the pullout strength between 6.5 mm standard cancellous and 7.3 mm self-tapping cannulated bone screws, which were inserted in tapped and non-tapped pilot holes respectively at the proximal metaphysis, mid-diaphysis and distal metaphysis. The study found 6.5 mm cancellous and 7.3 mm cannulated screws had similar pullout properties, but vary in insertion properties. For instance, the pullout results showed that the pullout strength of the 6.5 mm cancellous screws and 7.3 mm cannulated screws were similar at each location of insertion. The pullout power of both screws was significantly greater in the mid-diaphysis than in either metaphyseal location. On the other hand, insertion torques for the 7.5 mm cannulated screws inserted in the tapped pilot holes were greater than in non-tapped pilot holes, but their insertion torques were significantly lower than for the 6.5 mm cancellous screws.

Pfeiffer and Abernathie (2006) compared various pedicle screw designs using non-tapped and pre-tapped pilot holes in synthetic bone models of density similar to osteoporotic bone. A uniform synthetic bone model was utilised in the study to provide a consistent test for each screw by eliminating the variability seen in human bone. During testing, they observed that tapping some of the pilot holes caused degradation of the bone materials. Their results indicated that screw pullout strength from the tapped pilot hole in their osteoporotic bone model was lower than in the untapped case. They inferred that this could be due to the degradation of the bone by the tapping action.

In a similar study, Chen et al. (2009) investigated the pullout strength of cannulated pedicle screws in a synthetic bone model with a density similar to severely osteoporotic bone as part of a bigger study. They also discovered that pre-tapping of the pilot hole in a low-density bone decreased the screw pullout strength, with larger standard deviations, suggesting that the results from the pre-tapped case results are less repeatable than the non-tapped cases (Chen et al., 2009).

In summary, for higher-density bone (or normal bone quality), tapping had no demonstrable effect on screw pullout strength. Pre-tapping of the pilot hole prior to screw insertion, particularly in patients with dense bone, may be a desirable option in order to cut the thread profile into the bone. However, in the case of material of lower density, pre-tapping of a pilot hole decreased the pullout strength of the bone screw. Pre-tapping of the pilot hole may therefore be inadvisable in patients with osteoporotic bone quality.

3.9   Pullout Strength: The Effect of Bone Quality

Bone serves as a foundation material for the anchorage of screw threads. Therefore, its quality (in terms of bone mineral density and micro-architecture) coupled with other factors highlighted in previous sections is pivotal in contributing to the success of screw fixation.

To investigate the effect of aBMD on screw pullout strength, Halvorson et al. (1994) compared the influence of the pullout strength of 6.5 mm pedicle screws in

normal (average aBMD = 1.17 mg/cm^2) and osteoporotic (average aBMD = 0.82 mg/cm^2) human cadaveric spines. The pedicle screws were inserted into the spine using different insertion methods, untapped pilot holes, tapped pilot holes (size: 6.5 mm and 5.5 mm) and enlarged pilot holes packed with corticocancellous bone, followed by the pullout tests.

Their results showed that the average screw pullout strength in normal bone specimens (average pullout strength = 1540 ± 361 N) was approximately 8 times greater than in osteoporotic bone specimens (average pullout strength = 206 ± 159 N). In normal spines, the method of screw insertion did not influence the screw pullout strength. In contrast, the method of screw insertion in osteoporotic bone did alter the screw pullout strength significantly. In osteoporotic spine, the screw pullout strength either from an untapped or a 5.5 mm tapped pilot hole was significantly greater than screw pullout with 6.5 mm tapped pilot hole or the destroyed pilot hole with packed corticocancellous bone (pullout strength (N): untapped = 350.4 ± 115; 5.5 mm tapped = 400.3 ± 205; 6.5 mm tapped = 63.55 ± 48.2, and destroyed pilot hole packed with corticocancellous bone = 61.41 ± 47.0 $p < 0.0003$) (Halvorson et al., 1994).

Tingart et al. (2006) investigated the effect of bone mineral density on pullout strength using a metal screw-like suture anchor in fresh-frozen cadaveric humeri. Prior to insertion, pQCT was used to measure total, trabecular, and cortical bone mineral densities in different regions of the lesser and greater tuberosities of cadaveric humeri. Suture anchors were then inserted into individual regions of the humeri, and cyclic loading was applied in order to evaluate the influence of total,

trabecular and cortical bone mineral densities on the pullout strength of the anchors. Consistent with the previous studies, overall significant positive correlations were found between bone mineral densities and pullout strengths with coefficient of correlation R values ranging from 0.65 to 0.74 ($p < 0.01$).

Seebeck et al. (2004) investigated the holding strength of uni-cortical screws used in an internal fixator system by means of an axial and cantilever bending mode. The tibia bone mineral density was determined at the screw's insertion sites with the use of CT images. The screws were inserted at different sites of the metaphyseal and diaphyseal regions, followed by axial pullout and cantilever bending tests (Figure 3.2).
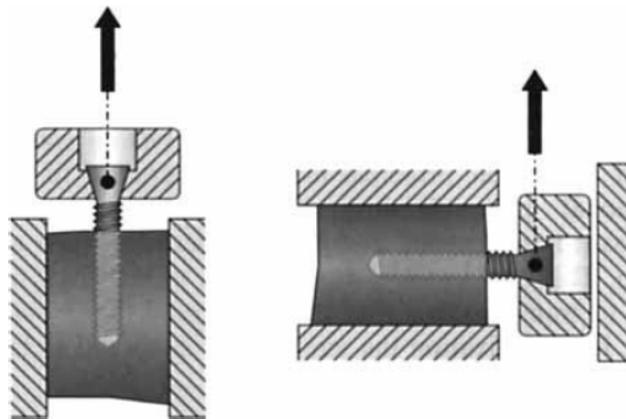
Figure 3.2 Experimental set-up for the axial pullout (left) and the cantilever bending tests (right), (Seebeck et al., 2004). Reproduced with permission from John Wiley and Sons.

Their stepwise multiple linear regression results revealed that trabecular bone density and cortical thickness explained 93% and 98% of the variance of the screw pullout strength in axial and cantilever bending modes respectively. Additionally, the study also found that loading of the screw in the cantilever

bending mode led to a significant increase, almost doubling the holding power of the screw compared to the axial loading situation.

Seebeck associated this phenomenon with the anisotropic material properties of the bone in which by using the screws in a cantilever bending mode, the bone was loaded along the direction of its highest compressive and tensile strength, while pullout in an axial mode produced a loading of the bone in its weakest transverse direction. This means that a screw which fails with axially loaded application, might still provide enough holding power if loaded in a cantilever bending mode, since it better uses the strength potential of the bone (Seebeck et al., 2004).

While most studies have concentrated on measures of bone density such as aBMD, only very few studies reported in the literature have investigated the influence of the other contributing factors of bone quality, such as the micro-architecture of trabecular bone on the pullout strength of bone screws in the laboratory setting (Poukalova et al., 2010; Yakacki et al., 2010). Poukalova et al. (2010) studied the relationships between trabecular micro-architecture and elastic modulus, compressive strength and pullout strength of cork-like screw suture anchors in the trabecular bone from human humeri.

The study evaluated the micro-architectural parameters and elastic moduli of the humeri bones from micro-CT images and stress-strain curve obtained from compression tests. After insertions of the cork-like screws to head contact at five locations in the greater tuberosity, lesser tuberosity, and humeral head, axial pullout tests were performed at a pullout rate of 1mm/sec. Their findings

suggested that the pullout strength of cork-like screws and compressive strength of the cadaveric humeri show significant correlations to bone volume fraction (BV/TV), structure model index (SMI), and trabecular thickness (Tb.Th).

Yakacki et al. (2010) investigated the effect of bone micro-architecture measured by micro-CT on the pullout strength of cork-like suture anchors. The cork-like screws were inserted in three different locations in human humeri bone specimens, i.e., at greater tuberosity, lesser tuberosity and humeral head. The micro-architectural parameters of the bone specimens however were evaluated after screw insertions, and thus the evaluated micro-architectural parameters were not taken directly from the actual sites of screws implantation, but rather from bone areas adjacent to the implantations. Their findings revealed that the trabecular bone micro-architecture, particularly the SMI had the highest correlation (R = - 0.81) with the pullout strength of the corkscrew, followed by Tb.Th (R = 0.71) and BMD (R = 0.64) (Yakacki et al., 2010).

Since the introduction of high resolution imaging technology such as quantitative CT (qCT), and MRI in clinics and micro-CT in laboratory environments, finite element analysis (FEA) has gained a strong momentum in orthopaedic research, particularly in the investigation of the peri-implant augmentation and stability in different bone quality (Wirth et al., 2011).

Wirth et al. (2009) developed micro finite element models (micro-FE) of bone-screw constructs and compared results of the FEA with data obtained from laboratory pullout strength tests performed on sheep vertebral bodies. Their

results showed a strong correlation (R^2 = 0.87) between laboratory and FEA pullout strength measurements and indicated that bone volume fraction (BV/TV) measured by micro-CT was a good predictor (R^2 = 0.86) of the experimentally measured pullout strength (Wirth et al., 2010).

In another FEA study, Wirth et al. (2011) investigated implant stability through the development of a model of trabecular bone of the humeral heads from micro-CT images. The screws were digitally inserted into the humeral head finite element model and a virtual biopsy of the bone was taken at the implant site to quantify bone structural quality (micro-architectural parameters) and the stiffness of the bone-screw construct as a measure of implant stability (instead of the pullout test). Their findings indicated that the local bone micro-architecture at the place of screw implantation accounted for 91% of the variability observed in the bone-screw stiffness, compared to 52% from the global bone micro-architecture.

In summary, bone quality, particularly aBMD, has shown a significant relationship with screw pullout strength. This implies that bone of a high aBMD provides better foundation for the anchorage of screw threads, and hence, produces a strong fixation. Measures of bone micro-architecture also show a good relationship with the screw pullout strength, in particular BV/TV, SMI and Tb.Th.

3.10 Pullout Strength: The Effect of Insertion Torque

Once screw head contact is reached, the torque required to further tighten the screw and compress the bone fragments increases rapidly. Surgeons typically rely on their intuition to judge the torque at which to stop tightening before stripping occurs, with the aim of optimising stability of the bone-screw construct, while minimising the risk of screw stripping. This is based on the premise that continuing tightening beyond head contact increases the strength of the construct.

The question arises then, as to what effect the torque to which the screw is tightened beyond head contact has on construct strength. There have however been very few studies to address this directly; most studies have concentrated on the surgeon's ability to stop tightening prior to failure and what construct strength is achieved as a result of a surgeon's perceived optimal tightening torque.

In orthopaedic surgery, torque measuring devices are not commonly used; however, torque limiting screwdrivers are routinely used particularly for the insertion of locking screws in a theatre setting. Surgeons rely on their experience and intuition to judge the point at which to stop tightening once head contact has been reached. However, according to Stoesz et al. (2013), the ability of surgeons to optimise screw insertion torque for a good fixation based on their own judgement is not reliable in preventing and detecting screw stripping. In an investigation into screw and plate fixation constructs in three densities (0.08, 0.16 and 0.32 g/cm3) of synthetic trabecular bone, they discovered that surgeons stripped 109 (45.4%) of 240 screws and did not recognise stripping 90.8% of the

time when it occurred. They also found there was a disparity in the frequency of stripping between surgeons, ranging from 16.7% to 83.3% stripped, suggesting that proprioception and/or aggression varies between individuals (Stoesz et al, 2013).

Dinah et al. (2011) investigated the risk factors for unintentional screw stripping and over-tightening during fixation of ankle fractures in elderly bone, including whether bone density, cortical thickness and screw insertion technique (uni- and bicortical purchases) are predictors of unintentional screw stripping and over-tightening. The study utilised cadaver ankle bones (10 pairs) of varying densities (ranging from 186 distally to 1138 mg/L proximally) measured by multi-slice CT scanner with self-tapping cortical and cancellous screws (200 screws). The screws were tightened to optimal torque judged by the surgeon. Their results showed that 9% (18 out of 200 screws) of the screws were unintentionally stripped and 12% (24 out of 200 screws) were over-tightened (defined by authors as having been tightened to a torque ranging from 90% T_{Max} to 99% T_{Max}). Despite 21% of the screws being stripped or being at risk for stripping, they found no significant predictors to warn of impending screw stripping.

Cordey et al. (1980) undertook a study to measure the tightening levels produced by 101 surgeons though a laboratory experiment. Each surgeon was assigned to tighten one screw into a cadaveric tibia and femur, respectively, to their judged optimal torque (T_{Opt}) for a good fixation. The torque was then increased to strip the thread (T_{Max}). The screw insertion parameters, T_{Opt} and T_{Max}, were recorded via an instrumented screwdriver. The cortical thickness was measured for both

bone types (cortical thickness [mm] mean [SD]: tibia = 5.5 [1.3] and femur = 5.5 [1.0]). The findings of the investigation revealed that the relationships between the T_{Opt} and T_{Max} in tibia and femur are relatively constant, with T_{Opt} in the tibia being 84% of T_{Max} and in the femur 88% of T_{Max}, hence, the overall average of T_{Opt} as a percentage of T_{Max} in bone (tibia and femur) being 86%. Cordey et al. concluded that, in the clinical setting, surgeons typically tighten screws based on judgements to an average torque of 86% of T_{Max} in order to achieve the optimal force between the screw and bone.

In a different study, Cordey et al. investigated the surgeons' perceptions in judging for the optimal insertion torque (T_{Opt}) for strong fixation in different bone qualities (measured by roentgenogram) (Cordey et al., 1980). The screws were inserted using three different techniques, that is via small and large pilot holes, made visible to surgeons and via pilot holes, which sizes unknown to surgeons performing the tests. 36 surgeons of various skills were involved in the study, producing a total of 108 screw insertions. The insertion data such as the applied torque (T), T_{Opt}, stripping torque (T_{Max}), stripping force (F_{Max}) measured between the screw head and bone as well as screw angular displacement (α) were recorded.

The findings showed a linear relationship between T_{Opt} and T_{Max}, which indicated T_{Opt} is proportional to T_{Max}. Of the 108 insertions, surgeons stripped the screws more than 10 times. A strong correlation was found between F_{Max} and bone density (R = 0.93) and a weak correlation between F_{Max} and bone cortical thickness (R = 0.71). No statistical differences in T_{Opt}, T_{Max} or F_{Max} were found

between different insertion methods. Based on these findings, Cordey concluded that the F_{Max} at T_{Max} varies between bones; hence, so does T_{Opt}. In general the surgeons are able to adapt well to judging the torque at optimal force when subjected to different screw insertion methods and in varying bone qualities. Nevertheless, Cordey et al. stated that in low-quality (osteoporotic) bone, the surgeons' judgement was found to be inconsistent.

In a later study, Siddiqui et al. (2005) compared screw pullout strength achieved by clinicians applying an insertion torque that they felt to be optimal for a good fixation. Four clinicians with a range of experience (nurse, senior medical officer, registrar, and consultant surgeon) were asked to insert a number of partially threaded cancellous screws to a uniform depth into chipboard blocks of non-uniform properties (density not specified) in which pilot holes of different sizes had been drilled previously. After each insertion, the clinician was asked to assign a value from 0 to 10, based on how strong the construct would be (in terms of expected magnitude of pullout strength).

The results of the four clinicians indicated a strong correlation between the judged and true screw pullout strength measured by pullout testing (correlation coefficient [R] ranged from 0.47 to 0.67 [p < 0.001]). The consultant of many years of experience had a much stronger correlation than the others (R = 0.67). All of the measured screw pullout strengths fell between a range of 600 and 1200 N.

Siddiqui et al. concluded that the variation in R values between clinicians indicates that some clinicians are better judges of insertion torque than others, with experience lending to an improvement in judgement. According to Siddiqui et al., the strong correlation between the judged and true screw pullout strength implies that the human perception of insertion torque is refined enough and the need for torque measuring devices is not a requirement in the operative setting.

Siddiqui et al. however, acknowledged that the correlation may be less strong in osteoporotic bone, which they did not study. Furthermore, their study was performed in chipboard blocks and its material structure is different from that of bone; thus, the correlation between the judged and true screw pullout strength in human bone (particularly trabecular bone) could be different. Until it is investigated, therefore, a question remains as to how accurate human judgement is in controlling the insertional torque of bone screws to achieve good fixation strength, particularly in low-bone quality material, such as osteoporotic bone.

A study from our laboratory (Cleek et al., 2007) investigated the effect on pullout strength of tightening of cortical screws performed on cortical bone of ovine tibiae to three levels of tightening torque (as a percentage of expected failure torque), 50%, 70% and 90% of T_{Max}. The results showed an increase in the pullout strength tightened at 70% T_{Max} compared to 50% T_{Max}, which was not significant. However, the pullout strength of the cortical screw decreased significantly by 13% at 90% T_{Max} compared to the pullout strength at 70% T_{Max}.

During the screw insertions, Cleek et al. monitored insertion torque via a torque transducer. Analysis of the insertion torque to failure curves revealed a linear regime at the initial phase of the curve, indicating the bone is behaving elastically in response to insertion forces. The subsequent phase of the curve, however, became non-linear as the bone began to yield. Cleek et al. therefore suggested the lower pullouts at 90% T_{Max} were a result of decreased strength of the construct resulting from the bone yielding around the screw threads. This is also in agreement with other work in our laboratory Ryan et al. (2015) which confirmed that yield occurs at approximately 85% T_{Max} (Ryan et al., 2015).

Tankard et al. (2013) replicated the Cleek et al. study in human cortical bone of the humeri with varying bone qualities, ranging from normal to osteoporotic. They hypothesised that the pullout strength of the self-tapping cortical screw inserted in humeri bone would be greatest in screws tightened to 70% T_{Max}, and significantly greater than in screws tightened to 50% T_{Max} and 90% T_{Max}. However, their results showed that tightening of the screw beyond 50% T_{Max} did not significantly increase the pullout strength of the screw in all bone qualities tested. The pullout strength value, although greatest at 70% T_{Max} in low-quality bone, was not significantly different from that tightened at 50% T_{Max} and 90% T_{Max}. Tankard claimed that screws tightened to beyond 50% T_{Max} did not improve the pullout strength and their overall findings failed to support the stated hypothesis (Tankard et al., 2013).

Reitman et al. (2004) and Ryken et al. (1995) evaluated the relationships between screw pullout strength and insertional torque judged to be optimal at varying bone

mineral densities in human cervical spine. Reitman performed the investigation on 54 cervical vertebrae in 12 cervical spines. aBMD of the specimens were obtained using DXA. Two 3.5 mm OD anterior cervical screws were used in the study for unicortical placement in each cervical spine. All screws were inserted into bone specimens by a single orthopaedic surgeon using a special screwdriver with a torque transducer to enable continuous acquisition of torque measurements as the surgeon was placing the screws. One screw was inserted to failure to obtain the maximum or failure torque (T_{Max}) (actual peak torque) and the second screw was inserted until the surgeon felt a sufficient amount of torque was achieved to maximise pullout strength without stripping the bone (perceived peak insertional torque), then performed pullout test.

They found that on average, the applied insertion torque produced by the surgeons was 85% of T_{Max}. The results showed a stronger correlation between aBMD and screw pullout strength (R = 0.710) than between applied insertion torque and screw pullout strength (R = 0.422). They concluded that the quality of bone is more instrumental in the success or failure of the screws than the insertional torque to which screws are placed (Reitman et al., 2004).

Similar to Reitman et al., but using different types of screws (uni- and bicortical Casper cervical plating screws), Ryken et al. (1995) investigated the relationships of screw pullout strength and insertional torque to varying bone mineral densities from 99 cadaveric vertebral bone specimens. The aBMD of the specimens was evaluated using DXA. Unicortical screws were inserted in 51 specimens and bicortical screws in 48 specimens at perceived optimal torque for a good fixation.

The average applied torque was 0.367 ± 0.243 Nm, and average pullout strength was 210.4 ± 158.1 N. Results indicated that the applied insertion torque shows a stronger correlation with screw pullout strength (R = 0.88, p < 0.0001) than does the aBMD with screw pullout strength (R = 0.54, p < 0.0001). In this study, the bone mineral density accounted for 28%, while insertion torque was 77%, of the observed variability in screw pullout strength.

Ryken concluded that although both bone mineral density and insertion torque are statistically significant variables, torque has the greater influence (Ryken et al., 1995). The contradiction in the order of strength of correlations between insertion torque and pullout strength and aBMD and pullout strength between Ryken et al. (1995) and Reitman et al. (2004) could be due to the effect of different screw designs used in their studies (Section 3.6).

3.11   Prediction of Point of Screw/Bone Construct Failure

The literature reviewed above shows that the pullout strength of a bone screw is related to the level of insertion torque although there is some discordance about the exact relationship (Cleek et al., 2007; Reitman et al., 2004; Ryken et al., 1995; Siddiqui et al., 2005; Tankard et al., 2013). Regardless of the exact relationship, it would appear that the level of torque applied should be controlled to avoid over-tightening and damaging the surrounding bone structure, leading to poor construct strength or complete failure due to stripping of the bone around the screw threads. However a simple torque control system (e.g. torque limiting screwdriver)

whereby the torque limit does not adapt to bone quality will not succeed due to the relationships between pullout strength, insertion torque and bone quality.

It has been demonstrated that torque at failure (T_{Max}) for cancellous screws is dependent on the density of the bone (Suhm et al., 2007). Furthermore, the torque measured during screw insertion prior to failure has also been found to be directly related to bone density and can be used, on its own, as a good predictor of ultimate failure torque of the bone.
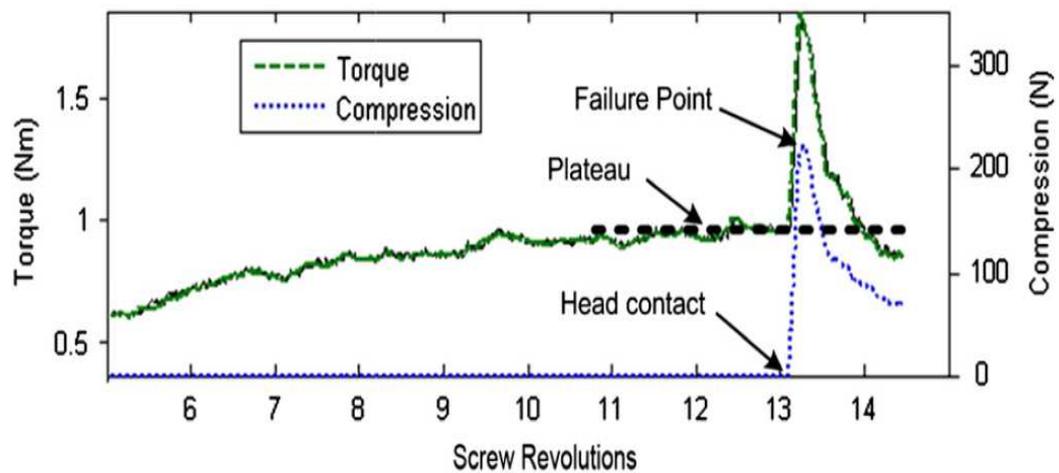
Figure 3.3 Torque and compression profiles of a synthetic bone to failure plotted against cancellous screw angular displacement (in revolutions), (Reynolds et al., 2013). Reproduced with permission from Elsevier.

A previous study from our laboratory (Reynolds et al., 2013) examined the torque, compressive forces, and rotations during automated cancellous screw insertion into synthetic (n=24), ovine (n=69) and human bone specimens (n=89). A typical graph of torque profile (insertion torque to failure versus screw angular displacement [revolution]) is shown in Figure 3.3. The plateau in torque just prior to head contact is a consequence of the fact that these screws are partially threaded; the plateau commences once all threads are engaged within the bone.

Results demonstrated a strong correlation between the torque value just prior to head contact ($T_{Plateau}$) and failure torque T_{Max} (synthetic: R = 0.90, p<0.001; ovine: R = 0.848, p<0.001 and human: R = 0.840, p<0.001), and showed that it is possible to predict failure torque (T_{Max}) solely from the insertion torque required to achieve bone-screw head contact. It was further established that variations related to bone density could be automatically detected through the effects of the bone on the rotational characteristics of the screw. These results and others (Hearn et al., 2004) from our laboratory indicate that it is possible to design an automated orthopaedic handpiece able to cease tightening at a safe level that avoids over-tightening and stripping and which adapts to bone quality. Further studies are warranted to identify the optimal level of tightening torque.

3.12   Summary

This chapter has reviewed the literature to identify a number of parameters that affect the fixation strength or pullout strength of bone screws. It has also briefly described the type, design and use of the bone screw, as well as possible fixation failure at different anatomy locations. Although fixation failure by pullout is uncommon among the screws of different types and designs seen in the clinical environment, pullout testing was chosen as the means to measure the screw fixation strength in vitro because of the simplicity of the experiment setup and protocol. The chapter also described different bone types (cadaver, animal and synthetic) that are commonly used as surrogates for living bones particularly human for the in-vitro testing along with work in our laboratory to develop smart

surgical instrumentation capable of adapting to bone density to improve fixation outcomes.

Of particular interest to this thesis, the level of applied insertion torque appears to influence screw pullout strength. However a surgeon's ability to identify the point at which to cease insertion is limited, and the optimal torque level for a good fixation is not established. Furthermore, bone quality has a significant influence on the screw pullout strength with higher density bone providing a better foundation for the anchorage of screw threads. Measures of bone micro-architecture also show a good relationship with the screw pullout strength, in particular BV/TV, SMI and Tb.Th.

This thesis aims to further our understanding of the actors affecting the stability of the bone-screw construct. The specific aims of the thesis will be described in the next chapter.

Chapter IV

Research Aims

4.0   Background

Most mechanical failures in screw fixation occur at the bone-screw construct interface due to the collapse of bone structure, which seems to suggest that the quality of the host bone does play a role in the stability of the bone-screw construct (Windolf and Perren, 2012) (see sub-chapter 3.9). Since the early days of implant development, many attempts have been made to improve the pullout strength of screw as described in chapter 3. However, the challenges still remain, particularly pertaining to the host bone quality and those challenges are highlighted below.

4.1   Current Challenges

Bone mineral density:

As previously mentioned, DXA aBMD is used in clinics to measure a patient's bone quality, but with some limitations. aBMD values represent measurements of bone mineral of the entire bone in the scan area, rather than the local density surrounding the screw implantation site. It is also not a true measure of density as it is normalised by the area of the scanned bone, instead of the volume, which can be biased to different bone sizes and orientations (Hernandez and Keaveny,

2006). Nonetheless, aBMD from DXA is the clinical measure of bone quality recognised by the World Health Organisation and globally referred to in the assessment of fragility fracture. Based on this, it is relevant from a clinical perspective to study aBMD's role in screw pullout strength. In addition, although measurements of a patient's aBMD are often lacking prior to surgery (Moroni et al., 2006), in some cases it may be available, possibly aiding surgeons in the the evaluation of the screw performance.

Bone Micro-architecture:

Bone micro-architectural parameters such as BV/TV, BS/TV, Tb.Th, Tb.Sp, Tb.N and SMI also define bone quality (see sub-chapter 2.3.1). Variations in micro-architectural parameters in human bone have shown to influence the mechanical strength of the bone (Cook et al., 2010; Mueller et al., 2009; Öhman et al., 2007; Perilli et al., 2012) and it could also be expected that they influence the stability of the bone-screw construct (Halvorson et al., 1994; Poukalova et al., 2010; Seebeck et al., 2004; Tingart et al., 2006; Wirth et al., 2009; Wirth et al., 2011; Yakacki et al., 2010) .

Unlike aBMD, the measurement of bone micro-architecture provides insight into the local bone area at which a screw is to be implanted, which is more advantageous than aBMD in the evaluation of screw performance. According to Seebeck et al. (2004) and Wirth et al. (2011), the quantity and micro-architectural quality of the bone in the vicinity of a screw may increase the predictability of screw pullout load. Although bone micro-architecture measurement in the clinical environment is still limited to peripheral skeletal sites, with the current rate of

technological developments, it could be expected that micro-architectural parameters may someday be used in the assessment of a patient's bone quality in the future.

Screw Insertion:

During screw insertion surgeons rely mainly on their personal judgement to apply the adequate insertion torque (T_{Insert}) for achieving optimum bone-screw stability and hence highest screw pullout strength ($F_{Pullout}$) (see sub-chapter 3.10). However, if any of the above mentioned bone micro-architectural parameters were found predictive of the insertion torque; these could then be used to predict the applied T_{Insert}, instead of relying on the surgeon's feel, which is subjective and inconsistent.

Based on the current challenges mentioned above, thus, there is a need for an investigation in laboratory environment to determine the respective roles of the cofounding factors of trabecular bone quality — aBMD and micro-architecture in contributing to screw $F_{Pullout}$ and T_{Insert} (including plateau torque or $T_{Plateau}$ — torque at screw head contact).

It is also important to determine the level of T_{Insert} for the optimal screw $F_{Pullout}$ before yielding occurs in trabecular bone of the femoral head, which has never been investigated before. This, therefore, leads to the research aims of this thesis and to an investigation of skeletal sites that are rich in trabecular bone (e.g., that which is found in human femoral heads).

4.2   Research Aims

The aims of the thesis are:

1. To determine the relationships between insertion torque at screw head-contact (or plateau torque, $T_{Plateau}$) and the aBMD and micro-architectural parameters of trabecular bone in human femoral heads of varying bone quality;

2. To determine the relationships between the pullout strength ($F_{Pullout}$) of a cancellous screw inserted in human femoral heads and the absolute applied insertion torque (T_{Insert}), aBMD and trabecular micro-architectural parameters of the bone;

3. To determine the effect of three different relative insertion torque levels (portion of maximum torque or T_{Max}) after head contact on the holding strength of the trabecular bone surrounding the cancellous screw, as assessed by screw pullout testing.

The aims of the thesis were investigated with partially threaded cancellous screws, typically used as lag screw in stabilising fractures at the trabecular rich anatomy such as the femoral neck. The partially threaded cancellous screws were used alone without a locking plate. This was to optimise contact between the screw and bone at tightening, hence, optimise the compression and fixation or pullout strength at the bone-screw construct. It is believed that this setup provides the precise means to investigate the effect of bone quality on the insertion torque and screw pullout strength compared to using a locking screw and plate, through which the bone may not be exposed to compressive force to its potential during

screw tightening as the forces are transferred rather to the plate (see sub-chapter 3.2.4 – Locking Screw).

It is hoped that the outcome of the present thesis will provide a valuable contribution to knowledge to enhance the understanding of the relationship between cancellous screw pullout strength, bone quality (aBMD and micro-architecture) and insertion torque; but also that these relationships may provide a basis to help clinicians to find a reliable mechanism to determine bone-specific insertion torque levels for achieving optimum screw pullout strength.

Chapter V

Study 1: Does Cancellous Screw Insertion Torque at Screw Head Contact Depend on Bone Mineral Density and/or Micro-architecture?

This chapter describes the experimental study performed to address the first aim of the thesis. That is, to determine the relationship between the absolute insertion torque at screw head-contact (plateau torque, $T_{Plateau}$) and bone quality (aBMD and the micro-architectural parameters) of trabecular bone tissue of femoral heads.

The results reported in this chapter have been published as Ab-Lazid R, Perilli E, Ryan MK, Costi JJ, Reynolds KJ, 2014, "Does cancellous screw insertion torque depend on bone mineral density and/or microarchitecture?' *J Biomech*, 2014 Jan 22; 47(2): 347-53. doi: 10.1016/j.jbiomech.2013.11.030. Epub 2013 Nov 27. The published paper was rewritten for this thesis.

5.0   Introduction

In a previous study from our laboratory, it was shown that during screw insertion of a partially threaded cancellous screw into human, ovine, and synthetic bone, the insertion torque level reaches a plateau at the engagement of all the screw threads prior to head contact (Reynolds et al., 2013) (see sub-chapter 3.11). This plateau torque ($T_{Plateau}$) was found to be a strong predictor of the maximum

(failure) torque (T_{Max}) occurring as the bone around the screw threads fails (R > 0.83 for all investigated bone types). $T_{Plateau}$ also showed strong positive correlations with volumetric bone mineral apparent density (g/cm^3) in ovine bone (R = 0.81, p < 0.001) and synthetic bone samples (R = 0.98, p = 0.001).

Based on these relationships, Reynolds et al. (2013) suggested that the measured $T_{Plateau}$ can be used to predict the point of failure during screw insertion and use this information to cease tightening of the screw before reaching T_{Max} or bone failure. However, their study did not explore the correlations between $T_{Plateau}$ and aBMD and between $T_{Plateau}$ and bone micro-architecture, and this was the aim of the present study. Human femoral heads were chosen for this study because of their high trabecular bone content and clinical relevance due to the high incidence of hip fractures (for example, intertrochanteric and femoral neck fractures) and the use of cancellous screws in the fixation of these fractures.

aBMD and bone micro-architecture vary both between and within patients (see Section 3.7). A patient's aBMD is measurable in clinics, and in some cases, is available prior to orthopaedic surgery. Micro-architectural parameters of the trabecular bone on the other hand, such as bone volume fraction (BV/TV), bone surface density (BS/TV), trabecular thickness (Tb.Th), trabecular separation (Tb.Sp), trabecular number (Tb.N), and structure model index (SMI), refer to measurements of trabecular bone structures obtained from micro-CT, and are currently only in use in pre-clinical research studies. However, with future technological developments, measurements of bone micro-architecture may become available clinically. Variations in micro-architectural parameters in

human bone have been shown to influence the stability of the bone-screw construct during laboratory failure testing (pull-out and push-in) (Mueller et al., 2013; Poukalova et al., 2010; Yakacki et al., 2010) (chapter 3) as well as the bone strength during bone compressive testing (Cook et al., 2010; Mueller et al., 2009; Öhman et al., 2007; Perilli et al., 2012). It could be speculated that these micro-architectural parameters, as well as aBMD, also influence $T_{Plateau}$ during screw insertion in human bone. However, to what extent is still unknown.

Therefore, the aim of this study was to investigate, for the first time, whether $T_{Plateau}$, measured during screw insertion prior to screw head contact, depends on aBMD or on bone micro-architectural parameters, or on their combination, in human femoral heads. In order to address the specified aims of this study, the following experimental procedures were implemented.

5.1   Materials and Methods

5.1.1 Ethics

Ethics approval was sought and granted from the Southern Adelaide Clinical Human Research Ethics Committee (SAC HREC) prior to the commencement of the collection and biomechanical testing of human specimens.

5.1.2 Bone Specimens

Fifty-two femoral heads, 45 retrieved from hip surgery (21 females, 24 males, mean [SD] age = 76.6 [10.2] years) due to neck of femur fracture or osteoarthritis,

and 7 from cadavers (1 female, 6 males, age = 82.1 [7.4] years) that had no history of fragility fracture or osteoarthritis, were collected from SA Pathology for testing.

5.1.3 Specimen Storage

The femoral head bone specimens were kept in a lockable medical freezer unit (MDF-U536, Sanyo Oceania Pty. Ltd, North Sydney, New South Wales, Australia) in the Biomechanics Laboratory at Flinders University with temperature set at - 20 °C. Prior to testing, the specimens were thawed for 24 hours in a refrigerator at 4°C.

5.1.4 Pre-preparation of Specimen

A floor-standing bandsaw was used to dissect the excised femoral head specimens at the femoral neck prior to DXA scans and biomechanical tests (Figure 5.1). A minimum head height of 35 mm was retained to provide sufficient depth and access for screw insertion.

Figure 5.1: A floor-standing bandsaw was used to cut the excised femoral heads from the femoral neck, level jagged edges, and trim off remnants of soft tissues, to allow easy access for the insertion of the cancellous screw into the femoral head specimens.

Remnants of soft tissue and jagged edges of bones that were left from surgery were also trimmed and cleaned. Upon completion, the heads were individually wrapped in gauze soaked with saline solution (0.9% sodium chloride) and placed in ziplock bags that were labelled with identification details (specimen number).

5.1.5 DXA Scanning - Measurement of aBMD

The aBMD of the excised femoral head specimens was measured using a clinical DXA scanner (GE Lunar Prodigy, Madison, WI, USA) (Figure 5.2) at the Nuclear Medicine & Bone Densitometry Department at the Royal Adelaide Hospital. The scanner operates with a narrow fan beam and has a small-animal software package, which is ideal for scanning small samples (weight < 2 kg) such as femoral head specimens (Bogden et al., 2008; Daley et al., 2010; Kiebzak et al., 1999).
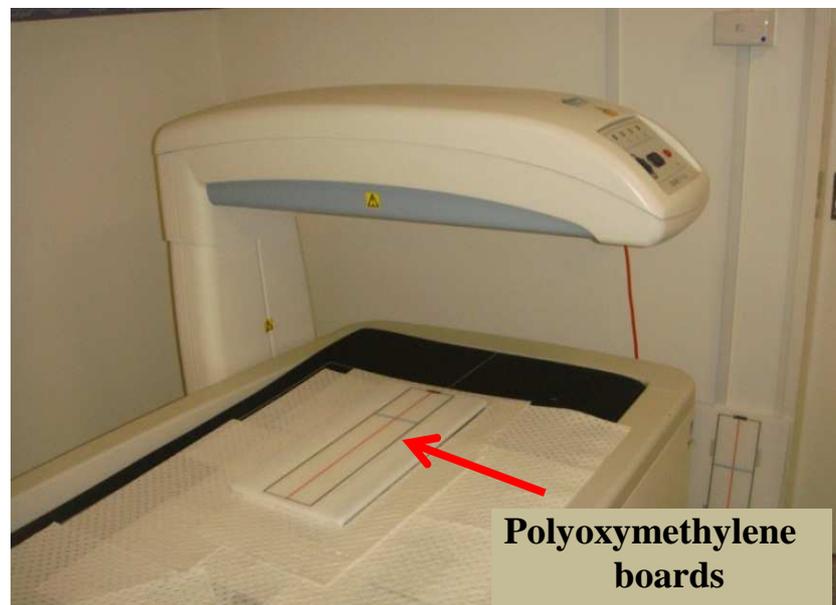
Figure 5.2: A DXA scanner (GE Lunar Prodigy, Madison, WI, USA), used in clinical departments for measuring patients' bone density, was used to measure areal bone mineral density (aBMD) of the femoral head specimens in vitro.

The scans were performed by an expert radiologist trained to perform DXA scans on patients. The femoral heads were placed in an anterior-posterior orientation on polyoxymethylene boards (Delrin®) (DuPont, Wilmington, Delaware, USA) (Figures 5.2 and 5.3) supplied with the scanner for simulating soft tissue (Farquharson et al., 1997), and scanned at an x-ray exposure of 1.8 µGy.
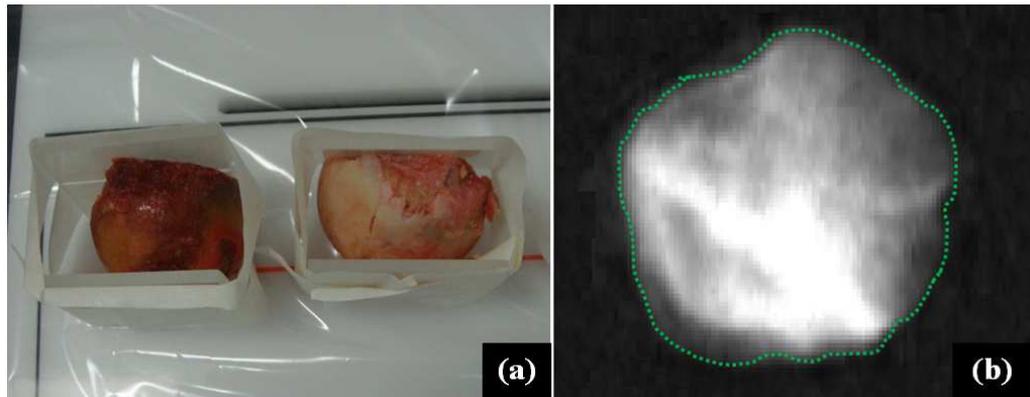
Figure 5.3: (a) The femoral head placed in anterior-posterior orientation on a Delrin board (served as soft tissue) for DXA scan. (b) A DXA image of the specimen. The areal bone mineral density was calculated based on the measured bone mineral content (BMC, g) divided by the bone area (cm^2) within the green boundary (aBMD = BMC (g)/ area (cm^2)).

At the completion of the scan, GE enCORE software (version 13.60, GE Healthcare Lunar, Madison, Wisconsin, USA) was used for the evaluation of bone mineral content (BMC) (measured in g) and bone area (measured in cm^2), from which aBMD was calculated (g/cm^2). The bone area within the DXA image was defined as a region of interest with size and shape adapted via software to the morphology of the femoral head by an expert radiologist.

5.1.6 Preparation for Screw Insertion

Before drilling of the pilot hole, both the femoral heads and specimen holders were manually sanded using a fine grade sand paper to provide better surface for

cyanocrylate adhesive (Loctite®) (Loctite 454, Henkel Corporation, North America) (Figure 5.4) to grip. This task was performed with great care to ensure that good contact was achieved between the specimen and holder to prevent them from coming unstuck during screw insertion resulting in a failed test. The centres of the cut surfaces of the specimens were marked with an "X" by a permanent blue marker to indicate the point of screw insertion (Figure 5.4 [b]). Once completed, final trimming of bone was performed on those specimens with larger head circumference. The bone areas that lay outside the circumference of the specimen holder, indicated by the circular blue line (Figure 5.4[b]), were trimmed off in order to fit the specimen holder (Figure 5.4 [c]).
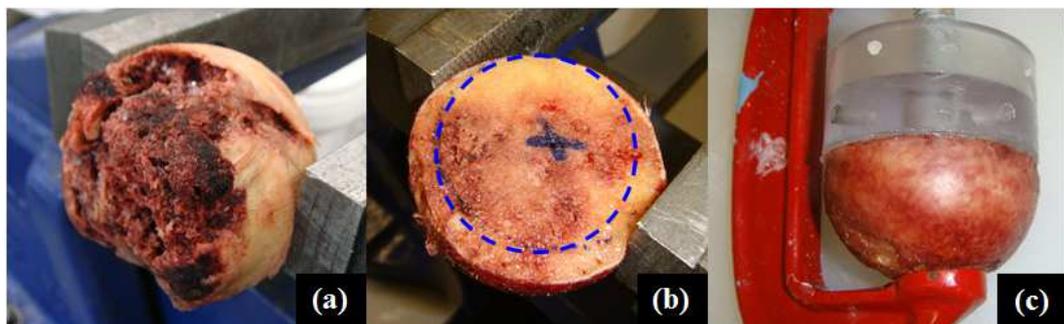
Figure 5.4: Photographs show different stages of femoral head specimen's preparation: (a) the initial condition of the femoral head specimen before trimming (levelling and smoothing) process, (b) after levelling and smoothing of the femoral head specimen surface area, further trimming of bone was made around the blue dotted circular line of the specimen holder circumference and (c) a G-clamp was used to hold the femoral head specimen and holder together after application of cyanoacrylate adhesive.

Once completed, the sanded femoral head specimen surfaces were wiped with gauze to remove bone debris, while the other surfaces of the specimen were covered with gauze soaked with 0.9% saline solution to keep the specimen moist. Cyanoacrylate adhesive (Loctite®) was applied onto the specimen holder (Figure 5.5) for gluing the femoral head and specimen holder together. The "X" on the

bone surface was carefully placed onto the central hole of the specimen holder for screw insertion.

(a)   (b)
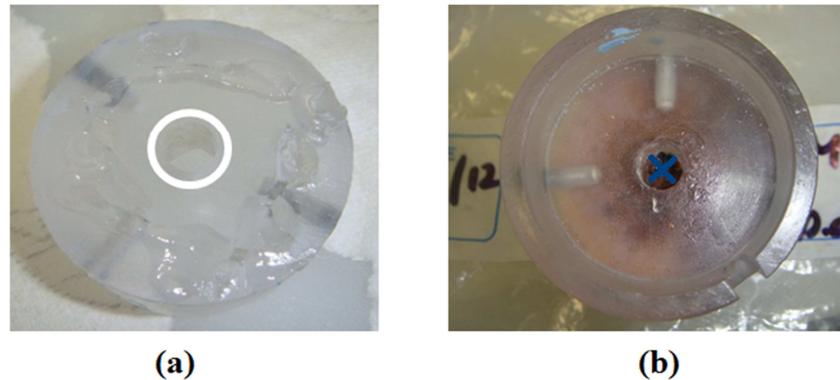
Figure 5.5: (a) Cyanocrylate adhesive (Loctite®) was applied to the surface of specimen holder, which the femoral head specimen was glued onto, and (b) the mark "X" was placed to face the central hole of the holder to allow for screw insertion.

A G-clamp was used to clamp the glued femoral head and the specimen holder together for about 15 to 20 minutes (Figure 5.4 [c]), until the adhesive was slightly dried and the bone and specimen holder construct became stabilised. The G-clamp was then removed and the specimen and holder construct were kept in the refrigerator at 4°C for the adhesive to set while thawing continued overnight.

Upon completion of 24 hours thawing time, the adhesive was properly set and the bone specimen and holder construct was removed from the refrigerator and transferred to the bench-top drill press for pilot hole drilling.

5.1.7 Cancellous Bone Screws

Partially threaded aluminium cancellous screws were used in the study. They were fabricated in-house to replicate a current orthopaedic cancellous screw

typically used in hip surgery (Smith and Nephew, London, UK [Catalog No. 7110-7050]).

The cancellous screws were of length 45.5 mm, outer thread diameter 6.9 mm, inner thread diameter 5.2 mm, thread length 16.5 mm, and thread pitch 2.0 mm (Figure 5.6). They were fabricated out of aluminium material instead of the original titanium to avoid artefacts during bone-screw imaging with high resolution micro-CT.
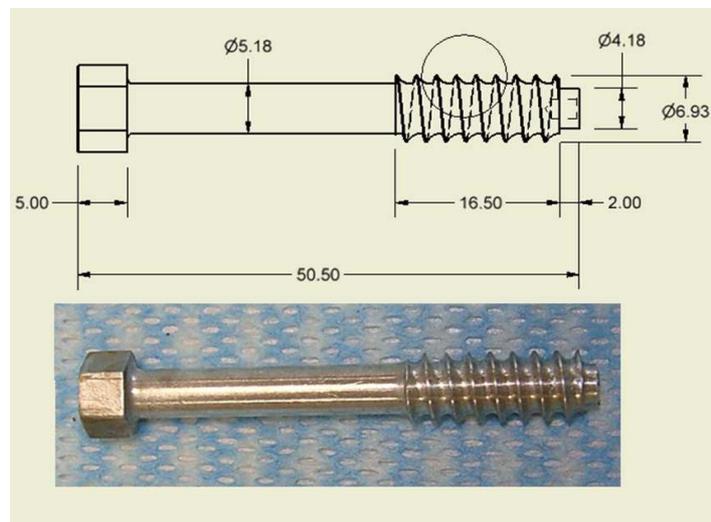
Figure 5.6: Dimensions of an aluminium cancellous screw that was replicated from a Smith and Nephew orthopaedic screw, commonly used in hip surgery.

5.1.8 Pilot Hole Drilling

Each of the 52 femoral head specimens was subjected to one screw insertion using a cancellous screw in a pilot hole. For the preparation of the pilot hole and initial placement of the cancellous screw into the pilot hole, a commercial bench-top drill press (Figure 5.7) from Ledacraft, Leda Machinery Pty. Ltd., North Plympton, South Australia was used. A drill bit of size 5.2 mm in diameter (size

recommended by Smith and Nephew, the manufacturer of the cancellous screw replicated in this study) was selected for drilling the pilot holes.

Figure 5.7: A commercial bench-top drill press was used for drilling the pilot hole and performing initial screw insertion prior to head contact.

Prior to drilling, the positioning and alignment of the femoral head specimens were checked with the aid of a spirit level and locator pin as shown in Figure 5.8 to ensure the pilot hole passage was drilled axially (not angled). Once ready, the drill was lowered, penetrating into the bone specimen to create an un-tapped pilot hole at the centre (X) of the cut surface (Figure 5.9 [a]) to a depth of 23.5 mm to allow penetration of all the screw threads (Figure 5.9 [b]).
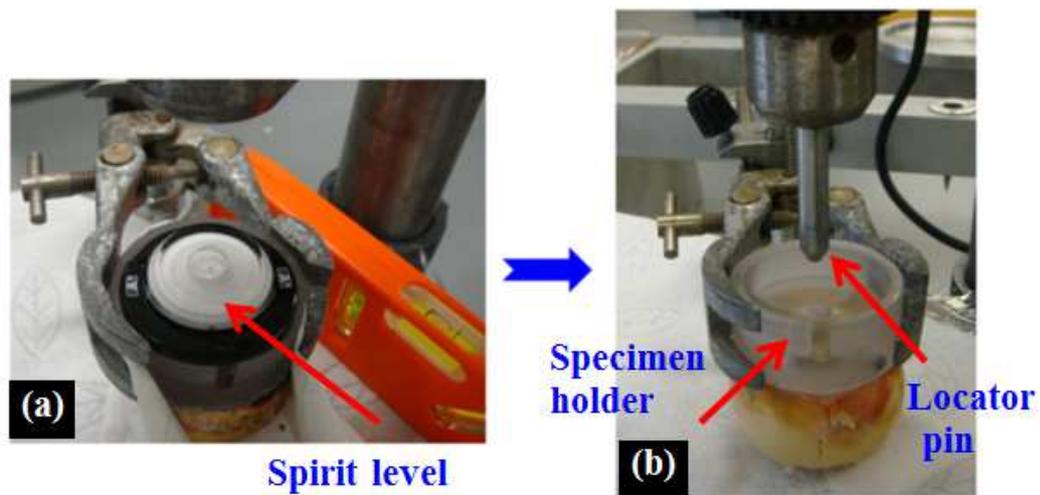
Figure 5.8: Photographs illustrating the alignment and positioning checks prior to pilot hole drilling. (a) A spirit level placed on top of the bone-specimen holder construct ensured that the bone surface was at level (not tilted) position with respect to the drill bit. This enabled drilling of the pilot hole into bone in axial direction. (b) A locator pin attached to the bench-top drill press was moved up and down, passing through the centre hole of the specimen holder to check that the locator pin was not touching any sides of the specimen holder's centre hole. This was to ensure no obstruction for the drill bit during drilling of pilot hole, preventing errors which might affect the measurement of insertion torque and pullout force.
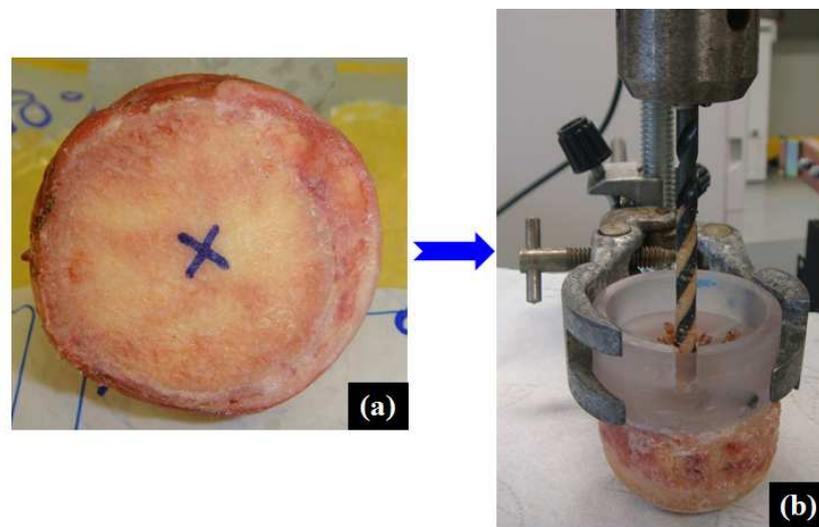
Figure 5.9: Photographs of the pilot hole drilling process, showing (a) the point of screw insertion, marked with an "X" at the centre of the femoral head specimen by a blue marker, and (b) drilling of pilot hole using 5.2 mm drill bit to the depth of 23.5 mm.

5.1.9 Manual Screw Placement into Pilot Hole

A partially-threaded cancellous screw was placed into the predrilled pilot hole in each specimen with the aid of a drill press and driver bit to a point approximately 2 to 3 mm between the screw head and washer (Figure 5.10). Further insertion and tightening of the screw was performed with the aid of a micro-mechanical test that had it affixed inside the micro-CT scanner.
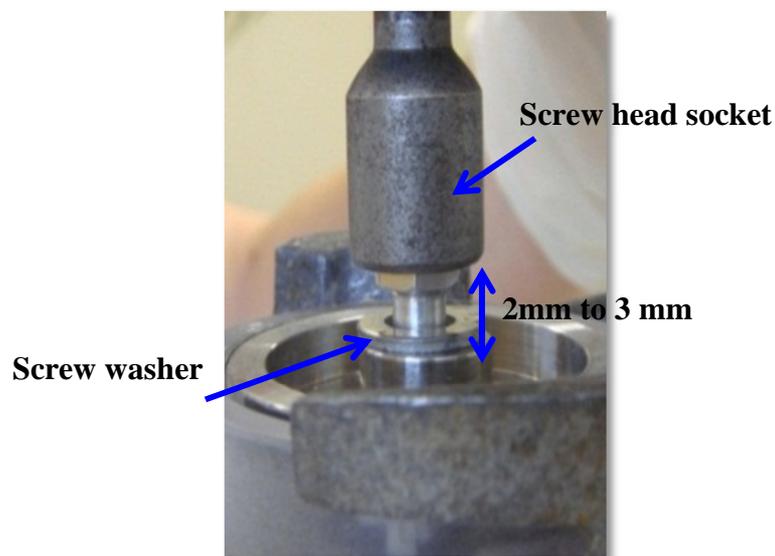
Figure 5.10: The photograph illustrates the initial insertion of the partially-threaded cancellous screw about 2 to 3 mm before reaching head contact.

5.1.10 Micro-Mechanical Test Device

A micro-mechanical test device (Figure 5.11) was used for an automated screw insertion inside a micro-CT scanner. The micro-mechanical test device was designed and built for a previous study performed by our group (Reynolds et al., 2013), using material that is compatible with the micro-CT scanner to avoid artefacts in the images of the bone-screw construct. The test device is small in size (50 mm in diameter) and can fit within the confined space of the micro-CT scanner. The device is able to perform the process of screw insertion inside the

micro-CT scanner, and the process is controlled via an in-house designed control system controlling the motor.

The micro-mechanical test device accommodates several components within it, including: a compression load cell (THB-250-S, Temecula, California, USA); torque transducer (TRT-100, Transducer Techniques, Temecula, California, USA); a digital-signal-processor-based motor and motor controller with rotary encoder (Part No. 315360, Maxon Motor Ag, Sachseln, Switzerland); a data transfer socket to/from the computer that is linked to a USB carrier (NI USB-9162, National Instruments, Austin, Texas, USA) placed outside the micro-CT scanner.
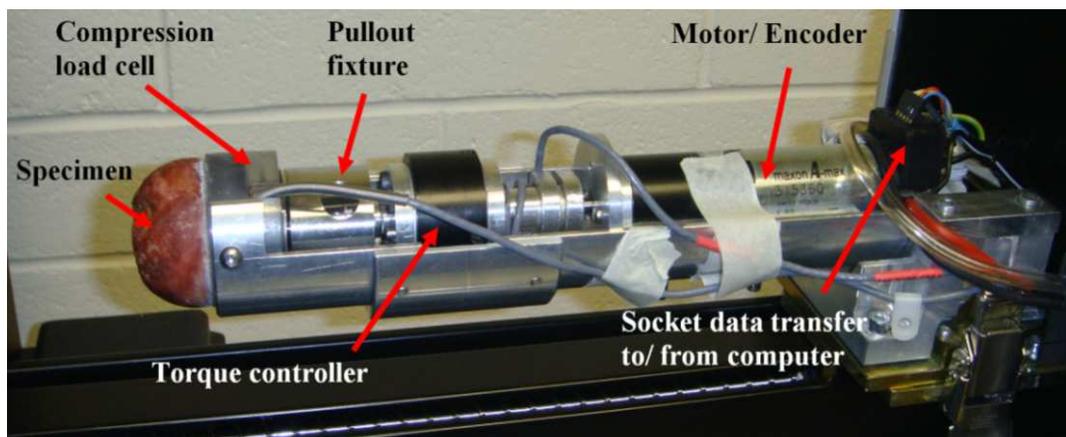
Figure 5.11: A software drive micro-mechanical test device, which is fitted within the micro-CT scanner ready to perform screw insertion automatically inside a micro-CT scanner.

Data from the torque transducer, compression load transducer, and rotary encoder captured at a sampling rate of 500 Hz during screw insertion (Figure 5.12) are transferred via a USB carrier to a laptop placed outside a micro-CT scanner where

they are downloadable in a common file format (CSV), which can be easily converted to the Microsoft Excel file format (.xlsx) for analysis.
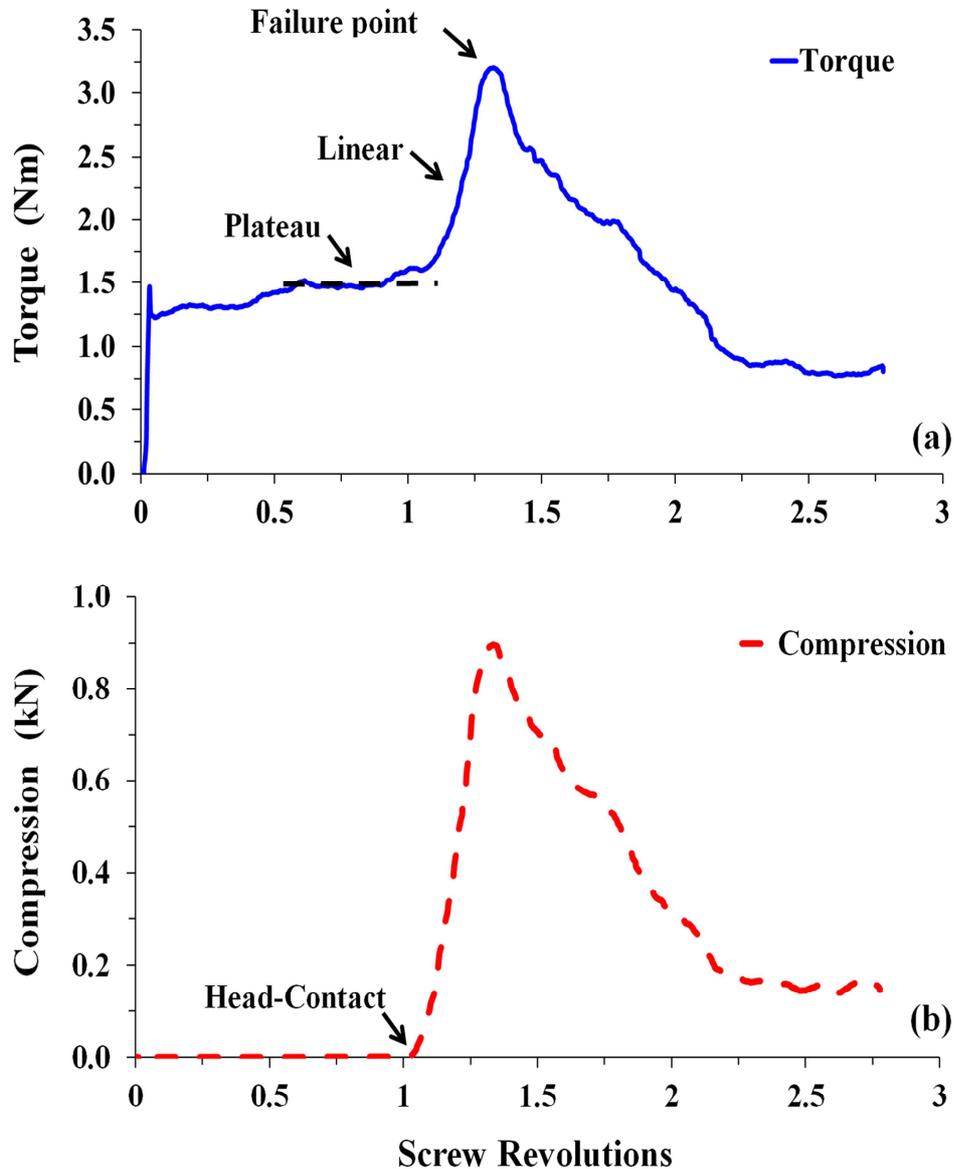
Figure 5.12: A. example of screw insertion profile to bone failure measured by the micro-mechanical test device automatically via its operating software: (a) torque vs. screw revolution (b) compression vs. screw revolution. One screw revolution corresponds to a full screw rotation over an angle of 360°. Screw head contact occurs once compression under the screw head exceeds the value of 2N. The profile has three distinct regimes: Plateau, which indicates progression of the screw thread purchase in the bone prior to head contact; Linear, which indicates that bone exhibits elastic behaviour; and Failure point, which indicates the point of bone failure where screw stripping occurs.

The 12 V DC motor/ gearbox is used to drive the cancellous bone screw into the bone. It is controlled by a digital-signal-processor-based motor controller, and software program (µCT Scanner Application, version 2.0vi) developed in-house, running on a laptop. The software was designed to enable screw insertions to be controlled either via "Torque Control," "Rotation Control," or "Position Control" modes. It displays and records the progressions of screw insertion torque and compression profiles in real time while the screw insertion is in progress as shown in Figure 5.13.
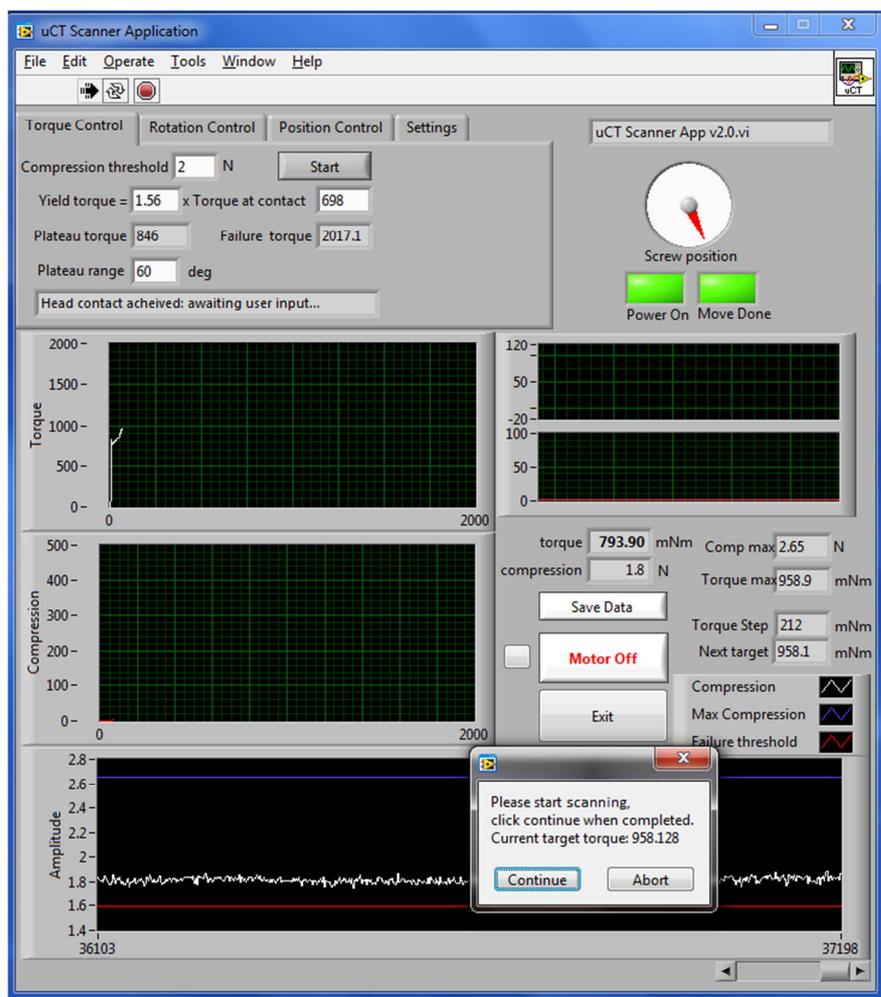
Figure 5.13: A screen shot of the micro-mechanical test device software captured at screw head contact, indicating "head contact achieved" and prompts to start micro-CT scanning. It also shows the screw insertion profile at screw head contact.

5.1.11 Automated Screw Insertion to Head Contact

For the purpose of this study, which was to correlate $T_{plateau}$ with aBMD and microarchitectural parameters, it was necessary for the control program to identify head contact, measure $T_{plateau}$, and cease tightening at head contact to allow a micro-CT scan to be performed at this point.

Once transferred from the drill press, the bone-screw construct was mounted onto the micro-mechanical test device (Figure 5.14). The head of the screw was then slotted into the screw head socket that is attached to the torque transducer of the test device.
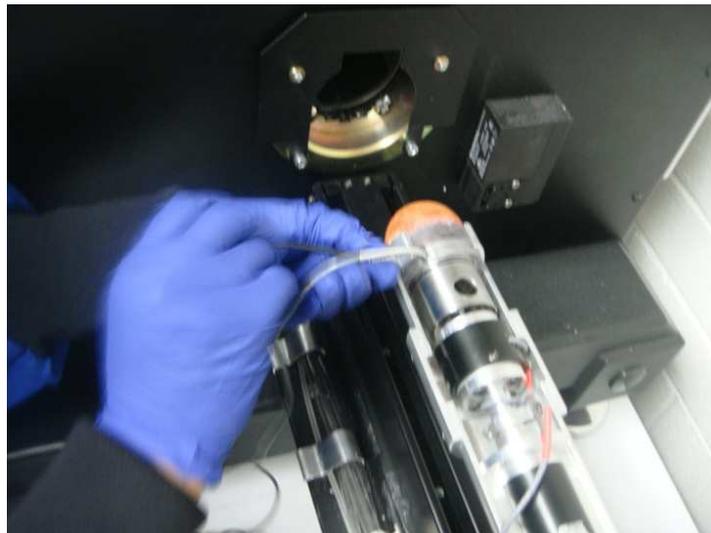
Figure 5.14: Mounting a specimen onto the micro-mechanical test device for an automated screw insertion inside a micro-CT scanner.

"Torque Control" mode was selected with compression threshold set to 2 N via a laptop. Then, "Start" button on the software was clicked to activate the micro-mechanical test device to commence screw insertion until head contact (Figure 5.15).

Screw head contact was defined as the point at which compression between the screw head and bone exceeded 2 N (Figure 5.12 [b] and 5.15 [b]), as measured by the compression load cell. At this point, the motor was stopped automatically by the control program, and $T_{Plateau}$ computed, based on the average of twenty torque data points measured at frequency of 500 Hz prior to head contact within the plateau region, as shown in the screw insertion profile (Figure 5.12 [a] and 5.15 [a]).
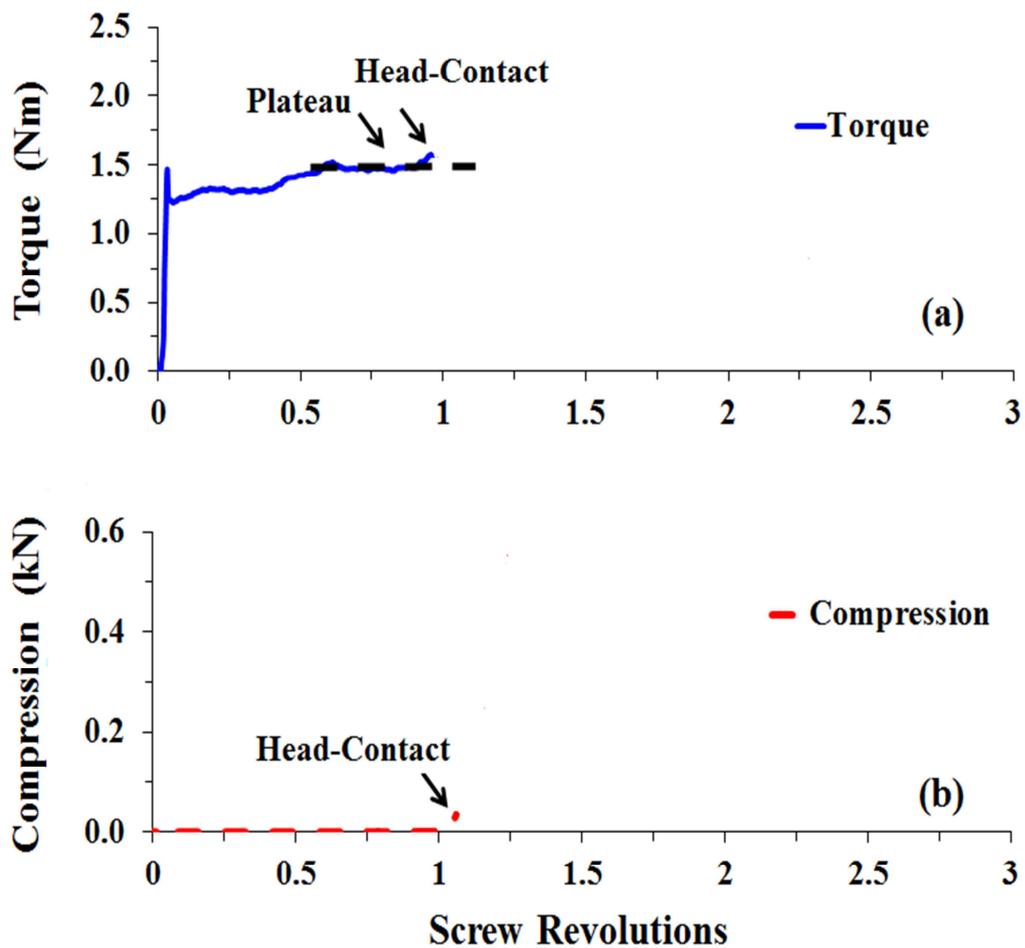
Figure 5.15: Screw insertion profiles: (a) torque vs. screw revolution, showing plateau torque ($T_{Plateau}$) prior to screw head contact, and (b) compression vs. screw revolution, showing compression force at head contact. The screw head contact was defined when the compression between the screw and bone achieved 2N.

At this point, the software prompted messages of "Head contact achieved" and "Please start scanning". Subsequently, the micro-CT scans on the bone-screw construct were performed.

5.1.12   Micro-computed Tomography (Micro-CT) Scanning – Acquiring Micro-CT Images of Bone-screw Construct

The micro-CT scanner used was a Skyscan model 1076, Skyscan, Kontich, Belgium) (Figure 5.16). The scanning protocol selected was; 17.3 µm isotropic pixel size, 35 x 35 mm (2024 x 2024 pixels) field of view, x-ray source voltage 100 kVp, current 80 µA, rotation step 0.4°, four frames averaging, rotation over 180°, using a 1.0 mm-thick aluminium filter for beam-hardening effect reduction, integration time of 885 ms (Perilli et al., 2012).

Figure 5.16:   The high resolution micro-computed tomography (micro-CT) scanner (Skyscan model 1076, Skyscan, Kontich, Belgium) that was used in this study. It has capability for in vivo and ex vivo scanning of small animals and bone specimens.

Other scanning protocols were previously tested using four other combinations of settings of exposure time, voltage, rotation step, filter, and frame averaging, however selected protocol provided the best compromise between noise and contrast. Refer to Appendix A1 for details.

5.1.13   Micro-CT Image Processing

The acquired projection images of the bone-screw constructs (Figure 5.17[a]) from the micro-CT scanner underwent three stages of image processing prior to morphometric analysis; cross-section image reconstruction, volume of interest (VOI) creation, and VOI image binarisation (segmentation).

Cross-section Image Reconstruction

Cross-sectional images, each 35 x 35 mm in size (2024 x 2024 pixels), and centred over the inserted screw, were reconstructed (NRecon software, version 1.6.6.0, Skyscan, Kontich, Belgium) and saved as 256 grey-level images (bitmap format files, 8 bit). For each femoral head, a stack of 900 cross-section slices, corresponding to a total height of 15.6mm, was reconstructed with slice thickness of 1 pixel (17.3 µm) (Figure 5.17[b]). Refer to Appendix A2 for detailed reconstruction protocols.

Volume of Interest (VOI) Selection

A ring-like region of interest (ROI), centered over the screw and consisting of two concentric circles, with outer diameter ($D_1 = 14$ mm) and inner diameter ($D_2 = 7.5$ mm) respectively, was first created to define the region of interest for bone morphology analysis (Figure 5.18 [top]) (software CT Analyser version 1.11,

Skyscan Bruker). Refer to Appendix A3 for the detailed creation of the ROI or

mask template.
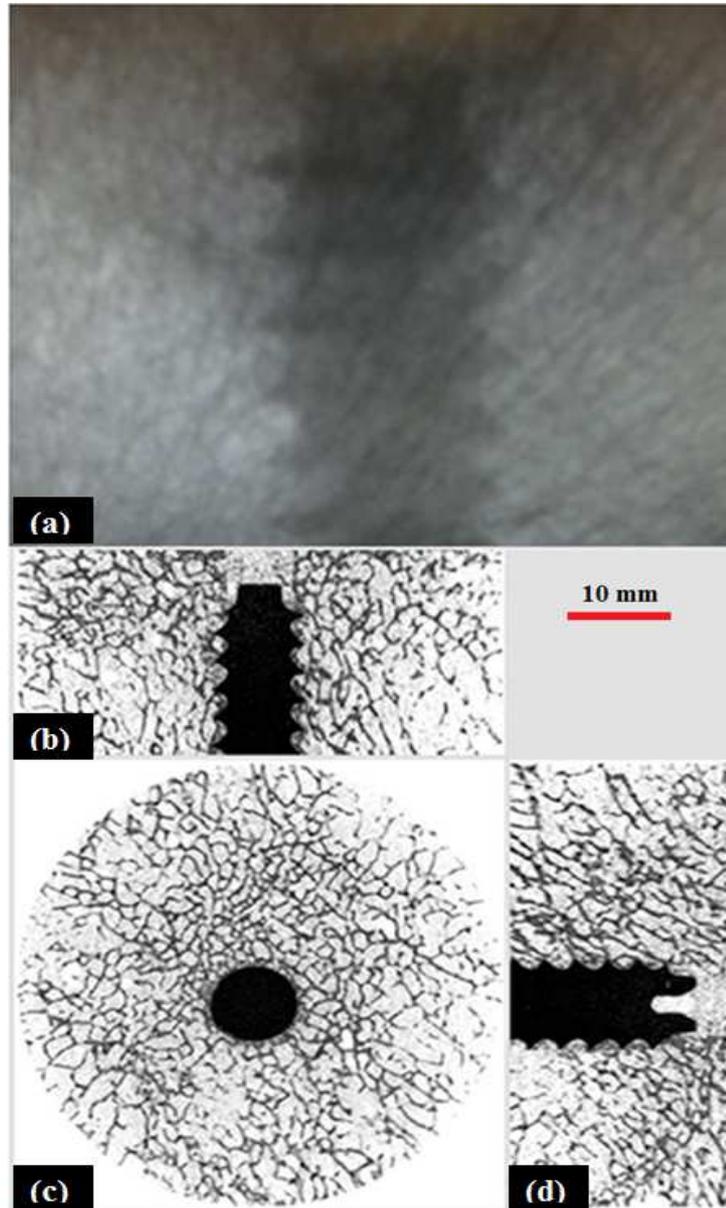
Figure 5.17: Micro-CT images of the bone-screw construct: (a) X-ray projection of the bone-screw construct. (b-d) Corresponding reconstructed cross-section images, (b) coronal view, (c) transaxial view (d) sagittal view. Images are at 17 μm pixel size.

The ROI's inner diameter (D_2 = 7.5 mm) was slightly bigger than the cancellous screw diameter (7.0 mm) to exclude bone debris adjacent to the screw produced during screw insertion. The ROI outer diameter (D_1 = 14 mm) was twice the screw diameter, since the trabecular structure within this proximity to the screw could be significantly strained during a screw push-in testing (Mueller et al., 2013; Wirth et al., 2011).

The ring-like ROI was placed centred on the screw cross-section images at three different heights along the screw (in a top, middle, and bottom slice), and interpolated over the entire stack of 694 slices (height = 12 mm) (Figure 5.18). This way a cylindrical VOI was created and saved, consisting of a trabecular bone annulus of height 12 mm, outer diameter 14 mm and inner diameter 7.5 mm (annulus thickness = 3.25 mm).

Binarisation and Three-Dimensional (3-D) Model

The binarisation (or segmentation) of the selected VOIs was performed using CTAnalyser software (version 1.11, Skyscan, Kontich, Belgium). A global three-dimensional Otsu thresholding algorithm was used for segmenting bone as a solid and removing the background consisting of air and marrow (bone minimum values: average [SD]: 65[4.5], maximum value = 255) (Otsu, 1987; Parkinson et al., 2008). Upon binarisation, the VOIs were transformed into 3D models via CTAnalyser software for morphological analysis of trabecular bone micro-architectural parameters (Figure 5.18). Refer to Appendix A4 for the detail of binarisation of the VOI.
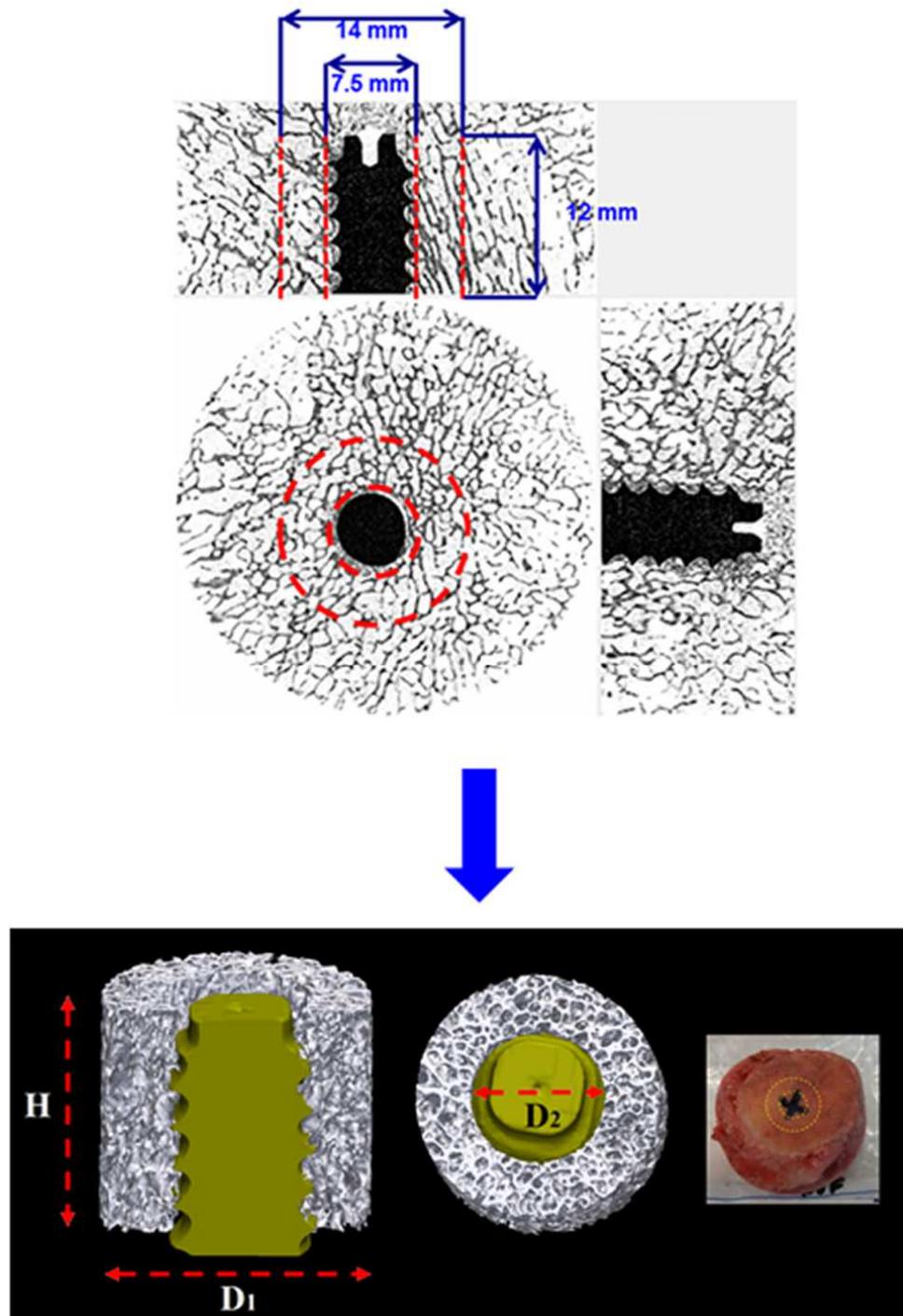
Figure 5.18: Top: Micro-CT images, process of extracting an annular volume of interest (VOI) from the stack of two-dimensional reconstructed images of the bone-screw construct. Bottom: 3D rendering of the annular VOI of trabecular bone surrounding the screw (left images), obtained from micro-CT images of the specimen (right image), over which morphometric parameters were quantified. H (12 mm) is the height of the VOI; D_1 (14 mm), outer diameter of the VOI; D_2 (7.5 mm), inner diameter of the VOI.

5.1.14 Bone Morphology Analysis

Morphological analysis was performed using CT Analyser software over the VOI of micro-CT images to calculate the following micro-architecture parameters of trabecular bones surrounding the screw:

- BV/TV (%)

- SMI

- Tb.Th (µm)

- Tb.Sp (µm)

- Tb.N (mm^{-1})

- BS/TV (mm^{-1})

5.1.15 Statistical Analysis

IBM SPSS Statistics software, version 20 was utilised for the statistical analyses. All data distributions were tested for assumptions of normality (Shapiro-Wilks test), homogeneity of variance (Levene's test), linearity and homoscedasticity (scatter plot of residuals).

Descriptive statistics were used to summarise the bone parameters measured from DXA (aBMD) and micro-CT (micro-architectural parameters), and the mechanical parameter $T_{Plateau}$. Pearson's correlation coefficient (R) was used to evaluate the associations between $T_{Plateau}$, aBMD and the micro-architectural parameters.

Pearson's correlation coefficient was also used to evaluate the interrelationships between aBMD and the measured micro-architectural parameters, and the interrelationships among the micro-architectural parameters themselves. Correlation coefficients of $|R| \geq 0.68$ were interpreted empirically as strong, those of $0.36 \leq |R| \leq 0.67$ as medium, and $|R| \leq 0.35$ as weak (Taylor, 1990).

Stepwise forward multiple regression analysis was performed to evaluate whether a combination of aBMD and micro-architectural parameters would improve the prediction of $T_{Plateau}$ beyond the regressions with single parameters. The significance level of all the tests was set to $p = 0.05$.

5.2   Results

5.2.1 Biomechanical Testing and Imaging

Of the 52 femoral heads, 46 (17 females, 29 males, mean [SD] age = 78.2 [9.6]) successfully underwent DXA scanning, micro-CT scanning and biomechanical testing. Six femoral heads did not complete the study due to technical errors encountered during specimen preparation (such as premature setting of adhesive that caused specimens to break away from the sample holder of the automated micro-mechanical test device), and were excluded from the analysis. Refer to Appendix A5 for detailed results performed on the femoral head specimens.

Table 5.1: Summary of aBMD obtained by DXA, micro-architectural parameters obtained by micro-CT, and $T_{Plateau}$ measured by the micro-mechanical test device, over the femoral heads (n = 46).

		Mean (SD)	Min-Max
DXA:			
aBMD	(g/cm^2)	0.8 (0.2)	0.5 - 1.2
MicroCT:			
BV/TV	(%)	29 (5)	17 - 42
SMI	-	0.9 (0.4)	-0.12 - 1.7
BS/TV	(mm^{-1})	4.5 (0.7)	2.9 - 5.9
Tb.Th	(μm)	235 (21)	184 - 285
Tb.Sp	(μm)	631 (112)	444 - 949
Tb.N	(mm^{-1})	1.2 (0.2)	0.8 - 1.7
In-vitro screw insertion:			
$T_{Plateau}$	(Nm)	1.1 (0.4)	0.4 - 1.9

Table 5.1 presents a summary of the values measured by DXA (aBMD), micro-CT (micro-architectural parameters), and biomechanical testing ($T_{Plateau}$). In all of the measured parameters, the tests for assumptions of normality, homogeneity of variance, linearity and homoscedasticity, revealed no violations (p > 0.05 for all the tests).

5.2.2 Correlation between $T_{Plateau}$, aBMD and Micro-architectural Parameters

$T_{Plateau}$ exhibited significant correlations with aBMD, as well as with each of the investigated micro-architectural parameters (Table 5.2). $T_{Plateau}$ showed the strongest correlation with SMI (R = - 0.82, p < 0.001), followed by BV/TV (R =

0.80, p < 0.01) and aBMD (R = 0.76, p < 0.01) (Table 5.2 and Figure 5.19). $T_{Plateau}$ exhibited moderate but significant correlations with the remaining micro-architectural parameters (BS/TV, Tb.Th, Tb.Sp, and Tb.N, with |R| ranging from 0.38 to 0.48) (Figure 5.20).

Table 5.2: Summary of correlation coefficient (R), coefficient of determination (R^2), and p-value, of $T_{Plateau}$ vs. aBMD and micro-architectural (n = 46).

	R	R^2	p-value
$T_{Plateau}$ vs. aBMD	0.76	0.58	p<0.01
$T_{Plateau}$ vs. BV/TV	0.80	0.64	p<0.01
$T_{Plateau}$ vs. SMI	-0.82	0.67	p<0.001
$T_{Plateau}$ vs. BS/TV	0.43	0.18	p<0.05
$T_{Plateau}$ vs. Tb.Th	0.48	0.23	p<0.05
$T_{Plateau}$ vs. Tb.Sp	-0.48	0.23	p<0.05
$T_{Plateau}$ vs. Tb.N	0.38	0.14	p<0.05

$$y = 0.07x - 0.85$$
$$R^2 = 0.64$$
$$p < 0.01$$

(b)

$$y = 2.16x - 0.65$$
$$R^2 = 0.58$$
$$P < 0.001$$

(c)
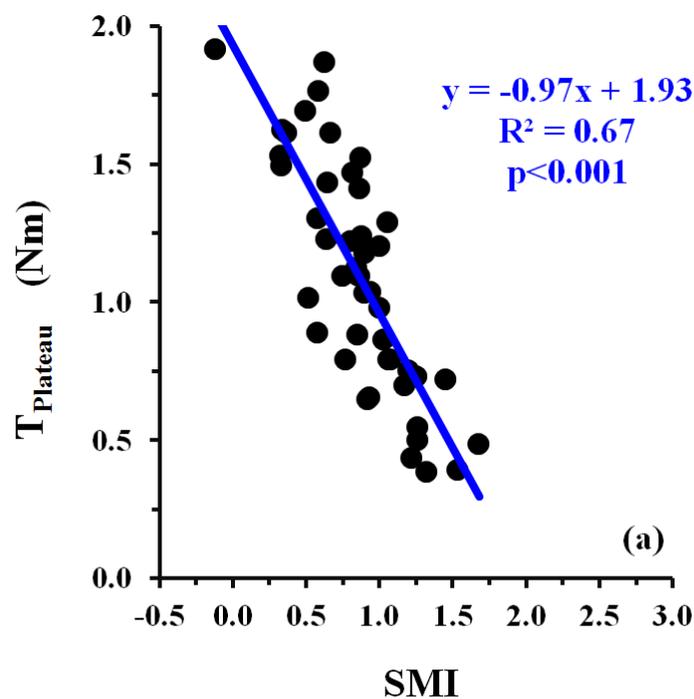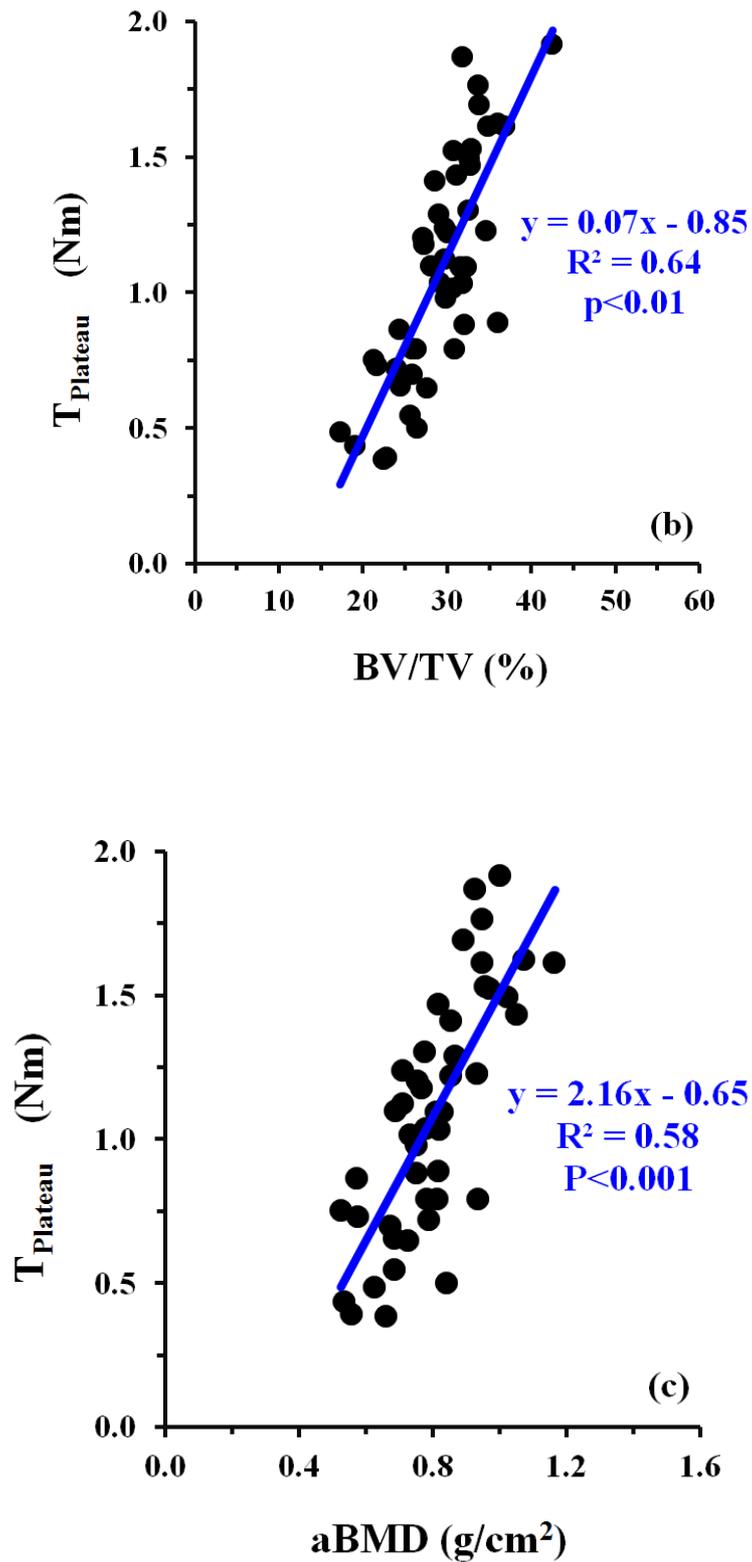
Figure 5.19: Scatter plots and best-fit line of the linear regression between $T_{Plateau}$ versus SMI, BV/TV and aBMD (a, b, and c, respectively).

(a) Scatter plot of $T_{Plateau}$ (Nm) versus BS/TV (mm^{-1}) with regression line:
$$y = 0.25x - 0.06$$
$$R^2 = 0.18$$
$$p < 0.01$$

(b) Scatter plot of $T_{Plateau}$ (Nm) versus Tb.N (mm^{-1}) with regression line:
$$y = 0.78x + 0.11$$
$$R^2 = 0.14$$
$$p < 0.01$$
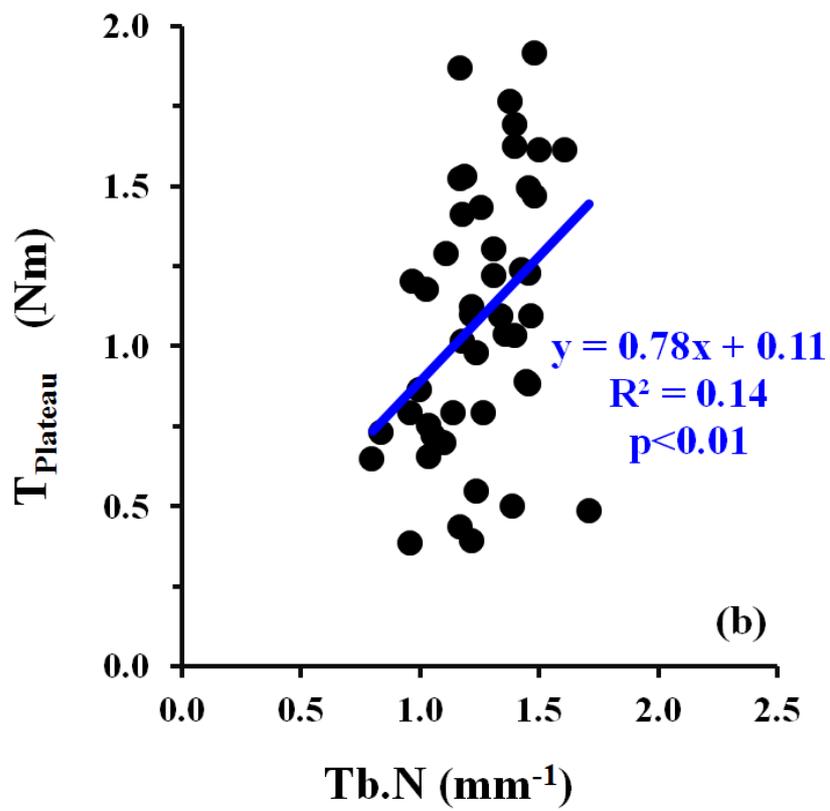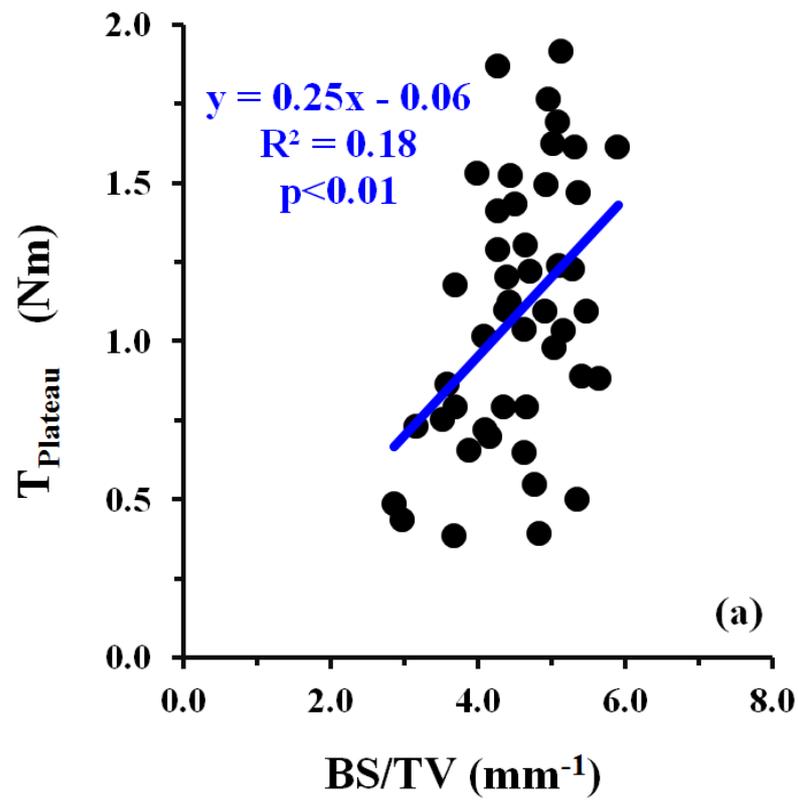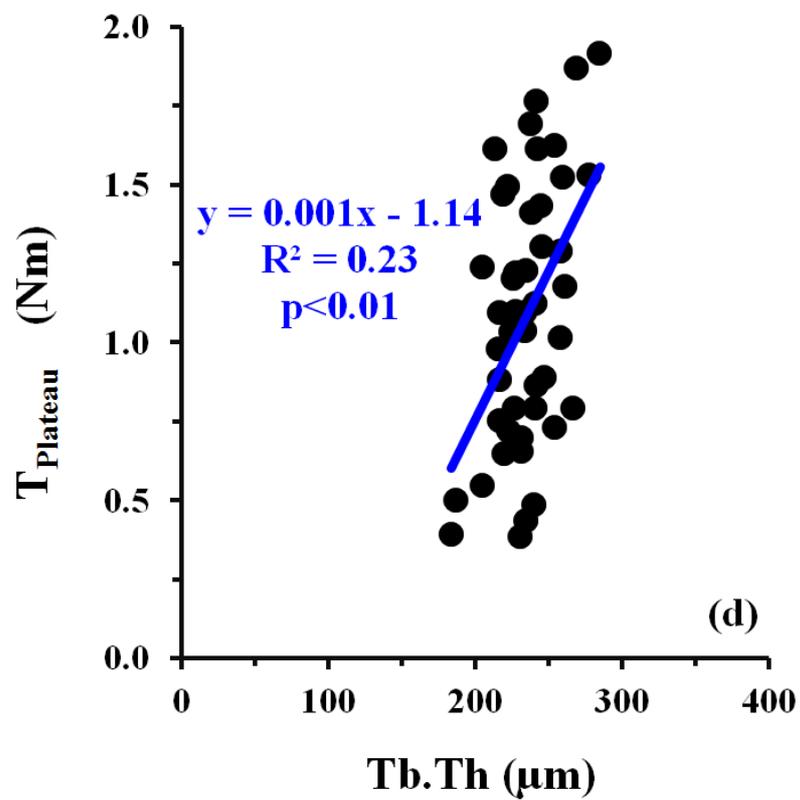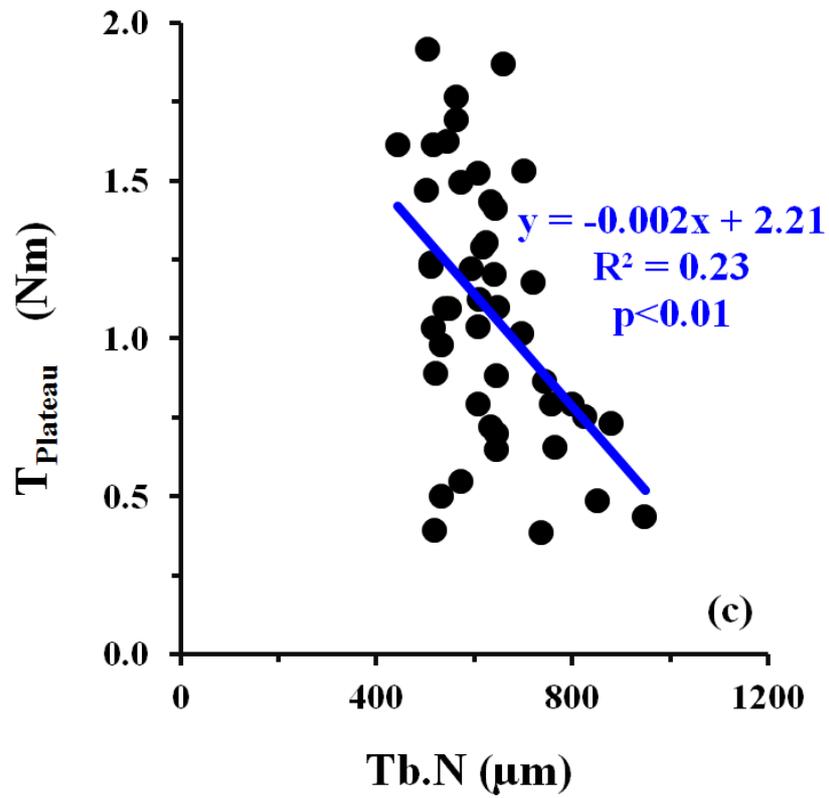
Figure 5.20: Scatter plots and best-fit line of the linear regression between $T_{Plateau}$ versus BS/TV, Tb.N, Tb.Sp and Tb.Th (a, b, c, and d, respectively).

5.2.3 Inter-correlation Between aBMD and Micro-architectural Parameters, and Among Micro-architectural Parameters

The inter-correlations between aBMD and the examined micro-architectural parameters were all significant ($p < 0.05$ for all comparisons) except between "Tb.Sp vs. Tb.Th" and "Tb.N vs. Tb.Th" (Table 5.3). aBMD exhibited the strongest correlation with BV/TV ($R = 0.80$, $p < 0.001$), followed by SMI ($R = -0.74$, $p < 0.001$), and moderate correlations with BS/TV ($R = 0.55$), Tb.Th ($R = 0.36$), Tb.Sp ($R = -0.57$) and Tb.N ($R = 0.44$).

Table 5.3: Correlation coefficient (R) between aBMD measured by DXA and micro-architectural parameters by micro-CT.

	aBMD	BV/TV	SMI	BS/TV	Tb.Th	Tb.Sp
BV/TV	0.80***	-				
SMI	-0.74***	-0.90***	-			
BS/TV	0.55***	0.77***	-0.50***	-		
Tb.Th	0.36*	0.31*	-0.50***	-0.34*	-	
Tb.Sp	0.57***	0.74***	0.45**	-0.92***	0.27	-
Tb.N	0.44**	0.52***	-0.37*	0.61***	-0.15	-0.57***

*** $p<0.001$, ** $p<0.01$, * $p<0.05$

Among the micro-architectural parameters, BV/TV exhibited the strongest correlation with SMI ($R = -0.90$, $p < 0.001$), followed by BS/TV ($R = 0.77$, $p < 0.001$) and Tb.Sp ($R = 0.74$, $p < 0.001$), and moderate correlations with Tb.N ($R = 0.52$) and Tb.Th ($R = 0.31$) (Table 5.3). The parameter SMI, apart from the strong correlation with BV/TV ($R= -0.90$), exhibited moderate correlations with the remaining micro-architectural parameters, respectively, BS/TV ($R = -0.55$),

Tb.Th (R = - 0.50), Tb.Sp (R = 0.45) and Tb.N (R = - 0.37). Among the other

inter-correlations, a strong correlation between BS/TV and Tb.Sp was found (R =

- 0.92, p < 0.001).

5.2.4 Stepwise Forward Regression Analysis: $T_{Plateau}$ vs. aBMD and Micro-architectural Parameters

Stepwise forward regression analysis revealed an increase for the prediction of

$T_{Plateau}$ when micro-architecture was combined with aBMD. In particular "$T_{Plateau}$

vs. SMI + aBMD" (R^2 = 0.72) and "$T_{Plateau}$ vs. BV/TV + BS/TV + aBMD" (R^2 =

0.74) showed an increase in prediction, compared to the single regressions

"$T_{Plateau}$ vs. SMI" (R^2 = 0.67), "$T_{Plateau}$ vs. BV/TV" (R^2 = 0.64) or "$T_{Plateau}$ vs.

aBMD" R^2 = 0.58) (Table 5.2 compared to Table 5.4). Including the other

parameters into the analysis did not increase the prediction of $T_{Plateau}$ beyond the

single regression model; hence these parameters were removed from the analysis.

Table 5.4: Summary of stepwise regression analysis, with $T_{Plateau}$ as dependent variable, and aBMD and micro-architectural parameters as independent variables. The R^2 increased, compared to the single regression model (Table 5.2).

	R^2	p
$T_{Plateau}$ vs. SMI + aBMD	0.72	p<0.001
$T_{Plateau}$ vs. BV/TV + BS/TV + aBMD	0.74	p<0.001

5.3   Discussion

This study investigated whether $T_{Plateau}$, a strong predictor of failure torque (Reynolds et al., 2013), depends on aBMD and/or micro-architecture in bone from the human femoral head. To the best of our knowledge, this is the first study that relates the $T_{Plateau}$ measured experimentally during screw insertion to aBMD and micro-architectural measurements in human trabecular bone.

$T_{Plateau}$ exhibited significant correlations with all the examined bone parameters, the strongest correlations being with SMI, followed by BV/TV and aBMD. The remaining correlations, between $T_{Plateau}$ and BS/TV, Tb.Th, Tb.Sp and Tb.N, were moderate which suggests that variations in those parameters were not as influential. Furthermore, stepwise forward regression analysis showed that by combining aBMD with micro-architecture, there was an increase in $T_{Plateau}$ prediction, i.e., aBMD combined with SMI (R^2 increased from 0.58 to 0.72) and aBMD combined with BV/TV and BS/TV (R^2 increased from 0.58 to 0.74), compared to the models with single parameters (Table 5.2 compared to Table 5.4).

Strong inter-correlations between aBMD and micro-architectural parameters (Table 5.3) indicated that aBMD, a sole measurement for bone strength in clinics, can be a good surrogate parameter for bone micro-architecture in predicting bone strength. At present, measuring patient's bone micro-architecture in clinics is still hampered by limitations in medical imaging technology. Additionally, a strong inter-correlation between SMI and BV/TV also prompted collinearity problems if

SMI and BV/TV were paired in the stepwise multiple regression models (Table 5.4). Thus, two models were formed: model 1, comprised of SMI, aBMD and other micro-architectural parameters as predictor variables, while model 2, comprised of BV/TV, aBMD and other micro-architectural parameters.

The findings of SMI, BV/TV and aBMD having the strongest correlations with $T_{Plateau}$ during screw insertion, and the signs of the respective correlation coefficients, are in line with findings from screw pullout-testing or compressive testing of bone reported in the literature, where specimens exhibiting plate-like structure and high density (BV/TV or aBMD) exhibit higher pull-out strength (Poukalova et al., 2010; Yakacki et al., 2010) or higher compressive failure load than specimens with rod-like structure, low BV/TV and low aBMD (Gibson, 2005a; Karim and Vashishth, 2011; Perilli et al., 2008). Moreover, the finding that the combination of aBMD and micro-architectural parameters in a regression model exhibits an increase in prediction of $T_{Plateau}$ is also consistent with findings on the prediction of failure load in compressive testing of trabecular bone reported in the literature (Majumdar et al., 1998; Mittra et al., 2005; Roux et al., 2013; Wegrzyn et al., 2010).

Overall, these findings suggest that specimens characterized by a higher bone volume fraction and a more plate-like structure, likely offer a structural environment in which the screw threads have to cut into more material, which leads to an increased $T_{Plateau}$ as illustrated in Figure 5.21. As a result, this type of bone structure might offer an environment for increased maximum or failure

torque given the previous findings that $T_{Plateau}$ was directly proportional to the maximum torque (Reynolds et al., 2013).
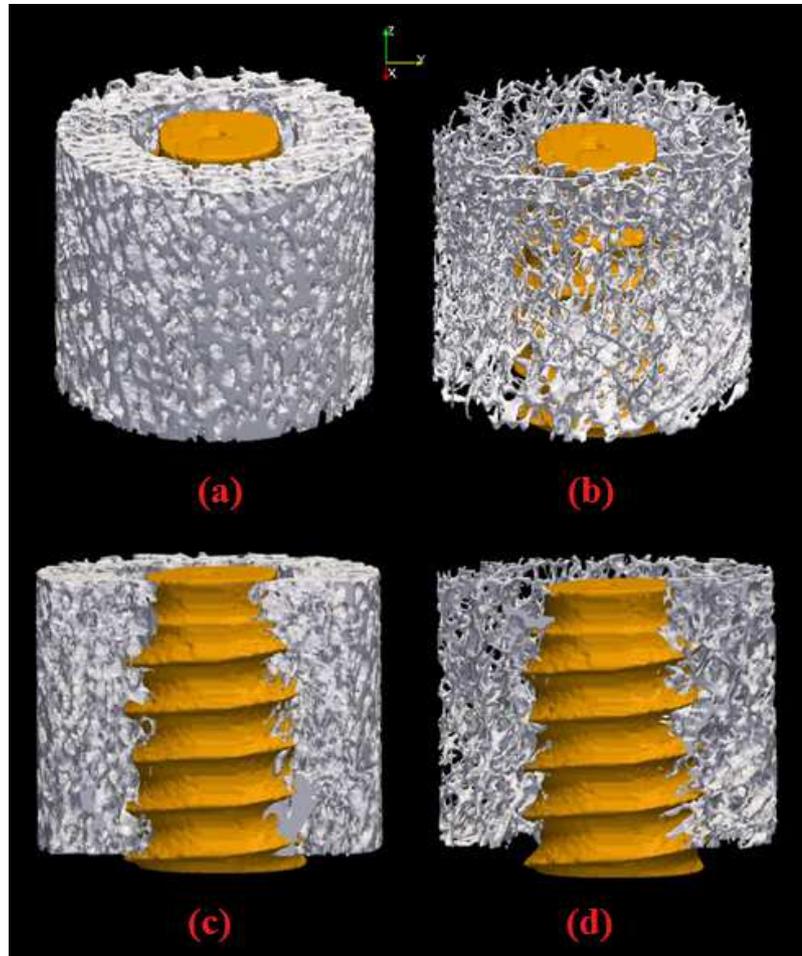
Figure 5.21: 3-D rendering of bone-screw constructs developed from micro-CT images using ParaView software (Sandia Corporation, Kitware Inc), visualising the trabecular bone (grey) and cancellous screw (orange) constructs:

(a) bone-screw construct showing trabecular bone of mostly plate-like structure (SMI = 0.33) and high bone volume fraction (BV/TV = 32.69%) and density (aBMD = 102.30 g/cm^2) . The screw is embedded within the bone.

(b) bone-screw construct showing trabecular bone of mostly rod-like structure (SMI = 1.68), low BV/TV (17.26%) and aBMD (62.60 g/cm^2).

(c, d) cuts through the bone of (a), (b), respectively, performed in inferior-superior direction. The screw has been left complete.

A limitation of the present study is that the bones used were taken from only one anatomic location, i.e., femoral head. Bone mechanical properties differ among anatomic locations (Goldstein, 1987; Helgason et al., 2008; Keaveny et al., 2001). Further research is required to investigate the effect of anatomic locations on $T_{Plateau}$. Another limitation is that the measurement of aBMD from DXA was done on excised specimens in vitro and did not account for the surrounding tissue variability among different patients. Hence, the measurements of aBMD represent rather a best-case scenario. Further studies are needed to explore aBMD from DXA on cadavers to account for this variability. Nonetheless, a strong relationship was found between $T_{Plateau}$ and aBMD measurements obtained with a device (DXA) commonly used in clinics.

5.4   Conclusion

In conclusion, our study indicates that $T_{Plateau}$, shown previously to be a strong predictor for bone failure torque (T_{Max}) during screw insertion, is significantly dependent on micro-architecture, particularly SMI and BV/TV, followed by aBMD. This implies that bone with a more plate-like structure and high bone amount produces higher $T_{Plateau}$ at screw head contact compared to bone composed of a more rod-like structure (or less plate-like structures) and lower bone volume. Overall, the study demonstrates that $T_{Plateau}$ detected from the screw insertion profile in human trabecular bone of the femoral head is directly related to bone quality, particularly micro-architecture and aBMD.

Chapter VI

Study 2: Does the Pullout Strength of Cancellous Screws in Human Femoral Heads Depend on Applied Insertion Torque, Trabecular Bone Micro-architecture and/or Areal Bone Mineral Density?

This chapter describes the experimental study performed to address the second aim of the thesis, that is, to determine whether the pullout strength ($F_{Pullout}$) of cancellous screws in femoral heads depends on applied insertion torque (T_{Insert}), trabecular bone micro-architecture and/or aBMD.

The results reported in this chapter have been published in *Journal of Mechanical Behavior of Biomedical Materials*: Ab-Lazid, R, Perilli, E, Ryan MK, Costi JJ, Reynolds KJ, 2014, "Pullout strength of cancellous screws in human femoral heads depends on applied insertion torque, trabecular bone micro-architecture and areal bone mineral density." *J Mech Behav Biomed Mater*. 2014 Dec; 40: 354-61. doi: 10.1016/j .jmbbm,.2014.09.009. Epub 2014 Sep 16. The published paper was rewritten for this thesis.

6.0   Introduction

Despite the body of published scientific literature, it is still unknown whether higher T_{Insert} values applied during cancellous screw insertion correspond with higher pullout strength values — that is, whether tightening indeed improves the

mechanical stability of the bone-screw construct, nor how this relates to the quality of the underlying bone with respect to bone's micro-architecture and density.

As described in chapters 2 and 3, variations in bone quality including mechanical properties, mineral density, and micro-architecture exist between patients and within patients (Bouxsein, 2003; Hernandez and Keaveny, 2006; Keaveny et al., 2001; Perilli et al., 2008; van der Meulen et al., 2001; van Rietbergen et al., 2002) and it was suggested that these variations influence the stability of the bone-screw construct during pullout and push-in testing in the laboratory (Mueller et al., 2013; Poukalova et al., 2010; Ruffoni et al., 2012; Yakacki et al., 2010) along with other factors relating to screw geometry, material, size, and insertion technique (e.g., tapping versus non-tapping and size of pilot hole) (Battula et al., 2006; Frandsen et al., 1984; Johnson et al., 2004; Muller et al., 1992; Oktenoglu et al., 2001; Ramaswamy et al., 2010; Seller et al., 2007; Tingart et al., 2006). However, the influence of T_{Insert} on $F_{Pullout}$ was not examined in those studies. In fact, in a recent study performed in the diaphysis of human humeri, the authors concluded that the relationship between applied screw insertion torque and pullout strength still remains undetermined (Tankard et al., 2013).

Furthermore, previous investigations have led to inconsistent conclusions, particularly, regarding the order of importance between aBMD and the applied insertion torque (T_{Insert}) in predicting $F_{Pullout}$ (Reitman et al., 2004; Ryken et al., 1995) (see sub-chapter 3.10). Those studies also did not investigate the effect of micro-architecture (another subset of bone quality) on $F_{Pullout}$. Even more so, the

values of the applied T_{Insert} used in the correlation with $F_{Pullout}$ were not clearly described. Reitman and colleagues described their applied T_{Insert} as based on a surgeon's perception of an "optimal" tightening torque (Reitman et al., 2004). Ryken and colleagues on the other hand, described their applied T_{Insert} as based on the clinician's perception of the utmost tightening before stripping (Ryken et al., 1995). It can be speculated that the applied T_{Insert} used in those studies could have been of different magnitude (whether in absolute or % T_{Max} values) and this might explain their inconsistent findings on the order of importance between aBMD and T_{Insert} in predicting $F_{Pullout}$. Also, those studies evaluated the $F_{Pullout}$ using unicortical and bicortical screws in human cervical spines, which might not apply to cancellous screws and to other anatomical sites, such as human femoral heads.

Previous studies as described in sub-chapter 3.10 have discovered that surgeons of different experiences and skills perceived the T_{Insert} for an optimum $F_{Pullout}$ differently (Cordey et al., 1980; Siddiqui et al., 2005). Therefore, it can be assumed that in the clinical environment, surgeons of different experiences may have been judging T_{Insert} for the optimum $F_{Pullout}$ at varying torque values, which can span anywhere between shortly after screw head contact to prior to screw stripping. To address this, our study was designed to include $F_{Pullout}$ measurements at varying T_{Insert} values, covering T_{Insert} values between 55% (shortly after screw head contact) to 99% (prior to screw stripping) of the maximum torque with the aid of a micro-mechanical test device.

According to our previous study using an automated micro-mechanical screw-insertion device on human femoral heads (sub-chapters 5.1.10 and 5.1.11), the

T_{Insert} measured at screw head contact ($T_{Plateau}$) is influenced by the micro-architecture and aBMD of the host bone. In particular, bone specimens having a more plate-like trabecular micro-architecture and higher density (higher bone volume fraction and aBMD) exhibited higher T_{Insert} at screw head contact compared to those with a more rod-like structure and lower density. It could be reasonable to expect that these specimens would also withstanding higher T_{Insert} to exhibit greater pullout strength. However, to the best of our knowledge, this has not been studied before, particularly over a wide range of T_{Insert} values.

Thus, the aim of this study performed on cancellous bone screws inserted in excised human femoral heads was to determine the relationship between pullout strength ($F_{Pullout}$), insertion torque (T_{Insert}), aBMD, and micro-architectural parameters when cancellous screws are inserted into trabecular bone tissues of femoral head.

6.1   Materials and Methods

The laboratory tests performed in Study 2 were a continuation of the laboratory tests performed in Study 1, and described in detail in sub-chapter 5.1.

6.1.1   Human Femoral Head Specimens, DXA and Micro-architectural Data

The same cohort of human femoral head specimens (46 femoral heads retrieved from hip replacement surgery (17 females, 29 males, mean [SD] age = 78.2 [9.6]), with DXA and micro-architectural data shown in Table 5.1 were used in this pullout study.

6.1.2   Screw Insertion

The screw insertions (tightenings) in this study resumed from where they had stopped in Study 1, i.e., from screw head contact. Once the micro-CT scan of the bone-screw construct at head contact was completed (sub-chapter 5.1.11), each screw was then further tightened randomly by the micro-mechanical test rig to a torque level or $T_{Insert,}$ ranging from 55% to 99% of the predicted maximum torque (T_{Max}) (Figure 6.0), while the specimens were still in the scanner This was followed by a micro-CT scan of the bone-screw construct.
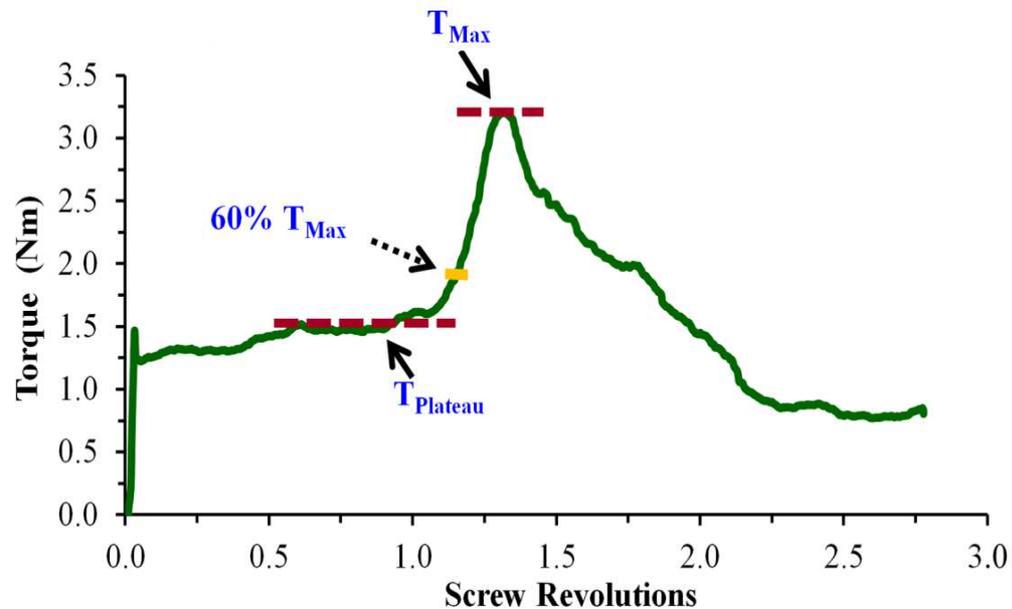
Figure 6.0:   Screw insertion profile ("Torque (Nm) vs. Screw Revolutions") recorded by the micro-mechanical test device. Plateau torque ($T_{Plateau}$) is the insertion torque measured at screw head contact, while maximum torque (T_{Max}) is the predicted failure torque (stripping). The applied screw insertion torque (T_{Insert}) was within the linear region of the graph $T_{Max} - T_{Plateau}$, and ranged from 55% to 99% of T_{Max}. As an example, a dotted arrow points to an applied T_{Insert} of 60% of T_{Max}.

The micro-CT images of bone-screw constructs that were subjected to tightening torque were not used for this thesis to study the deformation behaviour of the

bone tissues surrounding the screws as this was beyond the scope of the thesis. Nevertheless, these bone-screw construct images will provide good resources for the Flinders bone research team to conduct such a study in the future.

The previously published study by our group (Reynolds et al., 2013) demonstrated that it is possible to predict the torque at which the screw will strip (T_{Max}) based on measurement of $T_{Plateau}$ through a linear relationship between $T_{Plateau}$ and T_{Max} (R = 0.840, p < 0.001). The linear relationship applied in this study for the prediction of T_{Max} was derived from 21 tests performed on human femoral head samples, and was given by the equation: $T_{Max} = 1.56\ T_{Plateau} + 698$ mNm. This linear relationship was used to develop an algorithm for the prediction of T_{Max}. This algorithm was programmed into the controller for the mechanical test rig, and allowed the user to select a torque level (as a percentage of predicted T_{Max}) at which to stop insertion. This allows stoppage at any point during screw insertion before failure.

6.1.3 Screw Pullout Test

After tightening, the femoral heads were transferred to a servo hydraulics material testing machine (Model 8511, Instron Pty. Ltd., High Wycombe, UK) for screw pullout tests (Figure 6.1). To secure the femoral head specimen and screw construct onto the mechanical testing machine, custom-made fixtures were specially designed and built (Figure 6.2), according to ASTM, F543 (Cleek et al., 2007; Farrera and Ryken, 1999) to firmly grasp the bone-screw construct during the screw pullout tests.

Figure 6.1: A mechanical testing machine (Model 8511, Instron Pty. Ltd., High Wycombe, UK) was in operation for the pullout test and the acquisition software displayed on the computer screen captured the displacement of screw and pullout force ($F_{Pullout}$) data. A custom-made fixture was mounted onto the testing machine (illustrated inside the yellow dotted box) to firmly grip the specimen during testing.

The time between screw insertion and pullout test was standardised to 5 hours. In between procedures, the bone specimens were kept moistened in gauze soaked with saline solution. At the beginning of the tests, a preload of 10 N was applied, followed by screw pullout to failure at a displacement rate of 5 mm/min (Figure 6.3) (Cleek et al., 2007; Wirth et al., 2010). The screw displacement and the tensile force ($F_{Pullout}$) exerted on the load cell were recorded.
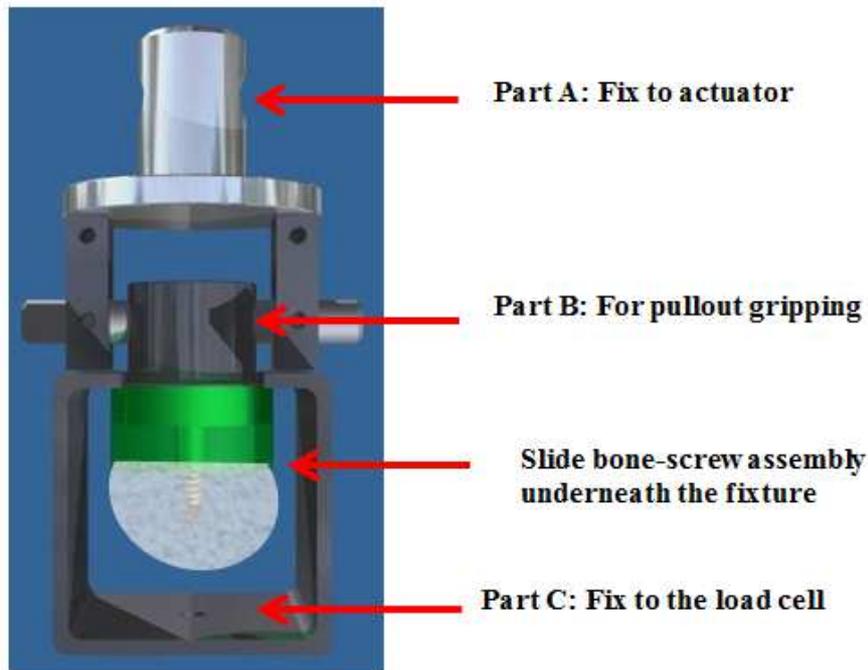
Figure 6.2: A close-up view of the custom-made fixture used to firmly grip the bone-screw construct during pullout tests performed with the Instron mechanical testing machine as illustrated in the red box in Figure 6.1.
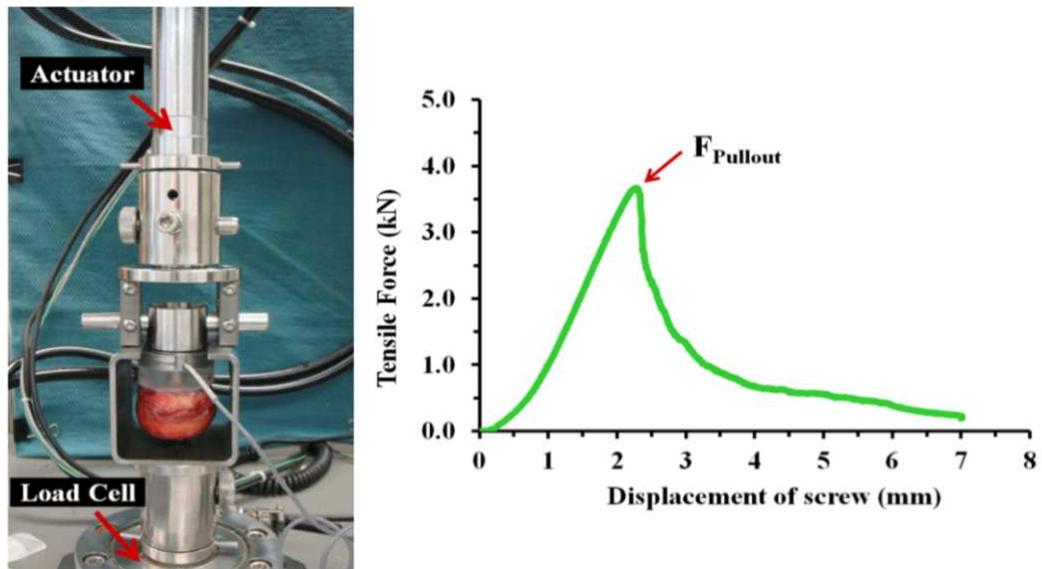
Figure 6.3: Illustration of screw pullout testing using a servo-hydraulic materials testing machine. The bone-screw construct was mounted into the custom-made fixture. The screw underwent tensile loading at a ramp rate of 5 mm/min until stripping occurred. The tensile force exerted on the load cell and the displacement of the actuator (reflecting the displacement of the screw) during the pullout tests were recorded, as shown in the graph "Tensile Force (kN) vs. Displacement of screw (mm)". The maximum tensile force achieved in the experiment is defined as the screw pullout strength ($F_{Pullout}$).

6.1.4 Statistical Analysis

IBM SPSS Statistics software (version 20) was utilised for the statistical analyses. All data distributions were tested for assumptions of normality (Shapiro-Wilks test), homogeneity of variance (Levene's test) and linearity (scatter plot of residuals).

Descriptive statistics were applied to summarise the aBMD measured from DXA, micro-architectural parameters from micro-CT, and measurements from biomechanical testing (T_{Insert} and $F_{Pullout}$). The Pearson's correlation coefficient (R) and the coefficient of determination (R^2) were used to evaluate the relationships "$F_{Pullout}$ vs. aBMD", "$F_{Pullout}$ vs. micro-architectural parameters", and "$F_{Pullout}$ vs. T_{Insert}."

In chapter 5 (study 1), it was found that T_{Insert} measured at screw head contact ($T_{Plateau}$) was significantly correlated with SMI, BV/TV and aBMD. Thus, in the correlations and regressions with $F_{Pullout}$ in the present study, we investigated the applied T_{Insert} first without, and then with, normalisation by each of these three bone quality parameters separately to evaluate if there is added predictive value to T_{Insert} that is independent of aBMD and micro-architecture (SMI and BV/TV). Correlation coefficients of $|R| \geq 0.68$ were interpreted empirically as strong, those of $0.36 \leq |R| \leq 0.67$ as medium, and $|R| \leq 0.35$ as weak.

Stepwise forward multiple regression analysis was performed to evaluate whether the combination of aBMD with micro-architectural parameters and T_{Insert} would

improve the prediction of $F_{Pullout}$ beyond the regressions with single parameters. The significance level of all tests was set to p = 0.05.

6.2 Results

6.2.1 Biomechanical Testing of Screw Pullout

All of the 46 femoral heads (17 females, 29 males, mean [SD] age = 78.2 [9.6]) successfully underwent screw pullout tests. The descriptive statistics of T_{Insert} applied with the micro-mechanical testing device, and $F_{Pullout}$ obtained from tensile testing in the materials testing machine are summarised in Table 6.0. In all the measured parameters, the tests for assumptions of normality, homogeneity of variance, and linearity, revealed no violations (p > 0.05 for all).

Table 6.0: Descriptive statistics of the values of screw insertion torque (T_{Insert}) applied by using the micro-mechanical testing device, and pullout strength ($F_{Pullout}$) obtained from tensile testing in the material testing machine.

	units	Mean (SD)	Min-Max
*T_{Insert}	(Nm)	1.9 (0.6)	0.9 - 3.9
$F_{Pullout}$	(kN)	1.60 (0.6)	0.5 - 3.2

*ranging from 55% to 99% of T_{Max}, that is, within the region of T_{Max} - $T_{Plateau}$

6.2.2 Correlations Between $F_{Pullout}$, aBMD and Micro-architectural Parameters

$F_{Pullout}$ exhibited statistically significant correlations with all the investigated bone parameters (Table 6. 1). $F_{Pullout}$ showed the strongest correlation with SMI (R= -

0.81, p < 0.001), followed by BV/TV (R = 0.73, p<0.001) and aBMD (R = 0.66, p

< 0.001). $F_{Pullout}$ exhibited moderate correlations with the remaining micro-

architectural parameters (BS/TV, Tb.Th, Tb.Sp and Tb.N, with |R| ranging from

0.31 to 0.46). Figure 6.4 shows scatter plots and best fit lines for "$F_{Pullout}$ vs.

SMI", "$F_{Pullout}$ vs. BV/TV," and "$F_{Pullout}$ vs. aBMD," respectively. Figure 6.5

shows scatter plots and linear regression lines between "$F_{Pullout}$ vs. BS/TV",

"$F_{Pullout}$ vs. Tb.N", "$F_{Pullout}$ vs. Tb.Sp" and "$F_{Pullout}$ vs. Tb.Th."

Table 6.1: Pearson correlation coefficients (R) and coefficients of determination
(R^2) for $F_{Pullout}$ vs. aBMD from DXA, and for $F_{Pullout}$ vs. micro-architectural bone
parameters from micro-CT.

			R	R^2	p-value
$F_{Pullout}$	vs.	aBMD	0.66	0.44	p<0.001
$F_{Pullout}$	vs.	BV/TV	0.73	0.53	p<0.001
$F_{Pullout}$	vs.	SMI	-0.81	0.65	p<0.001
$F_{Pullout}$	vs.	BS/TV	0.35	0.12	p<0.05
$F_{Pullout}$	vs.	Tb.Th	0.46	0.21	p<0.01
$F_{Pullout}$	vs.	Tb.Sp	-0.36	0.13	p<0.05
$F_{Pullout}$	vs.	Tb.N	0.31	0.1	p<0.05

$$y = -1.37x + 2.79$$
$$R^2 = 0.65$$
$$p < 0.001$$

(a)

$$y = 0.10x - 0.93$$
$$R^2 = 0.53$$
$$p < 0.001$$

(b)
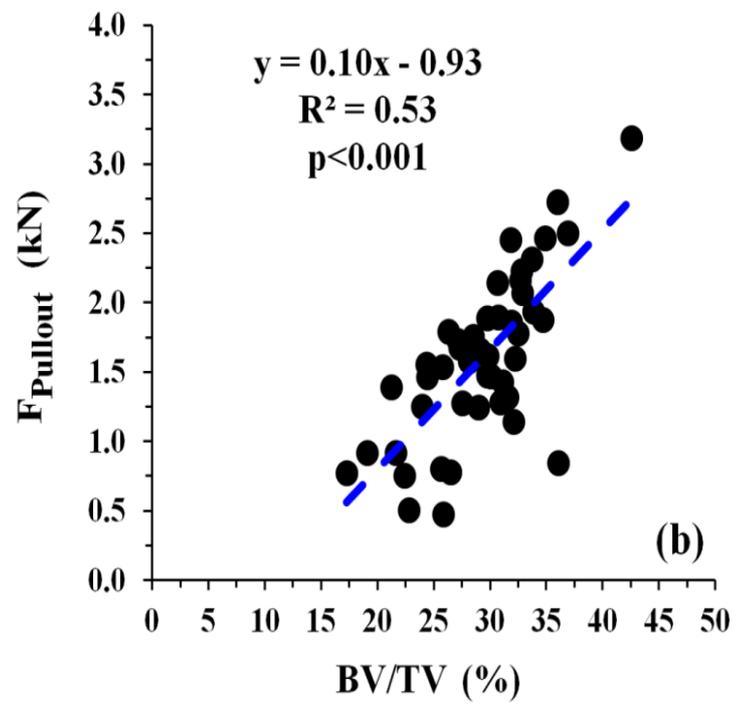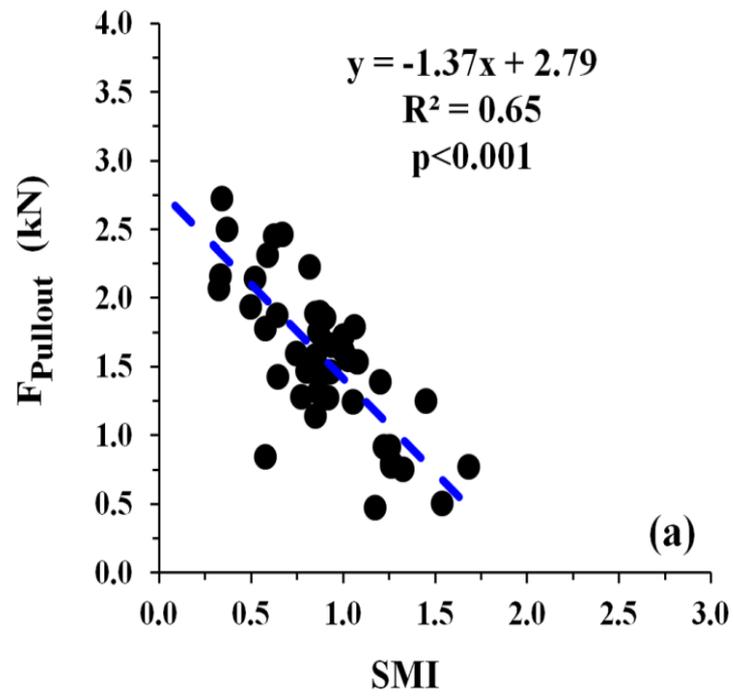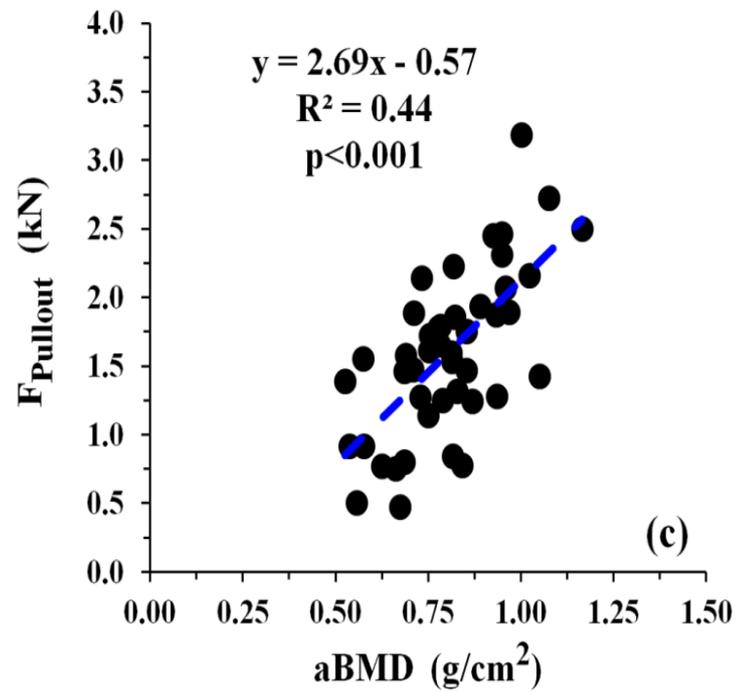
Figure 6.4: Scatter plots and linear regression lines between $F_{Pullout}$ versus SMI (a), BV/TV (b) and aBMD (c).

$y = 0.92x + 0.45$
$R^2 = 0.10$
$P < 0.05$

(b)

$y = -0.002x + 2.80$
$R^2 = 0.13$
$P < 0.05$

(c)
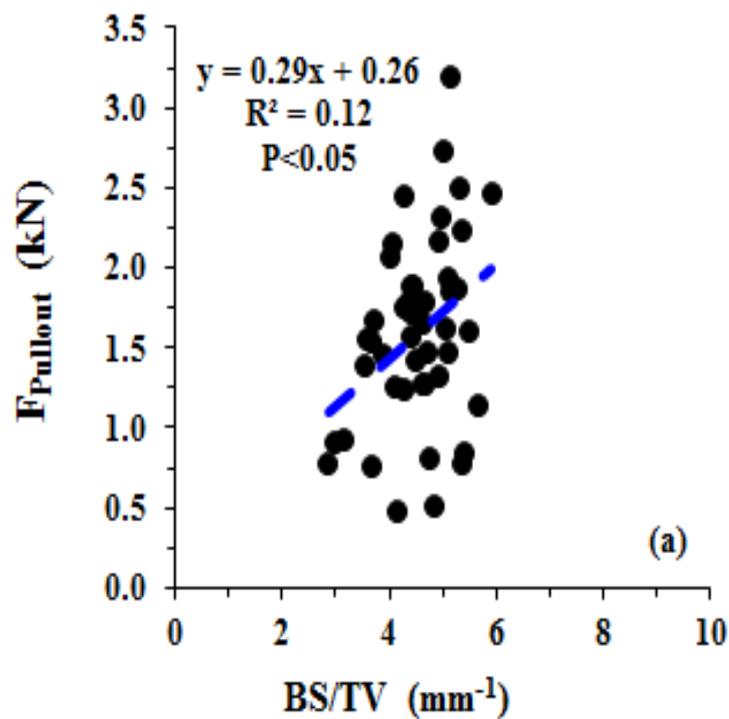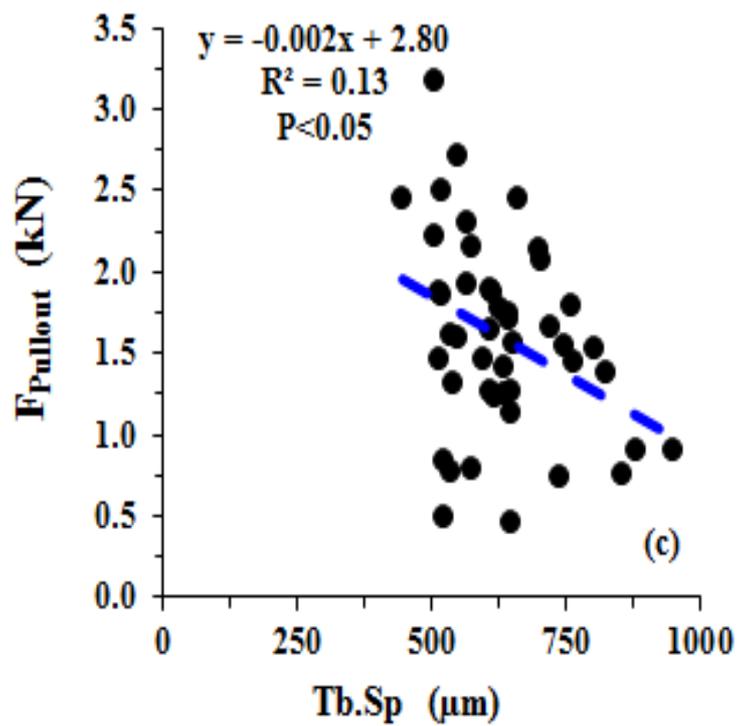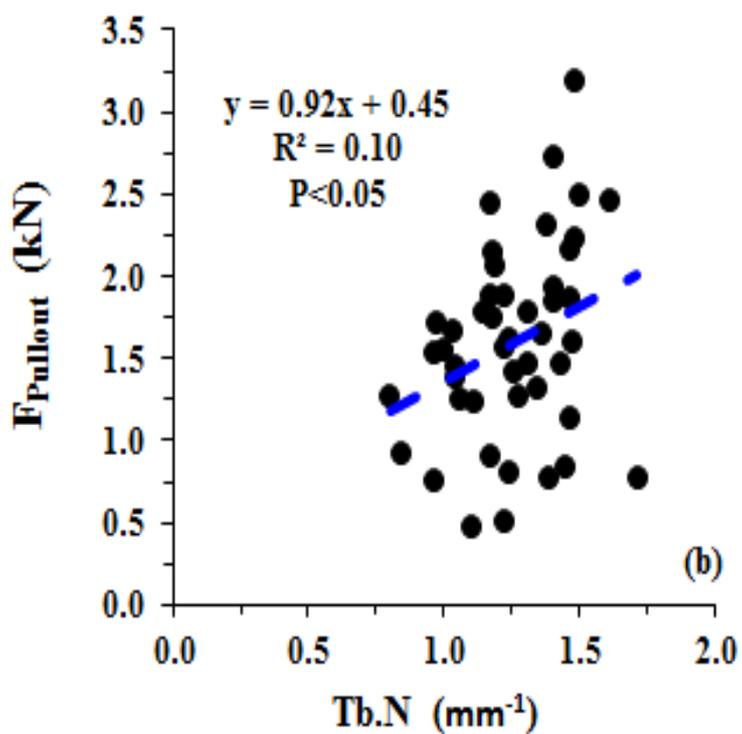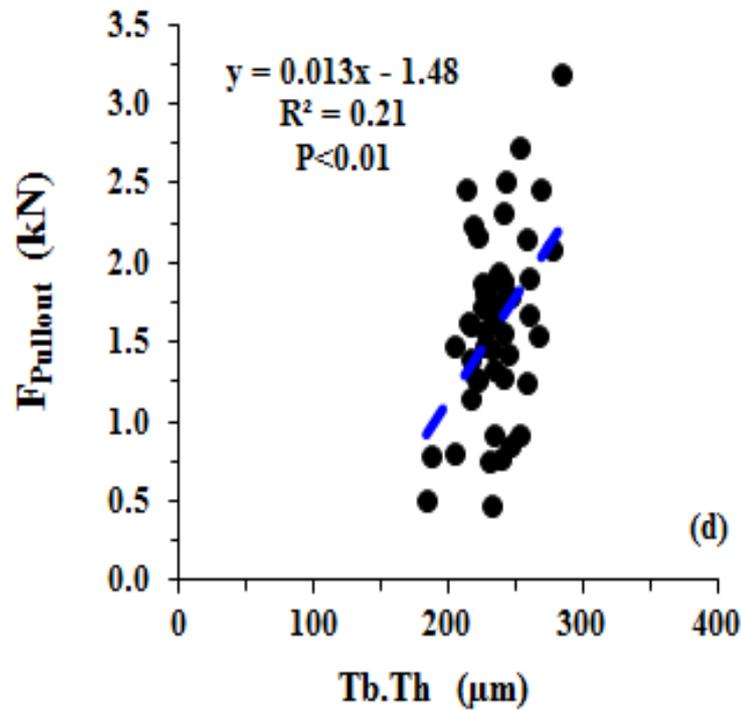
Figure 6.5: Scatter plots and linear regression lines between $F_{Pullout}$ versus BS/TV (a), Tb.N (b), Tb.Sp (c) and Tb.Th (d).

6.2.3   Correlations Between $F_{Pullout}$, T_{Insert} and Normalised T_{Insert}

$F_{Pullout}$ exhibited a significant correlation with T_{Insert} (R = 0.88, p < 0.001), as well as with T_{Insert} after normalisation for SMI, BV/TV and aBMD (R = 0.76, R = 0.75, and R = 0.68 respectively, p < 0.001 for all) (Table 6.2). Figure 6.6 shows scatter plots and best fit lines for "$F_{Pullout}$ vs. T_{Insert}," and "$F_{Pullout}$ vs. normalised T_{Insert}," respectively.

$y = 0.80x + 0.010$
$R^2 = 0.77$
$p < 0.001$

(a)

$y = 0.21x + 1.01$
$R^2 = 0.57$
$p < 0.001$

(b)
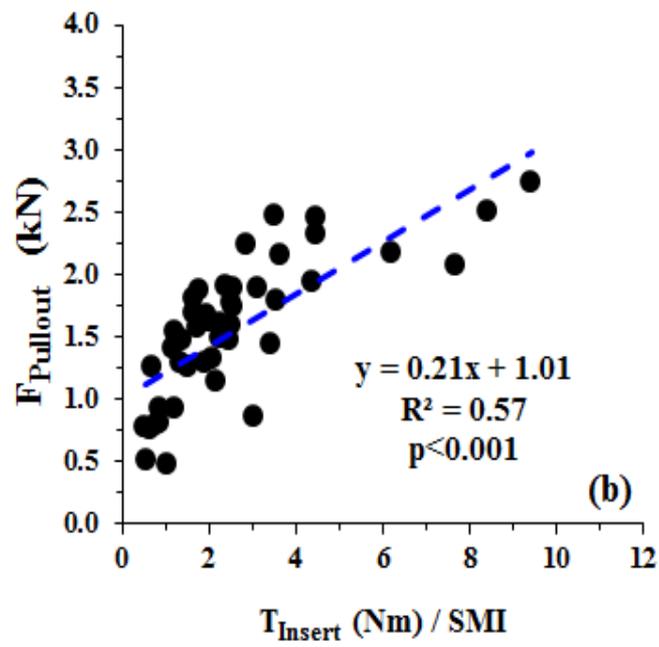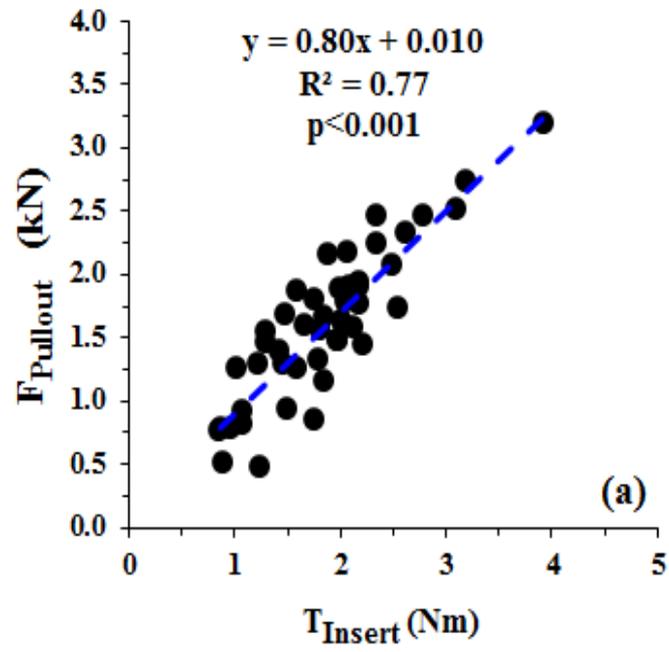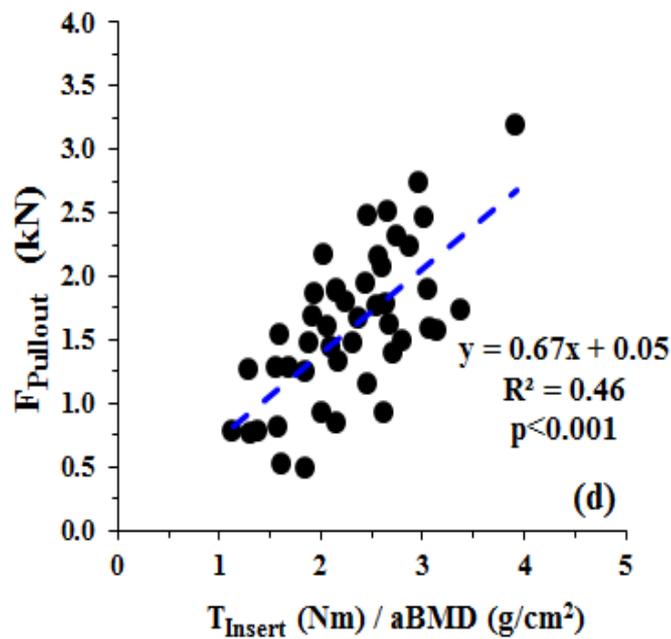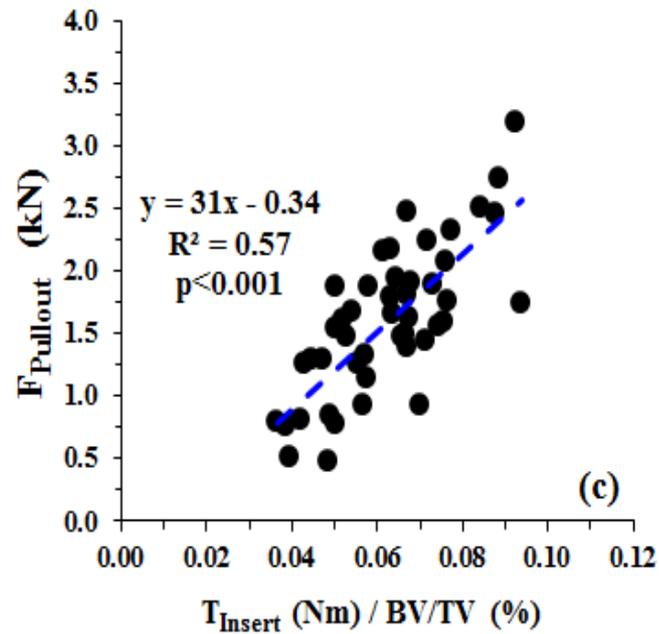
Figure 6.6: Scatter plots and linear regression lines of "$F_{Pullout}$ vs. T_{Insert}" (a), and "$F_{Pullout}$ vs. T_{Insert} normalised for aBMD, BV/TV and SMI" (b, c, d, respectively), i.e., the bone quality parameters that are highly correlated with T_{Insert} at head-contact ($T_{Plateau}$).

6.2.4 Stepwise Forward Regression Analysis: $F_{Pullout}$ vs. aBMD, Micro-architectural Parameters and T_{Insert}

Stepwise forward regression analysis revealed that the combination of aBMD and micro-architectural parameters BV/TV, SMI, BS/TV, Tb.Th, Tb.Sp, and Tb.N did not improve the prediction of $F_{Pullout}$ compared to the single regression of "$F_{Pullout}$ vs. SMI" ($R^2 = 0.65$, Table 6.1).

Stepwise forward regression analysis also revealed that by combining T_{Insert} with aBMD and micro-architectural parameters, there was no improvement in the prediction of $F_{Pullout}$ beyond the single regression model "$F_{Pullout}$ vs. T_{Insert}" ($R^2 = 0.77$, Table 6.2).

Table 6.2: Pearson correlation coefficients (R) and coefficients of determination (R^2) for "$F_{Pullout}$ vs. T_{Insert}", and for "$F_{Pullout}$ vs. T_{Insert} normalised for aBMD, BV/TV, and SMI", i.e., the bone quality parameters that have strong correlations with T_{Insert} at head-contact ($T_{Plateau}$) (Table 5.3).

			R	R^2	p-value
$F_{Pullout}$	vs.	T_{Insert}	0.88	0.77	p<0.001
$F_{Pullout}$	vs.	T_{Insert} / aBMD	0.68	0.44	p<0.001
$F_{Pullout}$	vs.	T_{Insert} / BV/TV	0.75	0.57	p<0.001
$F_{Pullout}$	vs.	T_{Insert} / SMI	0.76	0.57	p<0.001

6.3   Discussion

Overall, the present findings confirm that $F_{Pullout}$ is significantly influenced both by the level of applied insertion torque, as well as by the quality of the host bone. In particular, the $F_{Pullout}$ of cancellous screws exhibited the strongest correlations with T_{Insert} (R = 0.88), followed, in order of decreasing |R| values, by the micro-architectural parameters SMI (R = - 0.81) and BV/TV (R = 0.73), and moderate correlation with aBMD (R = 0.66).

The correlations between $F_{Pullout}$ and the remaining micro-architectural parameters BS/TV, Tb.Th, Tb.Sp, and Tb.N were significant but lower (|R| = 0.31 - 0.46), suggesting that variations in those parameters were not as influential. Using the T_{Insert} combined with micro-architectural parameters and aBMD did not improve the prediction beyond the single regression model "$F_{Pullout}$ vs. T_{insert}," which confirms T_{Insert} as the overall best predictor of $F_{Pullout}$.

Furthermore, the correlations between $F_{Pullout}$ and T_{Insert} remained significant even after normalizing T_{Insert} by aBMD, BV/TV, and SMI. This suggests that T_{Insert} is the primary factor affecting $F_{Pullout}$, and that for a specimen with a given bone micro-architecture and density, increases in the applied T_{Insert} will lead to increases of $F_{Pullout}$.

This study also shows that, at a given absolute insertion torque level (measured in Nm), those bone specimens presenting a more plate-like structure and higher

density (i.e., lower SMI, higher BV/TV and aBMD), will have a higher $F_{pullout}$. There have been mixed findings regarding the relationships "$F_{Pullout}$ vs. T_{Insert}" and "$F_{Pullout}$ vs. aBMD" in human bones reported in the literature; some studies have shown statistically significant relationships, yet contradict the order of correlation strength (Reitman et al., 2004; Ryken et al., 1995), hence leaving the question still open to further investigate the effect of T_{Insert} and bone quality such as aBMD on $F_{Pullout}$.

In the present study, an important experimental difference from the previous studies is that an insertion test device was used, which can automatically measure bone-specific T_{Insert} in a percentage of T_{Max} during screw insertion, providing greater reliability and flexibility to include a wide range of T_{Insert} values in the investigation of $F_{Pullout}$ compared to the previous studies by Reitman et al. (2004) and Ryken et al. (1995) (sub-chapter 3.10). Reitman and Ryken each performed $F_{Pullout}$ measurements at only one level of torque based on surgeon's subjective perceived T_{Insert} for the optimal fixation strength. Reitman et al. (2004) measured $F_{Pullout}$ at torque value of mean $\pm$ SD = 2.16 $\pm$ 1.28 Nm or 85% T_{Max}; while Ryken et al. (1995) measured $F_{Pullout}$ at torque of 0.312 $\pm$ 0.230 Nm. Furthermore, the torque value published in Ryken's study lacked standard unit of measure of % of T_{Max}, which hampered one-to-one comparison in regards to their $F_{Pullout}$ findings with respect to bone's failure torque or T_{Max}. Thus, this limitation may be the reason for their conflicting findings, particularly on the importance of insertion torque and aBMD for predicting $F_{Pullout}$.

A recent study conducted on cortical screws in the diaphysis of human humeri concluded that the relationships "$F_{Pullout}$ vs. T_{Insert}" and "$F_{Pullout}$ vs. aBMD" still remain to be determined (Tankard et al., 2013). Tankard et al. (2013) also suggested that the $F_{Pullout}$ does not significantly increase with the applied T_{Insert} when the screw is tightened beyond head contact, in apparent contradiction with the present findings on cancellous bone screws. An explanation for this difference might be that cortical bone as used by Tankard et al. (2013) (diaphysis, human humeri) is compact and dense, compared to specimens containing mainly trabecular bone as used in this study (human femoral head).

Theoretically, during screw insertion in a compact solid, at the point of screw head contact, an optimal purchase of all the screw threads has already been achieved, and further tightening is unlikely to improve screw thread purchase. In trabecular bone however, which has high porosity compared to diaphyseal cortical bone (Morgan et al., 2013; Samuel et al., 2009), further tightening of a cancellous screw (below stripping torque) after head contact may cause deformation of the bone surrounding the screw, which in turn may cause compaction of any bone debris caused by cutting of the screw threads. As a result, the anchorage conditions are changing during the tightening phase, which may explain the increased $F_{Pullout}$ of the screw.

However, excessive tightening can lead to bone yielding and beyond that, to screw stripping. A previous study using cortical screws on the diaphysis of ovine tibiae suggested that the yield torque is beyond 70% of predicted T_{Max} (Cleek et

al., 2007). In human trabecular bone, the insertion torque of a cancellous screw after which the bone yields has yet to be explored (next chapter).

A limitation in the present study was the unavailability of apparent bone densitometry data from our donors' clinical records; hence measurements of aBMD were performed on the excised femoral heads in-vitro, which represent a best-case scenario environment, where the same amount of soft tissue was simulated (with polyoxymethylene board) for each sample.

6.4 Conclusion

In conclusion, this study used a computer-controlled micro-mechanical screw insertion device, micro-CT and DXA imaging, and experimental pullout testing on a cancellous bone screw in human femoral heads to investigate the effect of bone micro-architecture, aBMD, and the applied T_{Insert} on the $F_{Pullout}$ of cancellous screws. We found, in descending order of importance, that the $F_{Pullout}$ was most strongly correlated with the applied T_{Insert}, the micro-architectural parameters (in particular SMI and BV/TV), and aBMD of the host bone. The combination of applied T_{Insert} with micro-architectural parameters and/or aBMD did not improve the prediction of $F_{Pullout}$ beyond the single regression model "$F_{Pullout}$ vs. T_{Insert}." The applied T_{Insert} remained significantly correlated with $F_{Pullout}$ even after normalisation for SMI, BV/TV, and aBMD.

This indicates that, for a bone specimen with a given trabecular bone micro-architecture and density, increases in applied tightening torque beyond head

contact within the linear range will increase $F_{Pullout}$ of the screw. Thus, this implies that tightening of a screw after screw head contact improves screw fixation strength in stabilising the fractured bones, stabilisation being a primary factor for fracture healing. The level of tightening torque after which bone yielding occurs, and how $F_{Pullout}$ will be affected once this level is reached, should however be examined in greater detail in future studies on cancellous bone screws in human bone.

Chapter VII

Study 3: Comparison between the Cancellous Screws Pullout Strength at Three Levels of Tightening Torque in the Human Femoral Head

This chapter describes the study performed to address the third (final) aim of this thesis, that is, to compare the $F_{Pullout}$ (pullout strength) of cancellous screws in human trabecular bone of the femoral head at three relative insertion torque levels (T_{Insert}) (portion of maximum torque or T_{Max}), i.e., tightened to an average of 70% T_{Max}, 80% T_{Max}, and 90% $T_{Max.}$

The results reported in this chapter have been published as Ab-Lazid, R, Perilli, E, Ryan, MK, Costi, JJ, Reynolds, KJ, 2015, "Comparison between the cancellous screws pullout strength at three levels of tightening torque in the human femoral head" as an abstract in Proceeding of the Australian and New Zealand Orthopaedic Research Society (ANZORS) 21st Annual ANZORS conference, 2-4 October 2015, University of Auckland, New Zealand. Website: http://www.anzors.org.au. The published abstract was rewritten for this thesis.

7.0   Introduction

Unintentional screw stripping may go undetected during fracture repair surgery and this poses concern among surgeons about poor fixation. Clinically, surgeons estimate the level of tightening torque required for optimal fixation based on their

perception. According to a study, a surgeon's perception of optimal tightening torque is not reliable for detecting and preventing stripping of the bone around the screw. Out of 340 tests performed on synthetic trabecular bones, 109 (45%) screws were inadvertently stripped by the surgeons, and in 91% of these cases the surgeons did not recognise that stripping had occurred (Stoesz et al., 2014) (sub-chapter 3.10).

Dinah et al. (2011) (sub-chapter 3.10) found that 9% of screws inserted into human cadaveric ankle bones were inadvertently stripped, while 12% were over tightened. No significant predictors such as bone mineral density, bone micro-architecture, or insertion torque were found that could warn of impending screw stripping (Dinah et al., 2011). The Reynolds study later found $T_{Plateau}$ (or torque at screw head contact) was a significant predictor of bone stripping torque, which can be used as a control parameter to cease screw tightening before bone failure (Reynolds et al., 2013). Yet, clinically during screw tightening surgeons are still relying on their perceptions in engaging what is thought to be "optimal" torque, which is suggested as reaching 86% of the bone's maximum torque (T_{Max}) (Cordey et al., 1980). The question arises as to how much more tightening is required after the screw reaches head contact in order to obtain an optimum $F_{Pullout}$ of cancellous screw.

A previous study by our group suggested that tightening of screws to 70% T_{Max} in cortical bone ovine tibiae resulted in the highest $F_{Pullout}$ compared to torque at 50% T_{Max} and 90% T_{Max}; but tightening of screws beyond 70% T_{Max} had lowered

$F_{Pullout}$, from which it was concluded that tightening of cancellous screws past 70% T_{Max} (including the perceived "optimal" torque of 86% T_{Max}), exceeded the yield point of the cortical bone, which can cause damage leading to compromised pullout strength (Cleek et al., 2007).

In a similar study, Tankard et al. (2013) found that tightening of screws to 50% T_{Max} in the cortex of cadaveric humeri bone resulted the highest $F_{Pullout}$, and concluded that tightening of screws beyond 50% T_{Max} did not significantly increase the $F_{Pullout}$ of the screw compared to tightening to 70% T_{Max} and 90% T_{Max}. Tankard also suggested that tightening of screws beyond 50% T_{Max} may place bone at risk from damage, which might result in loss of fixation (Tankard et al., 2013).

Although previous studies have compared $F_{Pullout}$ at different tightening torque levels, mixed findings were demonstrated, contradicting each other. Moreover, the investigations were performed on cortical bone samples from animals and humans (Cleek et al., 2007; Tankard et al., 2013). It is still unknown whether a similar relationship exists in human anatomical sites that are rich in trabecular bone, such as the femoral head. Therefore, the aim of this study is to determine the effect of three tightening torque levels, i.e., group 1: T_{Insert} = 70% T_{Max}; group 2: T_{Insert} = 80% T_{Max}; and group 3: T_{Insert} = 90% T_{Max} on the pullout strength of cancellous screws in the human femoral heads.

7.1   Materials and Methods

7.1.1   Pullout Data Selection

A subset of 18 out of 46 specimens that completed the biomechanical testing in the previously described studies was selected for this study. The specimens (n = 6 per group) were selected to meet the three tightening torque levels specified in the aims (Table 7.0). The specimens were chosen among those having similar aBMD and BV/TV (Table 7.1).

Table 7.0: The applied tightening torque of the 3 groups (n = 6 specimens per group), expressed as mean value, standard deviation (SD), minimum and maximum value.

Groups	Tightening Torque ($\%T_{Max}$)		
	Mean	SD	Min - Max
Group 1: 70 $\%T_{Max}$ (n=6)	70	2	65-72
Group 2: 80 $\%T_{Max}$ (n=6)	80	2	75-83
Group 3: 90 $\%T_{Max}$ (n=6)	90	2	85-91

Table 7.1: aBMD and BV/TV, of the 3 groups (n = 6 specimens per group), expressed as mean value, standard deviation (SD), minimum and maximum value.

Groups	aBMD (g/cm^2)			BV/TV (%)		
	Mean	SD	Min - Max	Mean	SD	Min - Max
Group 1: 70 $\%T_{Max}$ (n = 6)	0.9	0.1	0.7 - 1.0	32	2	28 - 34
Group 2: 80 $\%T_{Max}$ (n = 6)	0.9	0.1	0.7 - 1.0	32	2	29 - 35
Group 3: 90 $\%T_{Max}$ (n = 6)	0.8	0.5	0.7 - 0.8	30	3	26- 36

7.1.2 Statistical Analysis

IBM SPSS Statistic software (version 20) was utilised for the statistical analyses. All data distributions were tested for assumptions of normality (Shapiro-Wilks test), homogeneity of variance (Levene's test) and linearity (scatter plot of residuals).

Descriptive statistics were applied to summarise the data such as aBMD, BV/TV, tightening torque ($\%T_{Max}$) and $F_{Pullout}$. A one-way ANOVA analysis with Tukey HSD post-hoc was performed to compare the means of aBMD, BV/TV and $F_{Pullout}$ between the three groups and quantify significance level between the means.

Post-experimental power analysis — t tests, Means; Difference between two dependent means (matched pair) was performed with G*power software (version 3.0.10) to determine the sample size of the specimens that would be required to show a significant effect of the pullout strength between groups (n = 3). A medium effect size of f = 0.5 which is common in orthopaedic research (Freedman et al., 2001), an α error prob = 0.0166, and a power (1-β err prob) = 0.8 were used. The significance level of all tests was set to p=0.05.

7.2   Results

7.2.1 Comparison of aBMD, BV/TV and $F_{Pullout}$ Among Groups

Descriptive statistics of the specimens' aBMD and BV/TV mean (SD) [min – max]) and p-values of mean differences among groups from the one-way ANOVA analysis are summarised in Table 7.1.

The one-way ANOVA analysis indicated that the mean values of aBMD and BV/TV among the groups were not significantly different (aBMD, p = 0.06 and BV/TV, p = 0.54, respectively), while $F_{Pullout}$ values indicated significant differences among the groups (p = 0.03).

Table 7.2: The one-way ANOVA analysis was performed to compare aBMD, BV/TV and $F_{Pullout}$ (means [SD] [min – max]) among the groups. The p-values of aBMD (p = 0.54) and BV/TV (p = 0.06) suggested no significant difference in aBMD and BV/TV among the groups, while p-value of $F_{Pullout}$ (p = 0.03) suggested $F_{Pullout}$ was significantly different among the groups (p < 0.05 for both).

Parameters	70 %T_{Max} (n=6)	80 %T_{Max} (n=6)	90 %T_{Max} (n=6)	p-value
BV/TV (%)	32 (2) [28-34]	32 (2) (29-35)	30 (3) [26-36]	p = 0.54
aBMD (g/cm^2)	0.90 (0.10) [0.73-1.02]	0.90 (0.10) [0.73-0.96]	0.80 (0.50) [0.69-0.82]	p = 0.06
$F_{Pullout}$ (kN)	1.79 (0.31) [1.28-2.16)	2.07 (0.28) [1.66-2.45]	1.48 (0.40) [0.84-1.89]	p = 0.03

7.2.2 Comparisons of $F_{Pullout}$ between groups

$F_{Pullout}$ for cancellous screws tightened to 80% T_{Max} was greater than $F_{Pullout}$ for screws tightened to 70% T_{Max}, although not statistically significant (p = 0.33). $F_{Pullout}$ of screws tightened to 90% T_{Max} was significantly lower than for screws tightened to 80% T_{Max} (p = 0.02), and also lower than screws tightened to 70% T_{Max}, although not significantly different (p = 0.27) (Figure 7.0)
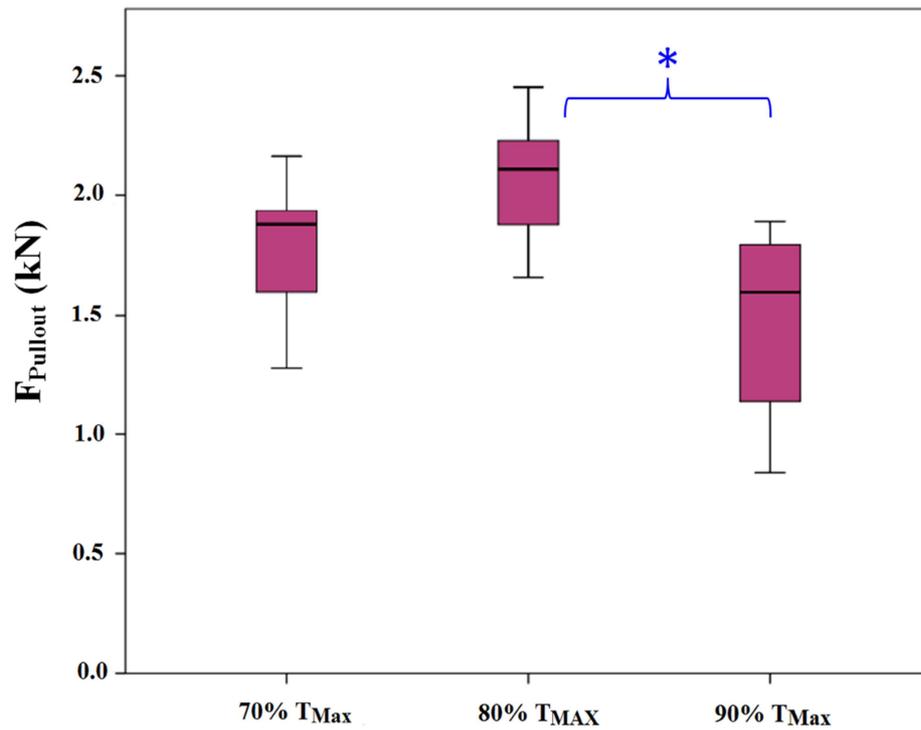
Figure 7.0: Boxplot of the $F_{Pullout}$ of screws tightened to $T_{Insert} = 70$ %T_{Max}, 80% T_{Max} and 90% T_{Max}. $F_{Pullout}$ of screws tightened to 80% T_{Max} was significantly different to $F_{Pullout}$ of screw tightened to 90% T_{Max} (*p = 0.019).

7.2.3 Post-experimental Power Analysis

The post-experimental power analysis revealed that the total sample size (n) of 69 (or 23 per group) are required to show a significant effect of the pullout strength between the groups for this study. Refer to Appendix A6 for the post-experimental power analysis screen shot.

7.3   Discussion

This study compared the effect of three torque levels on the pullout strength ($F_{Pullout}$) of cancellous screws in the femoral head bones of similar range of quality (aBMD and BV/TV) (Tables 7.1 and 7.2).

The results showed that $F_{Pullout}$ of the cancellous screws tightened to 80% T_{Max} was significantly greater than for screws tightened to 90% T_{Max} ($F_{Pullout}$ = 2.07 ± 0.28 kN vs. 1.48 ± 0.40 kN, p=0.019) and it tended to be greater than for screws tightened to 70% T_{Max} (1.79 ± 0.31 kN, p=0.33) (Figure 7.0). Although $F_{Pullout}$ at 70% T_{Max} was greater than at 90% T_{Max}, the difference was not significant (p=0.27). Based on these results, it could be speculated that tightening of screws beyond 80% T_{Max} led the trabecular bone around the screw to yield. As mentioned previously (sub-chapter 3.10), another study in our laboratory confirmed that yielding of the trabecular bone of the femoral heads occurs at approximately 85% of T_{Max} (Ryan et al., 2015).

Overall, the results of the current study are in line with Cleek in which $F_{Pullout}$ increased when the screws were tightened past 50% T_{Max}, but, $F_{Pullout}$ decreased between 70% and 90% of T_{Max} of tightening, which Cleek attributed to the yielding of bone structures (Cleek et al., 2007). In contrast, the results from Tankard et al. (2013) indicated that tightening of screws beyond 50% T_{Max} in human humerus cortical bone did not significantly increase the screw $F_{Pullout}$ and in fact they suggested that tightening of screws beyond 50% T_{Max} may expose the

cortical bone to the risk of yielding and consequently loss of fixation (Tankard et al., 2013).

In this case, it is hard to make a direct comparison between each of these three studies due to the screws and nature of bones used — Cleek used cortical screws in animal cortical bone (ovine tibiae), Tankard used cortical screws in human cortical bone (humeri), while the current study used cancellous screws in human trabecular bone (femoral heads). Thus, differences between results from the studies may be due to the characteristics of the specimens, particularly the bone quality and nature of the bone, as well as the screw designs. Tankard claimed the bone densities of the ovine tibiae used in the Cleek study were more homogeneous than those of the human humeri from their study, which had a wide range of densities (normal, osteopenic and osteoporotic). In addition, the average cortical thickness of the human humeri (mean $\pm$ SD = 8.60 mm $\pm$ 0.92) used in Tankard's study was about twice the thickness of the ovine tibiae (mean $\pm$ SD = 4.23 mm $\pm$ 0.42) used in Cleek's study; thus, the bones may have been less ductile and shown to fail at lower torque.

Szabó et al. (2011) indicated that bovine trabecular bone fails at a higher strain when subjected to force, and hence is more ductile; and the bone is accompanied by significantly increased micro-damage accumulation prior to failure compared to cortical bone. Thus, they suggested that these could contribute to the trabecular bone's ability to withstand higher damage tolerance compared to cortical bone (Szabó et al., 2011).

Similar occurrences could also happen during screw fixation. The ductile nature of the trabecular bone, coupled with the accumulation of micro-cracks prior to failure, may prevent the bone from yielding earlier. However, subsequent tightening of a screw beyond 80% T_{Max} resulted in significant reduction of screw $F_{Pullout}$, which is likely to be due to bone yielding.

Limitations of this study include small sample size to reach statistical significance in all comparisons and use of a single screw type. According to the post-experimental power analysis it was suggested that a sample size of 23 specimens per group (i.e., total specimens of 69 for the three groups) would be required to show a significant effect of the pullout strength between the groups for this study. Meanwhile, the aspect of the screw, such as the design (fully threaded cancellous screw) and dimension (length, diameter, pitch, thread profile, etc.) have been shown to influence the $F_{Pullout}$ (sub-chapter 3.5). Further study is required to investigate the effects of different screw designs and dimensions and in larger sample size.

7.4   Conclusion

In this study, the significantly reduced $F_{Pullout}$ for screws tightened to 90% T_{Max} compared to 80% T_{Max} may be a result of yielding of trabecular bone structures. $F_{Pullout}$ at 80% T_{Max} tightening was greater than $F_{Pullout}$ at 70% T_{Max}, although not significantly, which might be due to limited sample size. The result of this study

could provide useful insight in future work to develop a torque control system that considers the yield factor of the trabecular bones.

Chapter VIII
Summary, Conclusion and Future Work

8.0   Summary

Study 1 (chapter 5) results suggested that strong relationships exist between $T_{Plateau}$ and bone micro-architecture and aBMD of the femoral heads. This implies that $T_{Plateau}$ detected from the screw insertion profile is directly related to the quality of the host bone. Specimens exhibiting a more plate-like structure (as measured by SMI) and higher bone volume fraction (BV/TV), and also a higher aBMD, likely offer a structural environment in which the screw threads can cut into more material for better anchorage, which leads to an increase of $T_{Plateau}$. Thus, the applied T_{Insert} based on the percentage of maximum torque (% T_{Max}) can be predicted during screw insertion using the $T_{Plateau}$ value, instead of relying solely on the surgeon's feel for the prediction of the T_{Insert}, which is subjective. Additionally, the same type of structure might offer an environment for increased pullout strength, which was investigated in Study 2 (chapter 6).

In Study 2, the findings suggested that $F_{Pullout}$ of the cancellous screws has a strong relationship with $T_{Insert,}$ followed in order of strength of the coefficient of determination, by bone micro-architecture and aBMD. This implies that for a bone specimen with a given trabecular bone micro-architecture and density, increases in applied tightening torque (T_{Insert}) beyond head contact within the torque-versus-screw rotation linear range will increase $F_{Pullout}$ of the screw. The

level of tightening torque after which bone yielding occurs (post linear range), and how $F_{Pullout}$ will be affected once this level is reached, yet remained unknown. This was investigated in Study 3.

In Study 3, the results suggested that $F_{Pullout}$ reaches a maximum when screws are tightened to an average of 80% T_{Max} and $F_{Pullout}$ was significantly greater than for screws tightened to an average 90% T_{Max}. $F_{Pullout}$ at an average of 80% T_{Max} was also greater compared to $F_{Pullout}$ at an average of 70% T_{Max} (although not significantly), which could be due to small sample size. The significantly reduced $F_{Pullout}$ at an average 90% T_{Max} may be due to the yield of trabecular bone structures.

Overall, $T_{Plateau}$ and $F_{Pullout}$ of cancellous screws depend on bone micro-architecture and aBMD of the trabecular bone of the femoral heads. The T_{Insert} to be applied before stripping, based on the percentage of predicted maximum torque (% T_{Max}), can be predicted during screw insertion using the $T_{Plateau}$ value determined by the micromechanical screw insertion device, instead of relying on the surgeon's feel. In trabecular bone, increases in applied T_{Insert} beyond screw head contact to 80% T_{Max} were found to increase $F_{Pullout}$ of the screw. Further increases in T_{Insert} (or tightening) beyond 80% T_{Max} to 90% T_{Max} however resulted in significant decrease of screw $F_{Pullout}$ ($F_{Pullout}$ at 80% T_{Max} = 2.07 ± 0.28 kN versus $F_{Pullout}$ at 90% T_{Max} = 1.48 ± 0.40 kN; p=0.019). This is likely to be a result of yielding of the bone when exposed to T_{Insert} beyond 80% T_{Max}, consequently reducing the screw fixation strength.

8.1   Conclusion

The ability of surgeons to optimise screw insertion torque in cancellous screw fixation is important for fixation stability. Although the finding of this study suggested that fixation or pullout strength ($F_{Pullout}$) increases with an increase in insertion torque (T_{Insert}), it may however be limited by the bone yield point and could vary between bones. There is no mechanism currently in place to quantify the yield point of the bone while it is subjected to screw insertion. Nevertheless, the findings of this study also suggested that bone undergoes yielding when insertion torque exceeds 80% of the maximum torque (T_{Max}). Thus, at the present time, this value can be used as a point at which to stop screw tightening.

With current screw fixation methods, it requires manual intervention to estimate the optimal screw torque, as it cannot be standardised due to the variation in bone quality within and between patients. The current method depends on the feeling of screw purchase, which is assessed based on surgeon's perception that the screw is getting tightened rather than stripping. This method however is subjective and may vary between surgeons, depending on skills and experiences, hence, may not be reliable for optimal tightening and preventing and detecting screw stripping.

Therefore, a new approach on how to control screw insertion/ tightening torque may needed to improve screw fixations for better reliability and prevent complications such as accidental screw stripping during screw fixation in bone fracture surgery. Based on the findings of this thesis, the new approach to control

insertional torque for the optimal pullout strength could be adapted using torque at head contact or plateau torque ($T_{Plateau}$), the predictor of T_{Max}, which is also specific to bone density (measured by DXA) and micro-architecture (measured by micro-CT). The measured $T_{Plateau}$ can be used to determine torque levels based on the percentage of T_{Max} (% T_{Max}), which is specific to bone density and micro-architecture.

Since the bone mineral density or areal bone mineral density (aBMD) and local bone micro-architecture are highly correlated with $T_{Plateau}$, hence, T_{Max}, they also can be used as surrogate for T_{Max} to determine the % T_{Max} torque level. This option however currently is limited by the irregularity of aBMD measurement availability prior to surgery and lack of technology to measure bone micro-architecture in the clinical environment.

In conclusion, $T_{Plateau}$ could be the best option to use as surrogate parameter for T_{Max} to control for an optimal insertion torque and prevent from accidental screw stripping. This approach could also be the solution to replace the subjective method based on surgeon's perception.

8.2   Future Work

Bone of Different Anatomical Locations

It is known that the quality and mechanical strength of trabecular bone is site specific. Therefore, it would be beneficial to replicate the current studies using

trabecular bones from different anatomical locations to examine how this affects $T_{Plateau}$ and $F_{Pullout}$.

Cadaver Testing

The present study was performed using aBMD measured on the excised femoral head specimens without accounting for the surrounding soft tissues' variability between different patients. The measurements of aBMD performed in this thesis represent rather a best-case scenario as they were all done in vitro, with the same amount of soft tissue (polyoxymethylene board). Therefore, it could be worthwhile to replicate the study using aBMD measured on cadavers with intact soft tissues to explore this variability.

Use of Various Screw Designs

The aspect of screw designs (geometry, length, pitch, and thread profile) is reported to influence the T_{Insert} and $F_{Pullout}$ measurement (sub-chapter 3.5). For trabecular bones, there are two designs of screws typically used clinically, which are partially threaded (used in the present study) and fully threaded screws. Therefore, by replicating this work on different screw designs, particularly on the fully threaded screws, this could be beneficial to know how different designs of screws affect the $T_{Plateau}$ and $F_{Pullout}$.

Study on the Propagation of Micro-damage Surrounding the Bone and Screw

The present study had obtained multiple slices of micro-CT images of bone-screw constructs at different intervals of screw insertion torques and from different bone

qualities. These images provide a large dataset of bone-screw constructs, which are valuable to facilitate further studies particularly on the investigation of the propagation of micro-damage surrounding the bone and screw, which was not designed as part of the present thesis aims. Hopefully this future study will provide new insight into the factors leading to screw fixation failure.

Development of Finite Element (FE) Trabecular Bone Model

Also, the micro-CT images of the bone-screw constructs can be utilised for the development of FE model of the femoral head trabecular bone that can be used to investigate other parameters that may affect the mechanical stability of the bone-screw construct.

List of Publications

Conference Publications:

1. Ab-Lazid, R, Perilli, E, Ryan, MK, Costi, JJ, Reynolds, KJ, 2013. Trabecular bone screw pullout strength in human femoral heads: Does it depend on bone mineral density or micro-architecture, at a target insertion torque level? In ANZORS Proceeding. Australian and New Zealand Orthopaedic Research Society, 19th Annual Scientific Meeting. University of Sydney, NSW, Australia. September 2013, pp 39.

2. Ab-Lazid, R, Perilli, E, Ryan, MK, Costi, JJ, Reynolds, KJ, 2013.Does screw pullout strength at a specific insertion torque depend on trabecular bone mineral density or microarchitecture? In ABEC Proceeding. Australian Biomedical Engineering Conference. Sydney, NSW, Australia. October 2013.

3. Ab-Lazid, R, Perilli, E, Ryan, MK, Costi, JJ, Reynolds, KJ, 2014. Does screw pullout strength at a controlled insertion torque depend on trabecular bone bineral density and/or micro-architecture? Proceeding of the 23rd Australian Conference on Microscopy and Microanalysis (ACMM), 2-6 February 2014, Adelaide, South Australia.

4. Ab-Lazid, R, Perilli, E, Ryan, MK, Costi, JJ, Reynolds, KJ, 2014. The holding strength of cancellous screws depends on insertion torque, bone micro-architecture and areal bone mineral density. In ANZORS Proceeding. Australian and New Zealand Orthopaedic Research Society, 20th Annual Scientific Meeting. Flinders University, Adelaide, South Australia. September 2014, pp 135.

5. Perilli, E, Ryan, M, Ab-Lazid, R, Costi, JJ, Reynolds, KJ, 2015. Micro-CT imaging of surgical screw tightening in human trabecular bone. In Bruker microCT Proceeding. Bruker microCT, Annual User Meeting. Bruges, Belgium. May 2015.

6. Ab-Lazid, R, Perilli, E, Ryan, MK, Costi, JJ, Reynolds, KJ, 2015. Comparison between the cancellous screws pullout strength at three levels of tightening torque in the human femoral head. In ANZORS Proceeding. Australian and New Zealand Orthopaedic Research Society, 21st Annual Scientific Meeting. University of Auckland, New Zealand. October 2015.

Refereed Journal Articles:

1. Ab-Lazid, R, Perilli, E, Ryan, MK, Costi, JJ, Reynolds, KJ, 2014. Does cancellous screw insertion torque depend on bone mineral density and/or microarchitecture? J Biomech 47(2), 347-353.

2. Ab-Lazid, R, Perilli, E, Ryan, MK, Costi, JJ, Reynolds, KJ, 2014. Pullout strength of cancellous screws in human femoral heads depends on applied insertion torque, trabecular bone microarchitecture and areal bone mineral density. J Mech Behav Biomed Mater 40(Dec), 354-361.

Appendices

Appendix A1: Micro-CT Scanning Protocols

<u>Micro-CT Scanning Protocol</u>

- The purpose of the micro-CT scanning test was to determine the appropriate scanning settings/ protocols, which produced high x-ray attenuation, less noise, hence good image quality.
- This task was performed after having received the induction training by Ruth Williams from Adelaide Microscopy.
- Two sessions of micro-CT scanning were performed (on the 20th December 2011 and 13th January 2012), trying four different settings, to determine the appropriate scanning protocol to be used.
- Datasets of Tiff images obtained were saved at Rlazid\ PhD performed experiment_RL\ MicroCT_20_Dec_2011 and Rlazid\ PhD performed experiment_RL\ MicroCT_13_Jan_2011

	Title: Testing micro-CT scanning protocol on femoral head specimen			
	Experiment Date: 20th December 2011			
	Location: Adelaide Microscopy			
	Data storage: external hard drive. (rlazid:\PhD performed experiment_RL\ MicroCT_20_Dec_2011)			
No.	**Material and Task Lists**	**Yes**	**No**	**Remarks**
	Materials:			
1.	ESKE	✓		
2.	Plasticine	✓		
3.	Masking tape	✓		
4.	Tool box –scissor, knife, test pen and ruler		✓	
5.	Laboratory log book, pen and camera	✓		
6.	External hard-drive	✓		
	Tasks:			
a.	Thaw femoral head specimen in a refrigerator for 24 hours.	✓		Thawed for 24 hours, inside a refrigerator (4°C)prior to scanning
b.	Place femoral head and plasticine in ESKE, lock and tape ESKE lid with masking tape.	✓		

Title: Testing micro-CT scanning protocol on femoral head specimen				
c.	Attach a copy of micro-CT scanning protocols list.	✓		
d.	At micro-CT department, setup-up the micro-CT scanning machine.	✓		
e.	Connect external hard-drive to micro-CT's computer.	✓		
f.	Enter micro-CT scanning protocols as listed in the protocol list into the micro-CT programs	✓		
g.	Wear gloves and laboratory gown.	✓		
h.	Remove the femoral head specimen from ESKE. Unwrap gauze layer from femoral head.	✓		
i.	Place femoral head onto the specimen holder of micro-CT. Secure it with masking tape and plasticine as shown in Figure 1.	✓		
j.	Close the micro-CT and press 'start' to begin scanning.	✓		
k.	Record any observations.	✓		
	Image quality analysis			
	Analyse image noise (ring artefact)			

Femoral head and screw construct undergoing micro-CT scan to test different scanning protocols to achieve the optimum image quality

Scanning protocol test list

Scanning Protocols	Setting #1	Setting #2	Setting #3	Setting #4
X-ray source:	100kV	100kV	80kV	80kV
Current	80µA	80µA	120µA	120µA
Pixel size:	17µm/pix	17µm/pix	17µm/pix	17µm/pix
Filter:	1.0A1	1.0A1	1.0A1	0.5A1
Exposure Time:	885ms	885ms	885ms	590ms
Frame Averaging:	2	4	4	4
Rotation Step:	0.5°	0.4°	0.4°	0.4°
Scan Duration:	23min 20sec	43min 35sec	43min 32aec	29min 06sec
Line 510 attenuation				
Min:	7.1%	7.1%	5.1%	3.1%
Max:	21%	21.2%	17.3%	12.8%
Avg:	12.1%	12.1%	8.7%	6.5%
Start scan time:	10:12am	10:50am	12:23pm	11:44am
Finish scan time:	10:35am	11:33am	1:06pm	12.13pm
Reconstruction protocols				
Smoothing:	5	5	5	5
Ring Artefact:	10	10	10	10
Beam Hardening:	20	20	20	20
Object larger than FOV:	yes	yes	yes	yes
Grey level floating point				
Auto_Min:	0.001533	0.001603	0.001843	0.002119
Auto_Max:	0.042935	0.044884	0.051593	0.059339
Set_Min:	**0**	**0**	**0**	**0**
Set_Max (55.6% of auto-max):	**0.0239**	**0.0250**	**0.0287**	**0.0330**
Scanned on 20/12/2011				
Auto_Min:	0.001609	Nil	0.001847	0.002106
Auto_Max:	0.045066	Nil	0.051717	0.058965
Set_Min:	**0**	**Nil**	**0**	**0**
Set_Max (55.6% of auto-max):	**0.0251**	**Nil**	**0.0288**	**0.0328**
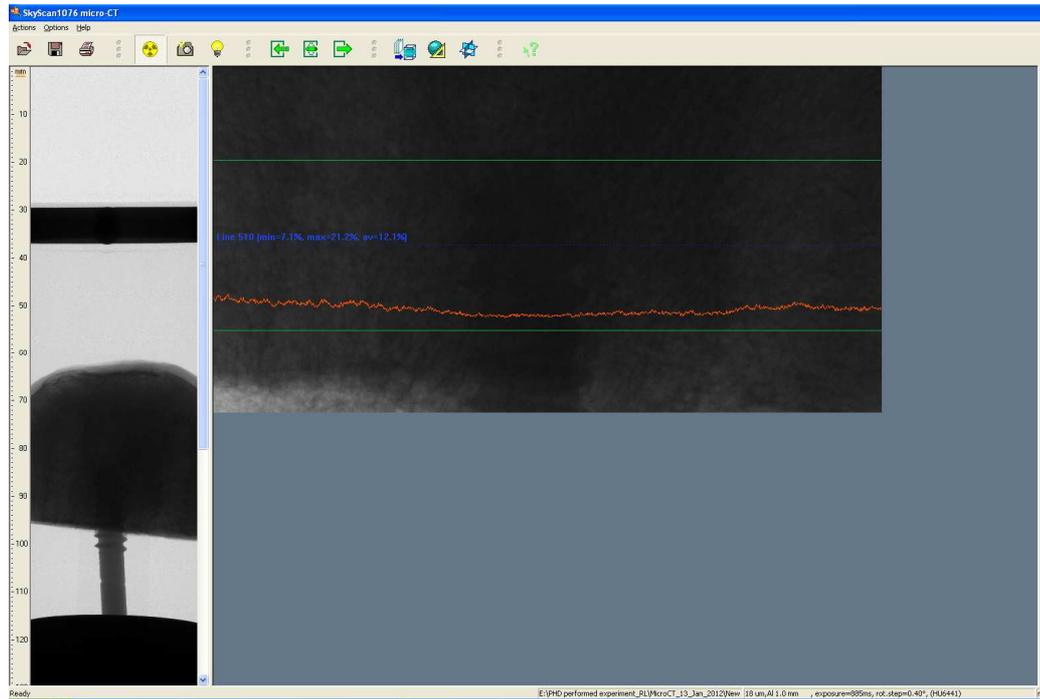
Micro-CT projection image of the bone screw construct scanned with setting # 1, showing x-ray intensity profile at line 510
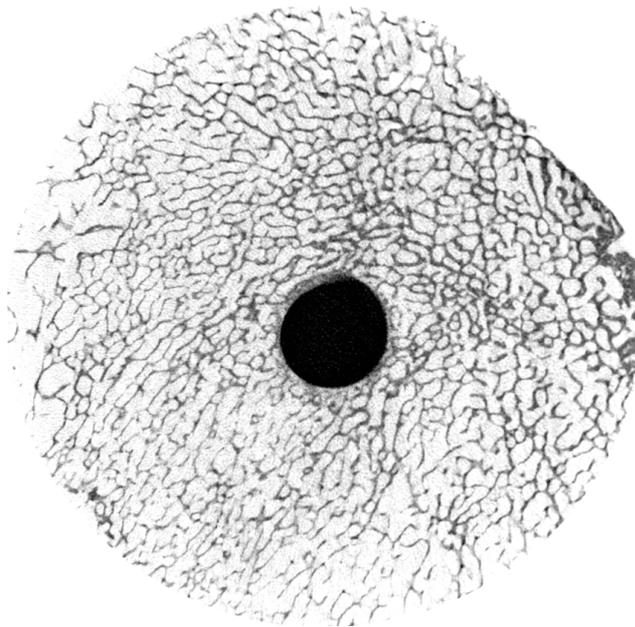
The reconstructed micro-CT image (from projection image) of the femoral head showing the screw at the centre of the bone

Results

- At line 510, Setting #1 and #2 (min: 7.1%, max: 21.2% and avg: 12.1%, for both settings) produced slightly higher x-ray intensities compared to settings #3 (min: 5.1%, max: 17.3% and avg: 8.7%) and #4 (min: 3.1%, max: 12.8% and avg: 6.5%)
- Setting #2 had higher frame averaging (4 compared to 2) and smaller rotation step (0.4° compared to 0.5°) compared to setting #1.

Conclusion

- Scanning protocol # 2 produced reasonably high x-ray attenuation compared with the other scanning protocols (#1, #3 and #4)
- Hence, scanning protocol #2 was utilised in the micro-CT scans of the femoral head and screw construct for research.

Appendix A2: Reconstruction Protocols of Micro-CT Images

Settings of reconstruction protocols of micro-CT images by NRecon software

<u>Excerpt from Nrecon reconstruction log</u>

Reconstruction settings undelined with red markers.

```
[Reconstruction]
Reconstruction Program=NRecon
Program Version=Version: 1.6.6.0
Program Home Directory=C:\Skyscan_SW\Nrecon\nreconLocal
Reconstruction engine=NReconServer
Engine version=Version: 1.6.6
Reconstruction from batch=Yes
Reconstruction servers= E418B
Option for additional F4F float format=OFF
Reconstruction mode=Standard
Dataset Origin=Skyscan1076
Dataset Prefix=NF_BJ429_11_50p_
Dataset Directory=F:\2012_Nov_PhD_Experimental_Data_Backup_\RL_PHD performed experiment_2011-2013\FemoralHea
Output Directory=F:\2012_Nov_PhD_Experimental_Data_Backup_\RL_PHD performed experiment_2011-2013\FemoralHead
Time and Date=Nov 30, 2012  22:50:11
First Section=67
Last Section=966
Reconstruction duration per slice (seconds)=5.218889
Total reconstruction time (900 slices) in seconds=4697.000000
Postalignment=-1.50
Section to Section Step=1
Sections Count=900
Result File Type=BMP
Result File Header Length (bytes)=1134
Result Image Width (pixels)=2000
Result Image Height (pixels)=2000
Pixel Size (um)=17.30254
Reconstruction Angular Range (deg)=196.80
Use 180+=OFF
Angular Step (deg)=0.4000
Smoothing=5
Smoothing kernel=0 (Asymmetrical boxcar)
Ring Artifact Correction=20
Draw Scales=OFF
Object Bigger than FOV=ON
Reconstruction from ROI=OFF
Filter cutoff relative to Nyquisit frequency=100
Filter type=0
Filter type meaning(1)=0: Hamming (Ramp in case of optical scanner); 1: Hann; 2: Ramp; 3: Almost Ramp;
Filter type meaning(2)=11: Cosine; 12: Shepp-Logan; [100,200]: Generalized Hamming, alpha=(iFilter-100)/100
Undersampling factor=1
Threshold for defect pixel mask (%)=0
Beam Hardening Correction (%)=20
CS Static Rotation (deg)=0.00
Minimum for CS to Image Conversion=0.005000
Maximum for CS to Image Conversion=0.023000
HU Calibration=OFF
BMP LUT=1
Cone-beam Angle Horiz.(deg)=16.275816
Cone-beam Angle Vert.(deg)=8.570329
[File name convention]
Filename Index Length=4
Filename Prefix=NF_BJ429_11_50p__rec
```

Reconstructed Micro-CT Images of Bone-Screw Construct Using Reconstruction Settings Highlighted in Yellow.

@ Head-Contact

Slice 648

Δ496

Slice 152

FF_BJ440_11

Reconstruction Settings:
Smoothing = 5; Ring artefact correction = 20;
Beam Hardening Correction = 20%
Object bigger than FOV = ON
Min_Floating_Point = 0.0050
Max_Floating_Point = 0.0230
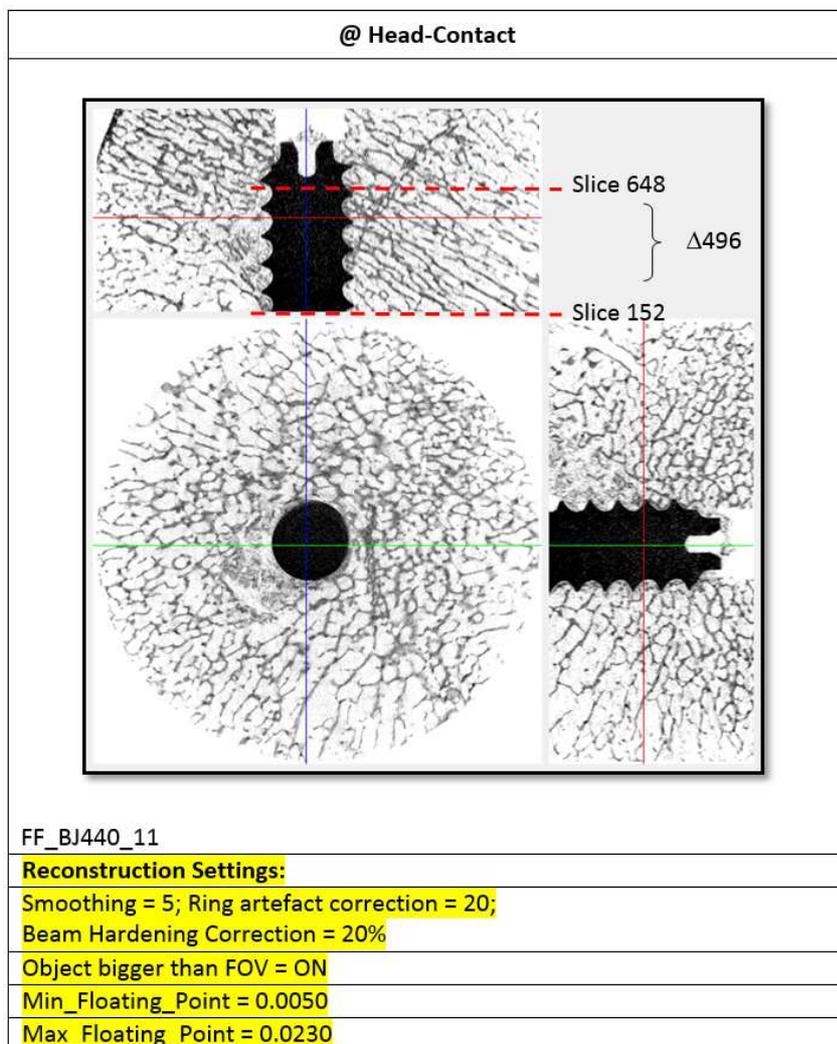
Appendix A3: ROI, VOI and Mask Creations

<u>**Creations of ROI, VOI and Mask**</u>

Creation of mask of ring-like region of region of interest (ROI) and volume of interest (VOI) that was used to remove screw image from the entire micro-CT images of bone-screw construct.
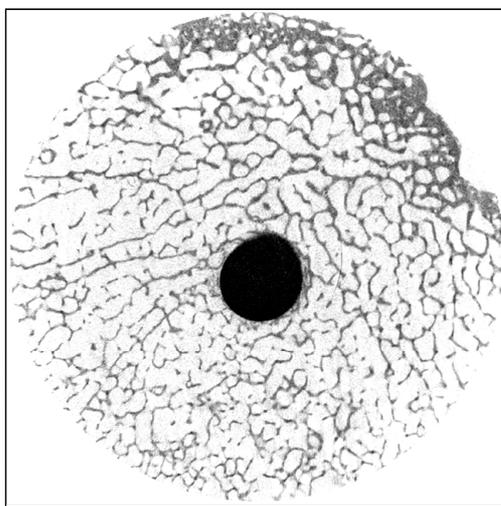
Load (2000 x 2000 pixel) image
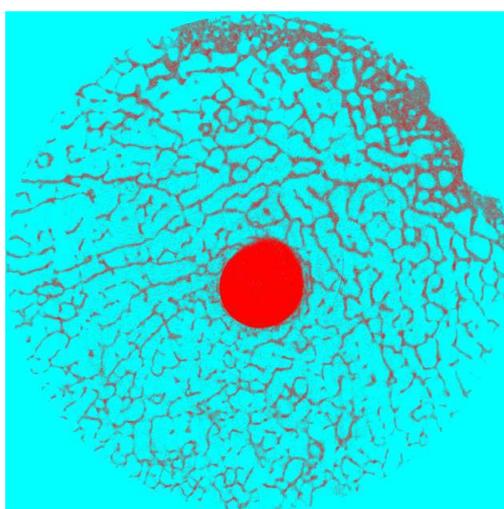
Used the entire image (2000 x 2000 pixel) as ROI (indicated by the blue region)
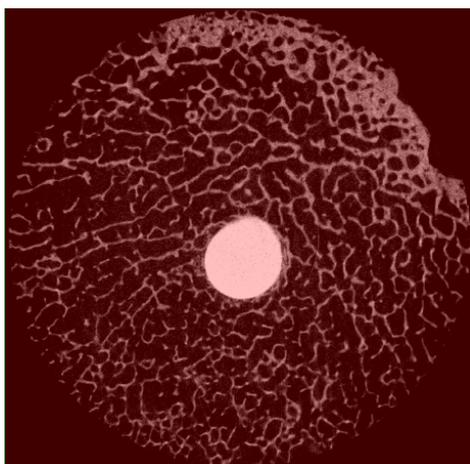
Then, threshold the image, min: 0 and max: 255.
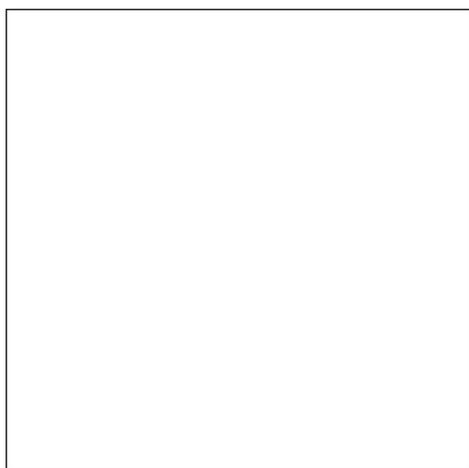
The result, white image of size 2000 x 2000 pixel image
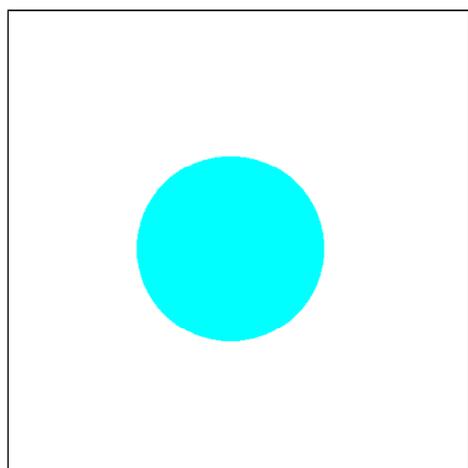
Then, create a round shape ROI, diameter = 14 mm (indicated with blue colour at the centre of the white image (2000 x 2000 pixel)
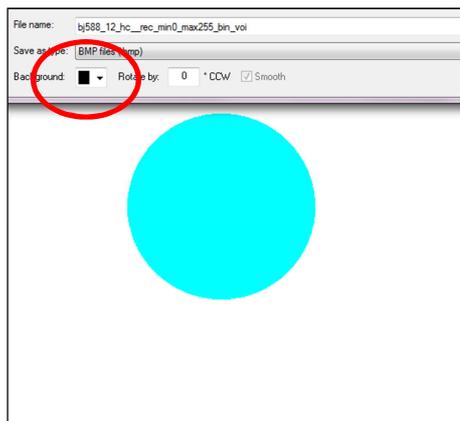
Save the image as ROI and VOI. When saving for VOI, select black background, from the background selection, indicated by a red circle.
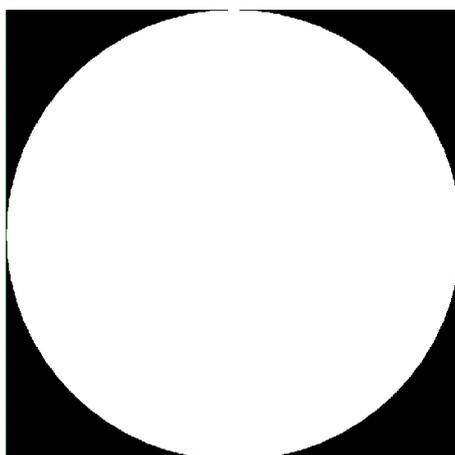
Load the VOI image with outer diameter of 14 mm (643 x 643 pixel)
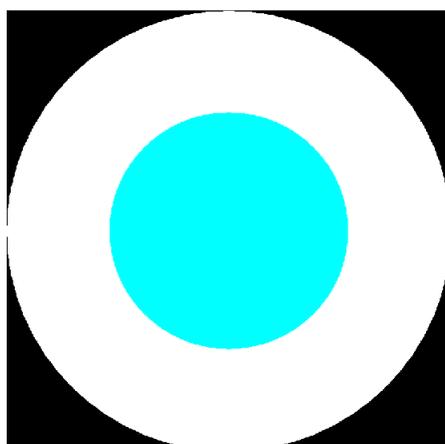
Create another round shape ROI, diameter = 7.51 mm (diameter of the screw that was slightly dilated) at the centre of 14 mm circle (indicated by blue colour). Save this as a new ROI.
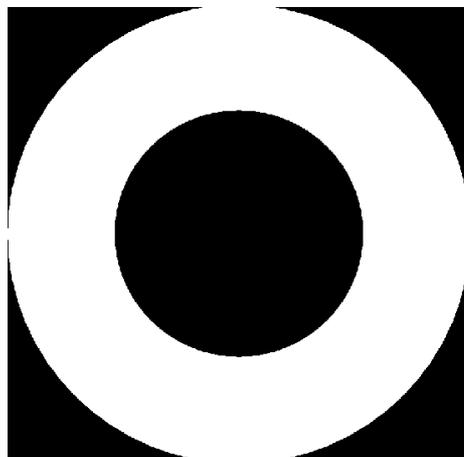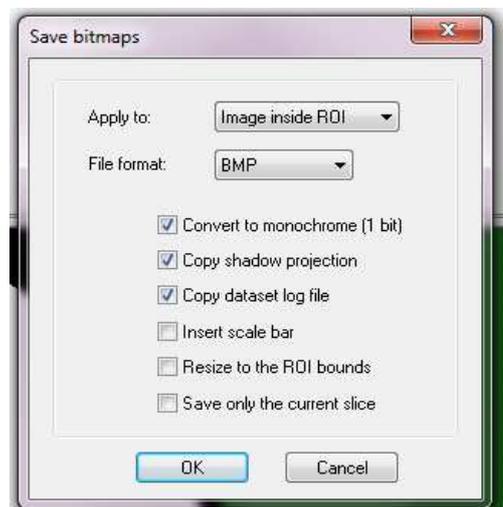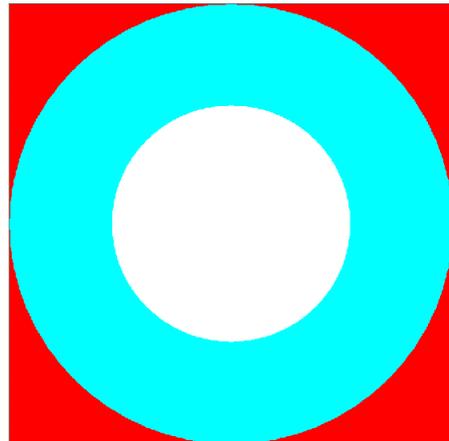
Load again the VOI image, outer diameter = 14 mm (643 x 643 pixel).

Place a 7.51 mm round shape ROI at the centre of the image.

Then, subtract the 7.51 mm ROI off the 14 mm (643 x 643 pixel) image and save as VOI with black background.

This forms the ring-like shape of VOI.

To transform VOI to a mask:

Threshold the ring-like VOI using a global threshold values, min: 255 and max: 255 via CTAn custom processing or via BATMAN.

Convert the ring-like VOI to monochrome (1 bit) image, and save in BMP image format.

This mask of ring-like shape can now be applied to remove screw image from the entire bone-screw micro-CT images.

Appendix A4: Binarisation/Segmentation of Ring-like or Annulus VOI:
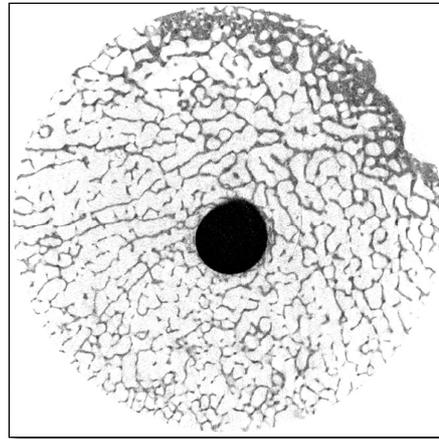
Load the bone-screw construct micro-CT images (2000 x 2000 pixel)
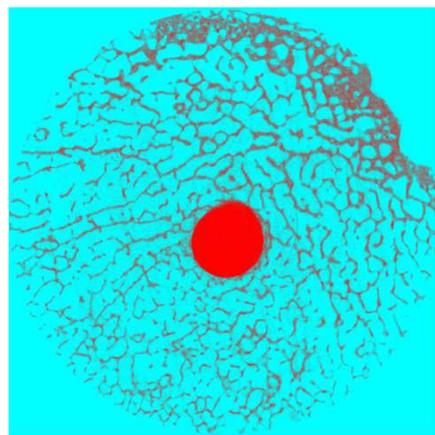
Used the entire image as ROI
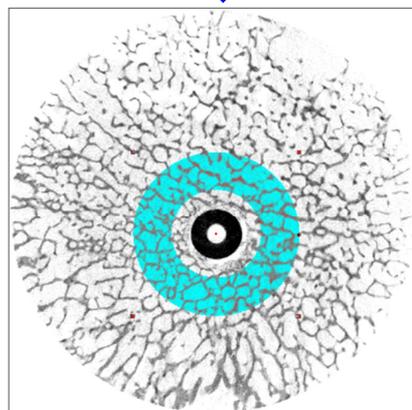
At the ROI menu (CTan), click on 'Image', then load the mask, a monochrome image as the ROI at the centre of the 2000 x 2000 pixel image

Interpolate the ROI across the stack of micro-CT images.

Save as new ROI and VOI.
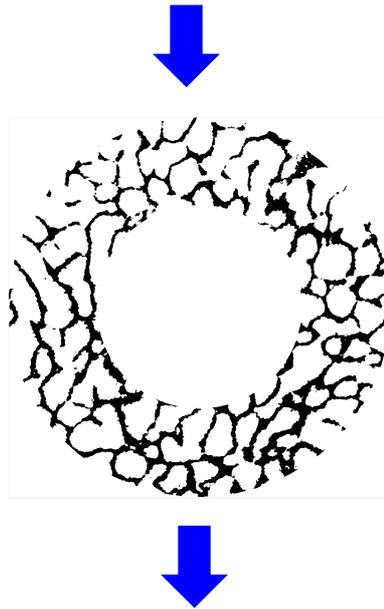
Load the ring-like reconstructed image for morphological analysis using either CTan custom processing or BATMAN.

Screen shot of the settings used to segment the ring-like reconstructed image of the trabecular bone via CTan is highlighted in yellow.

(Reconstruction protocol)

```
======================================================================================
CT Analyser
Version: 1.11.8.0
[ G:\MicroCT_Data\FRAGILITY\FF_70pc\FF_BJ521_12\BJ521_12_HC\VOI_Morph_Moving\bj521_12_hc__rec_voi????.bmp ]
[ 01/19/13 01:33:16 ]ROI
ROI filena G:\MicroCT_Data\FRAGILITY\FF_70pc\FF_BJ521_12\BJ521_12_HC\VOI_Morph_Moving\bj521_12_hc__rec_voi.roi


--------------------------------------------------------------------------------------
[ 01/19/13 01:33:56 ] Thresholding (3D space) inside VOI
Mode        Automatic (Otsu method)
Backgrour Dark
Lower gre          65
Upper gre          255
[ 01/19/13 01:33:59 ]Thresholding done


--------------------------------------------------------------------------------------
[ 01/19/13 01:33:59 ]Save bitmaps(image inside ROI):

Destination folder: G:\MicroCT_Data\FRAGILITY\FF_70pc\FF_BJ521_12\BJ521_12_HC\VOI_Morph_Moving\bj521_12_hc__rec_voi(1)
File format: bmp
Resize to the ROI bounds: Off
Number of saved files: 701


--------------------------------------------------------------------------------------
[ 01/19/13 01:34:20 ]Despeckle
Type: Sweep (3D space)
Remove: all exept the largest object
Apply to: Image
[ 01/19/13 01:34:27 ]Despeckle done


--------------------------------------------------------------------------------------
[ 01/19/13 01:34:27 ]Save bitmaps(image inside ROI):

Destination folder: G:\MicroCT_Data\FRAGILITY\FF_70pc\FF_BJ521_12\BJ521_12_HC\VOI_Morph_Moving\bj521_12_hc__rec_voi(2)
File format: bmp
Resize to the ROI bounds: Off
Number of saved files: 701


--------------------------------------------------------------------------------------
```

(Morphology analysis protocol)
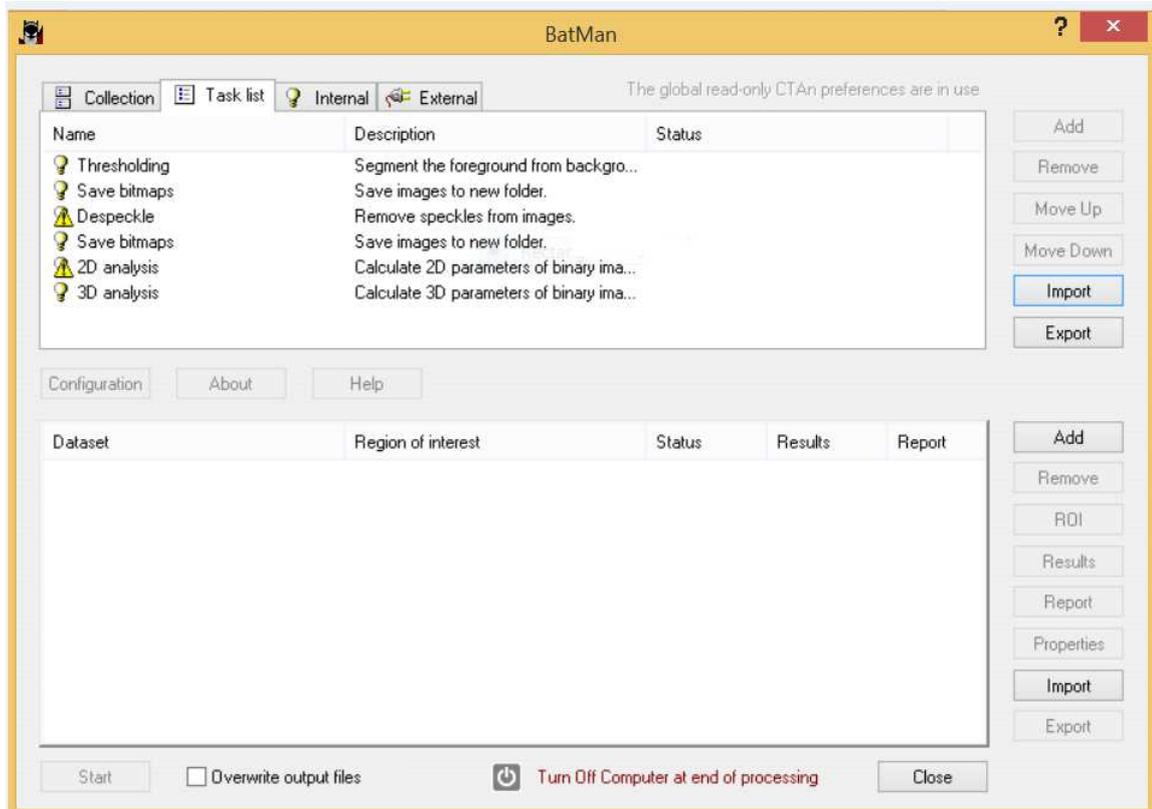
Appendix A5: The Overall Results from DXA and Micro-CT Scans and Biomechanical Testing (T_{Insert} and $F_{Pullout}$)

Specimen No	Sex	Age (Yr)	TMax (mNm)	TInsert (mNm)	TPlat (Nm)	%TMax	FPullout (kN)	aBMD (g/cm2)	BV/TV (%)	SMI	Tb.Th (µm)	Tb.SP (µm)	Tb.N (1/mm)	BS/TV (1/mm)	Potot	Connectivity
BJ511_12	F	86	1816.65	1031.06	0.72	29	1.3	0.79	23.989	1.449	223	634	1.06	4.11	76.31	11556
BJ264_10	F	85	2570.62	2552.25	1.20	99	1.7	0.76	27.137	1	226	641	0.97	4.4	73.17	12528
BJ144_10	F	85	1929.26	1302.74	0.79	45	1.5	0.82	25.819	1.078	267	801	0.96	3.69	74.44	9597
BJ515_12	F	78	1454.43	872.43	0.48	40	0.8	0.63	17.262	1.68	240	852	1.71	2.87	82.95	5870
BJ513_12	F	74	1373.81	1088.16	0.43	70	0.9	0.54	19.076	1.222	235	949	1.17	2.98	81.14	6271
BJ422_11	F	82	1835.97	1515.91	0.73	71	0.9	0.58	21.651	1.253	254	879	0.84	3.17	78.57	6689
BJ440_11	F	74	2083.67	1766.34	0.89	73	0.8	0.82	36.083	0.578	247	521	1.45	5.42	64.29	21280
BJ502_12	M	60	1309.55	901.19	0.39	55	0.5	0.56	22.778	1.537	184	520	1.22	4.83	77.60	18584
BJ517_12	F	65	1786.06	1252.75	0.70	51	0.5	0.68	25.853	1.174	232	645	1.1	4.16	74.44	11164
BJ530_12	M	79	1551.14	1085.86	0.55	54	0.8	0.69	25.655	1.263	205	574	1.24	4.77	74.70	17372
BJ536_12	M	81	2405.17	1806.12	1.09	54	1.3	0.83	31.602	0.864	234	540	1.34	4.92	68.75	14151
BJ521_12	M	84	1709.55	1238.80	0.65	56	1.3	0.73	27.564	0.918	220	645	0.8	4.63	72.77	16328
BJ514_12	F	80	2277.45	1891.40	1.01	69	2.1	0.73	30.652	0.52	258	698	1.18	4.08	69.62	7395
BJ538_12	M	81	1720.22	1299.91	0.66	61	1.5	0.69	24.447	0.93	232	765	1.04	3.89	75.83	10664
BJ229_10	F	92	1872.09	1428.55	0.75	60	1.4	0.53	21.274	1.201	217	825	1.04	3.53	78.98	7415
BJ503_12	M	55	3082.29	2502.81	1.53	63	2.1	0.96	32.868	0.326	278	702	1.19	4	67.41	5563
BJ540_12	M	88	2311.00	1854.49	1.03	64	1.7	0.78	29.109	0.937	234	609	1.36	4.63	71.22	14308
BJ509_12	F	77	2407.75	2131.54	1.10	79	1.6	0.69	28.123	0.85	228	649	1.22	4.39	72.19	11205
BJ535_12	M	84	2222.41	2019.56	0.98	84	1.6	0.75	29.809	1	216	533	1.24	5.04	70.56	16102
BJO51_10	F	68	2447.06	2179.13	1.12	80	1.9	0.71	29.776	0.847	241	611	1.22	4.43	70.54	10100
BJ248_10	M	90	2069.42	1856.36	0.88	82	1.1	0.75	32.093	0.85	217	647	1.46	5.65	68.32	28857
BJ300_10	M	91	1933.84	1763.35	0.79	85	1.8	0.78	26.283	1.062	227	758	1.14	4.35	74.03	14335
BJ488_11	F	91	2043.09	1812.75	0.86	80	1.6	0.57	24.362	1.028	242	744	1	3.59	75.89	6270
BJ429_11	F	77	2707.73	1606.76	1.29	22	1.2	0.87	29.005	1.054	258	618	1.11	4.27	71.30	10096
BJ547_12	M	89	1932.29	1467.93	0.79	59	1.3	0.94	30.928	0.772	241	608	1.27	4.67	69.41	13212
BJ593_12	M	81	3335.22	2180.04	1.69	30	1.9	0.89	33.833	0.497	238	565	1.4	5.08	66.53	16601
BJ551_12	F	75	2535.47	1482.13	1.18	22	1.7	0.77	27.274	0.896	261	720	1.03	3.7	72.99	5886
BJ587_12	M	70	3028.29	2075.15	1.49	38	2.2	1.02	32.688	0.334	222	574	1.46	4.93	67.66	11057
BJ582_12	M	77	1477.90	964.45	0.50	47	0.8	0.84	26.493	1.261	187	533	1.39	5.35	73.92	22453
BJ585_12	F	74	3682.91	3938.52	1.91	114	3.2	1.00	42.537	-0.121	285	505	1.48	5.14	57.82	12402
BJ595_12	M	73	3073.86	2089.51	1.52	37	1.9	0.97	30.757	0.872	260	608	1.17	4.44	69.57	11028
BJ599_12	M	78	2613.32	2012.22	1.23	57	1.9	0.93	34.689	0.641	235	512	1.46	5.29	65.69	15522
BJ597_12	M	73	3231.11	3202.55	1.62	98	2.7	1.08	36.019	0.339	254	545	1.4	5.02	64.34	14175
BJ141_10	M	86	3210.99	3115.82	1.61	94	2.5	1.17	36.898	0.37	243	518	1.5	5.32	63.48	15676
BJ548_12	M	86	2306.53	1606.66	1.03	45	1.9	0.82	31.879	0.902	225	518	1.4	5.16	68.50	16091
BJ553_12	M	61	3210.00	2348.12	1.61	46	2.5	0.95	34.864	0.668	214	444	1.61	5.9	65.57	22527
BJ218_10	M	76	2401.31	1680.75	1.09	45	1.6	0.81	32.250	0.746	217	549	1.47	5.47	68.15	21887
BJ552_12	M	66	2599.10	1986.38	1.22	56	1.5	0.85	30.088	0.801	228	594	1.31	4.71	70.26	12714
BJ580_12	M	72	3449.89	2623.01	1.76	51	2.3	0.95	33.753	0.588	242.1	564	1.38	4.96	66.61	13985
BJ581_12	M	51	3610.04	2795.39	1.87	53	2.5	0.93	31.836	0.623	269	659	1.17	4.27	68.47	8963
BJ588_12	F	89	2898.52	2192.54	1.41	53	1.8	0.85	28.533	0.865	239	643	1.18	4.28	71.77	9925
BJ600_12	M	89	2731.63	2057.62	1.30	53	1.8	0.78	32.486	0.577	246	624	1.31	4.65	67.85	12148
BJ591_12	M	72	2626.88	1990.52	1.24	54	1.5	0.71	29.773	0.878	205	512	1.43	5.1	70.61	14774
BJ594_12	M	80	2933.59	2221.03	1.43	53	1.4	1.05	31.138	0.645	245	634	1.26	4.51	69.19	11256
BJ592_12	M	84	1295.55	868.74	0.38	53	0.8	0.66	22.434	1.324	231	737	0.96	3.68	77.83	8916
BJ601_12	M	86	2990.35	2359.85	1.47	59	2.2	0.82	32.810	0.816	219	503	1.48	5.37	67.58	17235
BJ589_12	F	78	.	.	.	.		1.03	.	.	.	.	.	.	.	.
BJ586_12	M	43	.	.	.	.		1.01	.	.	.	.	.	.	.	.
BJ545_12	M	78	.	.	.	.		0.84	.	.	.	.	.	.	.	.
BJ557_12	F	69	.	.	.	.		0.86	.	.	.	.	.	.	.	.
BJ583_12	F	50	.	.	.	.		1.09	.	.	.	.	.	.	.	.
BJ544_12	F	69	.	.	.	.		0.64	.	.	.	.	.	.	.	.
BJ430_11	M	80	.	.	.	.		1.06	.	.	.	.	.	.	.	.
BJ500_12	M	59	.	.	.	.		0.96	.	.	.	.	.	.	.	.
BJ381_11	F	83	.	.	.	.		0.76	.	.	.	.	.	.	.	.
BJ578_12	F	81	.	.	.	.		0.70	.	.	.	.	.	.	.	.
BJ249_10	F	89	.	.	.	.		0.68	.	.	.	.	.	.	.	.
BJ539_12	M	85	.	.	.	.		0.89	.	.	.	.	.	.	.	.
BJ534_12	M	78	.	.	.	.		0.82	.	.	.	.	.	.	.	.

Failed tests

Appendix A6: Post-experimental Power Analysis
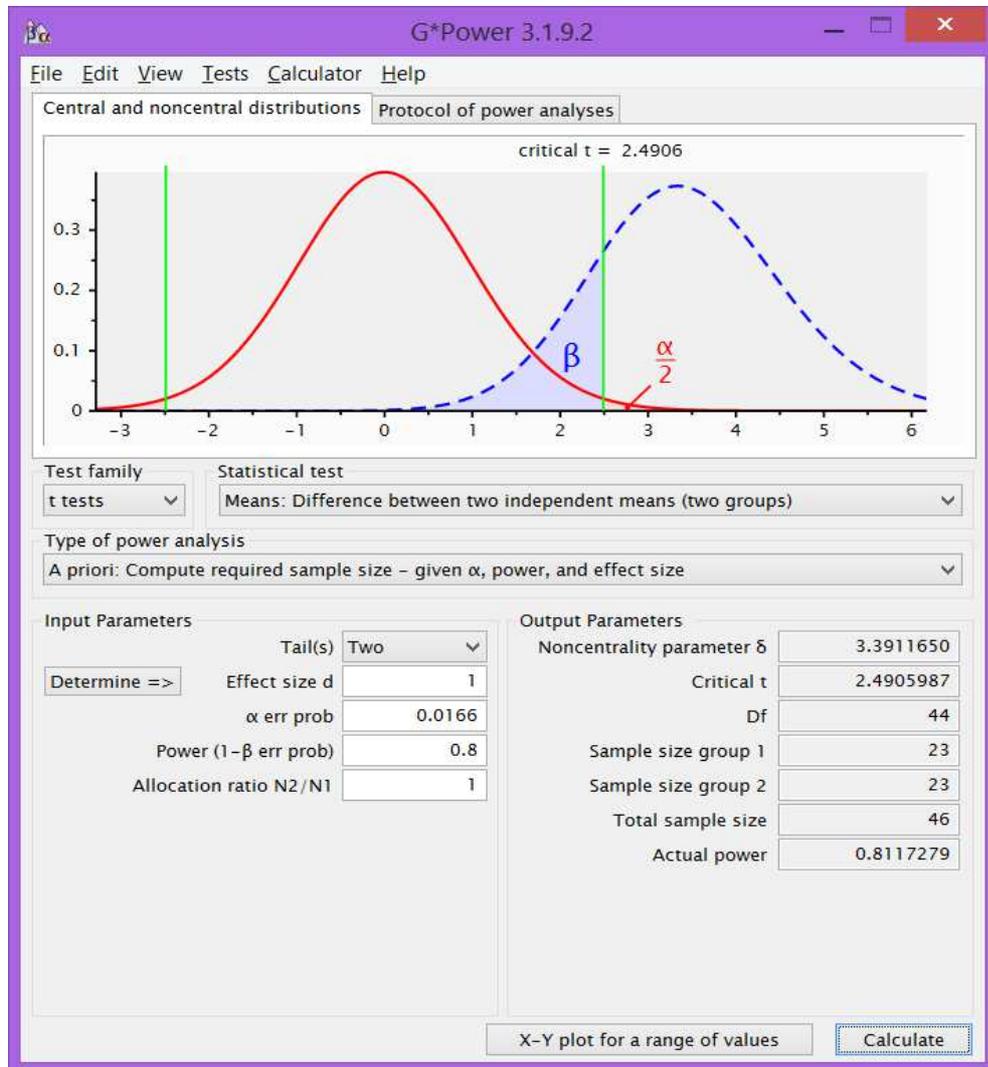
Screen shot of the post-experimental power analysis using G*Power software (version 3.1.9.2)

Bibliography

Abshire, B.B., McLain, R.F., Valdevit, A., Kambic, H.E., 2001. Characteristics of pullout failure in conical and cylindrical pedicle screws after full insertion and back-out. Spine J.1(6), 408-414.

AIHW 2014. Estimating the prevalence of osteoporosis in Australia. Cat. no. PHE 178. Canberra: AIHW.

Amirouche, F., Solitro, G.F., Magnan, B.P., 2016. Stability and spine pedicle screws fixation strength - A comparative study of bone density and insertion angle. Spine Deformity. 4(2016), 261-267.

Ansell, R., Scales, J.T., 1968. A study of some factors which affect the strength of screws and their insertion and holding power in bone. J Biomech. 1(4), 279-302.

Asnis, S.E., Ernberg, J.J., Bostrom, M.P.G., Wright, T.M., Harrington, R.M., Tencer, A., Peterson, M., 1996. Cancellous Bone Screw Thread Design and Holding Power. J Orthop Trauma. 10(7), 462-469.

ASTM F 543-07, Standard specification and test methods for for metallic medical bone screws.

Bartl, R., Frisch, B., 2009. Biology of bone, in: Bartl, R., Frisch, B. (Eds.), Osteoporosis: Diagnosis, Prevention, Therapy. Springer, pp. 7-28.

Basso, T., Klaksvik, J., Foss, O.A., 2014. Locking plates and their effects on healing conditions and sterss distribution: A femoral neck fracture study in cadavers. Clin Biomech (Bristol, Avon). 29(5), 595-598.

Bateman, D.K., Barlow, J.D., VanBeek, C., Abboud, J.A., 2015. Suture anchor fixation of displaced olecranon fractures in the eldery: a case series and surgical technique. J Shoulder Elbow Surg. 24(7), 1090-1097.

Battula, S., Schoenfeld, A., Vrabec, G., Njus, G.O., 2006. Experimental evaluation of the holding power/stiffness of the self-tapping bone screws in normal and osteoporotic bone material. Clin Biomech (Bristol, Avon). 21(5), 533-537.

Battula, S., Schoenfeld, A.J., Sahai, V., Vrabec, G.A., Tank, J., Njus, G.O., 2008. The Effect of Pilot Hole Size on the Insertion Torque and Pullout Strength of

Self-Tapping Cortical Bone Screws in Osteoporotic Bone. J Trauma. 64(4), 990-995.

Baumgaertner, M.R., Curtin, S.L., Lindskog, D.M., Keggi, J.M., 1995. The value of the tip-apex distance in predicting failure of fixation of peritrochanteric fractures of the hip. J Bone Joint Surg Am. 77(7), 1058–1064.

Baumgart, F.W., Cordey, J., Morikawa, K., Perren, S., Rahn, B., Schavan, R., Snyder, S., 1993. AO/ASIF self-tapping screws (STS). Injury. 24 Suppl 1, S1-17.

Bayraktar, H.H., Morgan, E.F., Niebur, G.L., Morris, G.E., Wong, E.K., Keaveny, T.M., 2004. Comparison of the elastic and yield properties of human femoral trabecular and cortical bone tissue. J Biomech 37(1), 27-35.

Bechtol, C.O., Ferguson, A., Laing, P., 1959. Metals and Engineering in Bone and Joint Surgery. Williams & Wilkins.

Bogden, J.D., Kemp, F.W., Huang, A.E., Shapses, S.A., Ambia-Sobhan, H., Jagpal, S., Brown, I.L., Birkett, A.M., 2008. Bone mineral density and content during weight cycling in female rats: effects of dietary amylase-resistant starch. Nutr Metab (Lond) 5, 34.

Bouxsein, M.L., 2003. Bone quality: where do we go from here? Osteoporosis Int. 14 Suppl 5, S118-127.

Burr, D.B., Allen, M.R., 2013. Basic and Applied Bone Biology. Elsevier Academic Press.

Burval, D.J., McLain, R.F., Milks, R., Inceoglu, S., 2007. Primary pedicle screw augmentation in osteoporotic lumbar vertebrae: biomechanical analysis of pedicle fixation strength. Spine (Phila Pa 1976). 32(10), 1077-1083.

Charnley, J., 1960. Anchorage of the femroal head prothesis to the shaft of the femur. J Bone Joint Surg Br. 42-**,**28-30.

Chen, L.-H., Tai, C.-L., Lai, P.-L., Lee, D.-M., Tsai, T.-T., Fu, T.-S., Niu, C.-C., Chen, W.-J., 2009. Pullout strength for cannulated pedicle screws with bone cement augmentation in severely osteoporotic bone: influences of radial hole and pilot hole tapping. Clin Biomech (Bristol, Avon). 24(8), 613-618.

Chen, C.-S., Chen, W.-J., Cheng, C.-K., Jao, S.-H., Chueh, S.-C., Wang, C.-C., 2005. Failure analysis of broken pedicle screws on spinal instrumentation. Med Eng Phys. 27(6), 487-496.

Cho, W.S., Youm, Y.S., 2009. Migration of polyethylene fixation screw after total knee arthroplasty. J Arthroplasty 24 (5), 852.e5–e9.

Christensen, F.B., Dalstra, M., Sejling, F., Overgaard, S., Bünger, C., 2000. Titanium-alloy enhances bone-pedicle screw fixation: mechanical and histomorphometrical results of titanium-alloy versus stainless steel. Eur Spine J. 9(2), 97-103.

Clarke, B., 2008. Normal bone anatomy and physiology. Clin J Soc Nephrol. 3 Suppl 3, S131-139.

Cleek, T.M., Reynolds, K.J., Hearn, T.C., 2007. Effect of screw torque level on cortical bone pullout strength. J Orthop Trauma. 21(2), 117-123.

Compston, J., 2010. Osteoporosis: Social and Economic Impact. Radiol Clin North Am. 48(3), 477-482.

Cook, R.B., Curwen, C., Tasker, T., Zioupos, P., 2010. Fracture toughness and compressive properties of cancellous bone at the head of the femur and relationships to non-invasive skeletal assessment measurements. Med Eng Phys. 32(9), 991-997.

Cordey, J., Rahn, B.A., Perren, S.M., 1980. Current concepts of internal fixation of fractures, in: Uhthoff, H.K., Stahl, E. (Eds.), Human Torque Control in the Use of Bone Screws, pp. 235-243.

Cotler, J.M., Star, A.M., 1990. Complications of spine fusions. In: Cotler J.M., Cotler, H.B., editors. Spinal fusion: science and technique. New York: Springer-Verlag. pp. 361–87.

Cowin, S.C., 2001. Bone Mechanics Handbook, Second Edition. Taylor & Francis.

Cowin, S.C., 2004. Bone Mechanics Handbook. Boca Raton, CRC Press

Cristofolini, L., Viceconti, M., Cappello, A., Toni, A., 1996. Mechanical validation of whole bone composite femur models. J Biomech. 29(4), 525–355.

Cummings, S.R., Melton, L.J., 2002. Epidemiology and outcomes of osteoporotic fractures. Lancet. 359(9319), 1761-1767.

Daley, E., Streeten, E.A., Sorkin, J.D., Kuznetsova, N., Shapses, S.A., Carleton, S.M., Shuldiner, A.R., Marini, J.C., Phillips, C.L., Goldstein, S.A., 2010. Variable bone fragility associated with an Amish COL1A2 variant and a knock-in mouse model. J Bone Miner Res. 25(2), 247-261.

Davis, T.R., Sher, J.L., Horsman, A., Simpson, M., Porter, B.B., Checketts, R.G., 1990. Intertrochanteric femoral fractures. Mechanical failure after internal fixation. J Bone Joint Surg Br. 72(1):26–31.

Demirhan, M., Kilicoglu, O., Akpinar S., Akman, S., Atalar, A.C., Göksan, M.A., 2000. Time-dependent reduction in load to failure of wedge-type polyglyconate suture anchors. Arthroscopy. 16(4), 383-390.

Dickman, C.A., Fessler, R.G., MacMillan, M., Haid, R.W., 1992. Transpedicular screw-rod fixation of the lumbar spine: operative technique and outcome in 104 cases. J Neurosurg. 77(6), 860–70.

Dinah, A.F., Mears, S.C., Knight, T.A., Soin, S.P., Campbell, J.T., Belkoff, S.M., 2011. Inadvertent screw stripping during ankle fracture fixation in elderly bone. Geriatr Orthop SurgRehabil. 2(3), 86-89.

Doblaré, M., García, J.M., Gómez, M.J., 2004. Modelling bone tissue fracture and healing: a review. J Eng Frac Mech. 71(13-14), 1809-1840.

Donnelly, E., 2011. Methods for assessing bone quality. Clin Orthop Relat Res. 469, 2128-2138.

Ehmke, L.W., Fitzpatrick, D.C., Krieg, J.C., Madey, S.M., Bottlang, M., 2005. Lag screws for hip fracture fixation: Evaluation of migration resistance under simulated walking. J Orthop Res. 23(6), 1329-1335.

Farquharson, M., Speller, R., Brickley, M., 1997. Measuring bone mineral density in archaeological bone using energy dispersive low angle X-ray scattering techniques. J Archaeological Sci. 24(8), 765-772.

Farrera, L.A., Ryken, T.C., 1999. Mechanical testing of bone and the bone-implant interface, in: Yuehuei, H.A., Draughn, R.A. (Eds.), Screw pullout testing. CRC press pp. 551-564.

Frandsen, P.A., Christoffersen, H., Madsen, T., 1984. Holding power of different screws in the femoral head. A study in human cadaver hips. Acta Orthop Scand. 55(3), 349-351.

Freedman, K.B., Back, S., Bernstein, J., 2001. Sample size and statistical power of randomised, controlled trials in orthopaedics. J Bone Joint Surg Br. 83-B(3), 397-402.

Giangregorio, L., Papaioannou, A., Cranney, A., Zytaruk, N., Adachi, J.D., 2006. Fragility Fractures and the Osteoporosis Care Gap: An International Phenomenon. Semin Arthritis Rheum. 35(5), 293-305.

Giannoudis, P.V., Schneider, E., 2006. Principles of fixation of osteoporotic fractures. J Bone Joint Surg Br. 88(10), 1272-1278.

Gibson, L.J., 2005. Biomechanics of cellular solids. J Biomech. 38(3), 377-399.

Goldstein, S.A., 1987. The mechanical properties of trabecular bone: dependence on anatomic location and function. J Biomech. 20(11-12), 1055-1061.

Gordon, C.L., Lang, T.F., Augat, P., Genant, H.K. 1998. Image-based assessment of spinal trabecular bone structure from high-resolution CT images. Osteoporos Int. 8(4), 317–325.

Gourion-Arsiquaud, S., Faibish, D., Myers, E., Spevak, L., Compston, J., Hodsman, A., Shane, E., Recker, R.R., Boskey, E.R., Boskey, A.L., 2009. Use of FTIR spectroscopic imaging to identify parameters associated with fragility fracture. J Bone Miner Res. 24(9), 1565–1571.

Halvorson, T.L., Kelley, L.A., Thomas, K.A., Whitecloud III, T.S., Cook, S.D., 1994. Effects of bone mineral density on pedicle screw fixation. Spine (Phila Pa (1976).19(21), 2415-2420.

Hambli, R., 2011. Numerical procedure for multiscale bone adaptation prediction based on neural networks and finite element simulation. Finite Elem Anal Des. 47(2011), 835-842.

Hawks, M.A., Kim, H., Strauss, J.E., Oliphant, B.W., Golden, R.D., Hsieh, A.H., Nascone, J.W., O'Toole, R.V., 2013. Does a trochanteric lag screw improve fixation of vertically oriented femoral neck fractures? A biomechanical analysis in cadaveric bone. Clin Biomech (Bristol, Avon). 28(8), 886-891.

Hayes, W.C., Bouxsein, M.L, 1997. Biomechanics of cortical and trabecular bone: implications for assessment of fracture risk. In *Basic Orthopaedic Biomechanics* 2nd ed. Mow V.C., Hayes W.C., Philadephia, Lippincott Williams & Wilkins.

Haynes, R.C., Pöll, R.G., Miles, A.W., Weston, R.B., 1997. An experimental study of the failure modes of the Gamma Locking Nail and OA Dynamic Hip Screw under static loading: a cadaveric study. Med Eng Phys. 19(5), 446-453.

Hearn, T., Cottrell, G., Reynolds, K.J., 2004. Automated surgical assessment of material density as a basis for the adaptive tightening of bone screws. In Proc. Australian Orthopaedic Association (SA Branch) Annual Scientific Meeting, Adelaide, Australia.

Hecker, A.T., Shea, M., Hayhurst, J.O., Myers, E.R., Meeks, L.W., Hayes, W.C., 1993. Pull-out strength of suture anchors for rotator cuff and Bankart lesion repairs. Am J Sports Med. 21(6), 874-879.

Heiner, A.D., Brown, T.D., 2001. Structural properties of a new design of composite replicate femurs and tibias. J Biomech. 34(7), 773-781.

Helgason, B., Perilli, E., Schileo, E., Taddei, F., Brynjolfsson, S., Viceconti, M., 2008. Mathematical relationships between bone density and mechanical properties: a literature review. Clin Biomech (Bristol, Avon). 23(2), 135-146.

Helgeson, M.D., Kang, D.G., Lehman, R.A., Jr., Dmitriev, A.E., Luhmann, S.J., 2013. Tapping insertional torque allows prediction for better pedicle screw fixation and optimal screw size selection. Spine J. 13(8), 957-65.

Hernandez, C.J., Keaveny, T.M., 2006. A biomechanical perspective on bone quality. Bone 39(6), 1173-1181.

Hildebrand, T., Laib, A., Muller, R., Dequeker, J., Ruegsegger, P., 1999. Direct three-dimensional morphometric analysis of human cancellous bone: microstructural data from spine, femur, iliac crest, and calcaneus. J Bone Miner Res. 14(7), 1167-1174.

Hildebrand, T., Ruegsegger, P., 1997. Quantification of Bone Microarchitecture with the Structure Model Index. Comp Methods Biomech Biomed Engin. 1(1), 15-23.

Johnson, N.L., Galuppo, L.D., Stover, S.M., Taylor, K.T., 2004. An in vitro biomechanical comparison of the insertion variables and pullout mechanical properties of ao 6.5-mm standard cancellous and 7.3-mm self-tapping, cannulated bone screws in foal femoral bone. Vet Surg. 33(6), 681-690.

Karim, L., Vashishth, D., 2011. Role of trabecular microarchitecture in the formation, accumulation, and morphology of microdamage in human cancellous bone. J Orthop Res. 29(11), 1739-1744.

Keaveny, T.M., Morgan, E.F., Niebur, G.L., Yeh, O.C., 2001. Biomechanics of trabecular bone. Annu Rev Biomed Eng. 3, 307-333.

Keaveny, T.M., Morgan, E.F., Yeh, O.C., 2003. Bone Mechanics, in: Kutz, M. (Ed.), Standard Handbook of Biomedical Engineering and Design. McGraw-Hill, pp. 8.1-8.11.

Kiebzak, G.M., Meyer, M.H., Meyer, R.A., 1999. Evaluation of Lunar small animal software for measuring bone mineral content in excised rat bones. J Clin Densitom. 2(1), 17-21.

Koranyi, E., Bowman, C., Knecht, C., Janssen, M., 1970. 36 Holding Power of Orthopedic Screws in Bone. Clin Orthop Relat Res. 72, 283-286.

Koval, K., Zuckerman, J., 2000. Treatment Principles, in: Hip Fractures: A Practical Guide to Management. Springer, pp.37-45.

Leite, V.C., Shimano, A.C., Gonçalves, G.A.P., Kandziora, F., Defino, H.L.A., 2008. The influence of insertion torque on pedicular screws' pullout resistance. Acta Ortop Bras. 16(4), 214-216.

Lin, L.-C., Chen, H.-H., Sun, S.-P., 2003. A biomechanical study of the cortex-anchorage vertebral screw. Clin Biomech (Bristol, Avon). 18(6), S25-S32.

Madsen, J.E., Naess, L., Aune, A.K., Alho, A., Ekeland, A., Strømsøe, K., 1998. Dynamic hip screw with trochanteric stabilizing plate in the treatment of unstable proximal femoral fractures: a comparative study with the Gamma nail and compression hip screw. J Orthop Trauma. 12(4), 241–248.

Majumdar, S., Kothari, M., Augat, P., Newitt, D.C., Link, T.M., Lin, J.C., Lang, T., Lu, Y., Genant, H.K., 1998. High-resolution magnetic resonance imaging: three-dimensional trabecular bone architecture and biomechanical properties. Bone 22(5), 445-454.

Mainds, C.C., Newman, R.J., 1989. Implant failures in patients with proximal fractures of the femur treated with a sliding screw device. Injury. 20(2):98-100.

Marti, A., Fankhauser, C., Frenk, A., Cordey, J., Gasser, B., 2001. Biomechanical evaluation of the less invasive stabilization system for the internal fixation of distal femur fractures. J Orthop Trauma. 15(7), 482– 487.

Matsuzake, H., Tokuhashi, Y., Matsumato, F., Hoshino, M., Kiuchi, T., Toriyama, S., 1990. Problems and solutions of pedicle screw plate fixation of lumbar spine. Spine (Phila Pa 1976). 15(11), 1159–65.

Mente, P.L., Lewis, J.L., 1987. Young's modulus of trabecular bone tissue. Trans Orthop Res SOC 12,49.

Meyer, D.C., Fucentese, S.F., Ruffieux, K., Jacob, H.A., Gerber, C., 2003. Mechanical testing of absorbable suture anchors. Arthroscopy. 19(2), 188-193.

Meyer, D.C., Gerber, C., 2004. Failure of anterior shoulder instability repair caused by eyelet cutout of absorbable suture anchors. Arthroscopy. 20(5), 521-523.

Mittra, E., Rubin, C., Qin, Y.X., 2005. Interrelationship of trabecular mechanical and microstructural properties in sheep trabecular bone. J Biomech. 38(6), 1229-1237.

Morgan, E.F., Barnes, G.L., Einhorn, T.A., 2013. The bone organ system: Form and Function, in: Marcus, R., Feldman, D., Dempster, K.W., Luckey, M., Cauley, J.A. (Eds.), Osteoporosis. Academic Press, pp. 3-20.

Morgan, E.F., Bouxsein, M.L., 2008. Biomechanics of Bone and Age-Related Fractures, in: Bilezikian, J.P., Raisz, L.G., Martin, T.J. (Eds.), Principles of Bone Biology: Two-Volume Set. Elsevier Science, pp. 29-51.

Moroni, A., Hoang-Kim, A., Lio, V., Giannini, S., 2006. Current augmentation fixation techniques for the osteoporotic patient. Scand J Surg. 95(2), 103-109.

Mueller, T.L., Basler, S.E., Muller, R., van Lenthe, G.H., 2013. Time-lapsed imaging of implant fixation failure in human femoral heads. Med Eng Phys. 35(5), 636-643.

Mueller, T.L., van Lenthe, G.H., Stauber, M., Gratzke, C., Eckstein, F., Muller, R., 2009. Regional, age and gender differences in architectural measures of bone quality and their correlation to bone mechanical competence in the human radius of an elderly population. Bone 45(5), 882-891.

Muller, M., Abel, E.W., McLeod, G., Rowley, D.I., 1992. Pull-out strengths for a range of screws inserted into the calcaneus: a preliminary study. Clin Biomech (Bristol, Avon) 7(2), 125-128.

Niu, C.C., Chen, W.J., Chen, L.H., Shih, C.H., 1996. Reduction-fixation spinal system in spondylolisthesis. Am J Orthop (Belle Mead NJ). 25(6), 418–24.

Nordin, S., Zulkifli, O., Faisham, W.I., 2001. Mechanical failure of dynamic hip screw (DHS) fixation in intertrochanteric fracture of the femur. Med J Malaysia. 56(Suppl. D), 12–7.

Öhman, C., Baleani, M., Perilli, E., Dall'Ara, E., Tassani, S., Baruffaldi, F., Viceconti, M., 2007. Mechanical testing of cancellous bone from the femoral head: experimental errors due to off-axis measurements. J Biomech. 40(11), 2426-2433.

Oktenoglu, B.T., Ferrara, L.A., Andalkar, N., Ozer, A.F., Sarioglu, A.C., Benzel, E.C., 2001. Effects of hole preparation on screw pullout resistance and insertional torque: a biomechanical study. J Neurosur. 94(1 Suppl), 91-96.

Oroszlany, A., Nagy, P., Kovacs, J.G., 2015. Compressive properties of commercially available PVC foams intended for use as mechanical models fir human cancellous bone. Acta Polytechnica Hungarica. 12(2), 89-101.

Ortner, D.J., Turner-Walker, G., 2003. The biology of skeletal tissue, in: Ortner, D.J. (Ed.), Identification of Pathological Conditions in Human Skeletal Remains. Elsevier Science, pp. 11-36.

Otsu, N., 1987. A treshold selection method from gray-level histograms. IEEE Trans. Syst., Man, and Cybern. 9(1), 62-66.

Parkinson, I.H., Badiei, A., Fazzalari, N.L., 2008. Variation in segmentation of bone from micro-CT imaging: implications for quantitative morphometric analysis. Australas Phys Eng Sci Med. 31(2), 160-164.

Patel, P.S., Shepherd, D.E., Hukins, D.W., 2010. The effect of screw insertion angle and thread type on the pullout strength of bone screws in normal and osteoporotic cancellous bone models. Med Eng Phy. 32(8), 822-828.

Peltier L. Fractures: A History and Iconography of Their Treatment. *San Francisco, Ca: Norman Publishing;*. 1990:273.

Perilli, E., Baleani, M., Ohman, C., Fognani, R., Baruffaldi, F., Viceconti, M., 2008. Dependence of mechanical compressive strength on local variations in microarchitecture in cancellous bone of proximal human femur. J Biomech. 41(2), 438-446.

Perilli, E., Baruffaldi, F., Bisi, M.C., Cristofolini, L., Cappello, A., 2006. A physical phantom for the calibration of three-dimensional X-ray microtomography examination. J Microsc. 222(Pt 2), 124-134.

Perilli, E., Briggs, A.M., Kantor, S., Codrington, J., Wark, J.D., Parkinson, I.H., Fazzalari, N.L., 2012. Failure strength of human vertebrae: prediction using bone mineral density measured by DXA and bone volume by micro-CT. Bone. 50(6), 1416-1425.

Perilli, E., Baleani, M., Ohman, C., Fognani, R., Baruffaldi, F., Viceconti, M., 2007. Structural parameters and mechanical strength of cancellous bone in the femoral head in osteoarthritis do not depend on age. Bone. 41(2007), 760-768.

Perilli, E., Parkinson, I.H., Reynolds, K.J., 2012b. Micro-CT examination of human bone: from biopsies towards the entire organ. Ann Ist Super Sanita 48(1), 75-82.

Pfeiffer, F.M., Abernathie, D.L., 2006. A comparison of pullout strength for pedicle screws of different designs: a study using tapped and untapped pilot holes. Spine (Phila Pa 1976). 31(23), E867-E870.

Poukalova, M., Yakacki, C.M., Guldberg, R.E., Lin, A., Saing, M., Gillogly, S.D., Gall, K., 2010. Pullout strength of suture anchors: effect of mechanical properties of trabecular bone. J Biomech. 43(6), 1138-1145.

Ramaswamy, R., Evans, S., Kosashvili, Y., 2010. Holding power of variable pitch screws in osteoporotic, osteopenic and normal bone: are all screws created equal? Injury. 41(2), 179-183.

Rapuri, V.R., Clarke, H.D., Spangehl, M.J., Beauchamp, C.P., 2011. Five cases of failure of the tibial polyethylene insert locking mechanism in one design of constrained knee arthroplasty. J Arthroplasty. 26 (6), 976, e21–e24.

Reitman, C.A., Nguyen, L., Fogel, G.R., 2004. Biomechanical evaluation of relationship of screw pullout strength, insertional torque, and bone mineral density in the cervical spine. J Spinal Disord Techn. 17(4), 306-311.

Reynolds, K.J., Cleek, T.M., Mohtar, A.A., Hearn, T.C., 2013. Predicting cancellous bone failure during screw insertion. JBiomech. 46(6), 1207-1210.

Rho J.Y., Ashman, R.B., Turner, C.H., 1993. Young's modulus of trabecular and cortical bone material: Ultrasonic and microtensile measurements. J Biomech. 26(2), 111-119.

Rho, J.Y., Tsui, T.Y., Pharr, G.M., 1997. Elastic properties of human cortical and trabecular lamellar bone measured by nanoindentation. Biomaterials. 18(20), 1325-1330.

Rhodes, N.P., 2014. Chapter 1 - Anatomy and Physiology, in: Taktak, A., Ganney, P., Long, D., White, P. (Eds.), Clinical Engineering. Academic Press, Oxford, pp. 3-20.

Rossouw, D.J., McElroy, B.J., Amis, A.A., Emery, R.J., 1997. A biomechanical evaluation of suture anchors in repair of the rotator cuff. J Bone Joint Surg Br. 79(3), 458-461

Roux, J.P., Wegrzyn, J., Boutroy, S., Bouxsein, M.L., Hans, D., Chapurlat, R., 2013. The predictive value of trabecular bone score (TBS) on whole lumbar vertebrae mechanics: an ex vivo study. Osteoporos Int. 24(9), 2466-60.

Ruffoni, D., Muller, R., van Lenthe, G.H., 2012. Mechanisms of reduced implant stability in osteoporotic bone. Biomech Model Mechanobiol. 11(3-4), 313-323.

Ryan, M.K., Mohtar, A.A., Costi, J.J, Reynolds, K.J., 2015. "Turn-of-the-nut" method is not appropriate for use in cancellous bone. J Orthop Trauma. 29 (11), 437-41.

Ryken, T.C., Clausen, J.D., Traynelis, V.C., Goel, V.K., 1995. Biomechanical analysis of bone mineral density, insertion technique, screw torque, and holding strength of anterior cervical plate screws. J Neurosurg. 83(2), 325-329.

Sabo, M.T., Pollmann, S.I., Gurr, K.R., Bailey, C.S., Holdsworth, D.W., 2009. Use of co-registered high-resolution computed tomography scans before and after screw insertion as a novel technique for bone mineral density determination along screw trajectory. Bone. 44(6), 1163-1168.

Salmon, P. L., Ohlsson, C., Shefelbine, S. J., Doube, M., 2015. Structure Model Index Does Not Measure Rods and Plates in Trabecular Bone. Front Endocrinol (Lausanne). 162(6), 1-10.

Samuel, S.P., Baran, G.R., Yen, W., Davis, B.L., 2009. Biomechanics, in: Khurana, J.S. (Ed.), Bone Pathology. Springer Dordrecht Heidelberg, pp. 70-71.

Sanders, A.P., Raeymaekers, B., 2014. The effect of polyethylene creep on tibial insert locking screw loosening and back-out in prosthetic knee joints. J Mech Behav Biomed Mater. 38(2014), 1-5.

Schatzker, J., 1991. Screws and plates and their application, Manual of internal fixation. Springer, pp. 179-290.

Schatzker, J., Sanderson, R., Murnaghan, J.P., 1975. The holding power of orthopedic screws in vivo. Clin Orthop Relat Res. (108), 115-126.

Seebeck, J., Goldhahn, J., Städele, H., Messmer, P., Morlock, M., Schneider, E., 2004. Effect of cortical thickness and cancellous bone density on the holding strength of internal fixator screws. J Orthop Res. 22(6), 1237-1242.

Seller, K., Wahl, D., Wild, A., Krauspe, R., Schneider, E., Linke, B., 2007. Pullout strength of anterior spinal instrumentation: a product comparison of seven screws in calf vertebral bodies. Eur Spine J. 16(7), 1047-1054.

Shah, S.N., Shurman, D.J., Goodman, S.B., 2002. Screw migration from total knee prostheses requiring subsequent surgery. J Arthroplasty. 17(7), 951–954

Shea, T.M., Laun, J., Gonzalez-Blohm, S.A., Doulgeris, J.J., Lee, W.E., Aghayev, K., Vrionis, F.D., 2014. Designs and techniques that improve the pullout strength of pedicle screws in osteoporotic vertebrae: current status. BioMed Res Int. 2014(2014), 1-15.

Shi, L., Wang, L., Guo, Z., Wu, Z.-x., Liu, D., Gao, M.-x., Wan, S.-y., Fu, S.-c., Li, S.-j., Lei, W., 2012. A study of low elastic modulus expandable pedicle screws in osteoporotic sheep. J Spinal Disord Tech. 25(2), 123-128.

Siddiqui, A.A., Blakemore, M.E., Tarzi, I., 2005. Experimental analysis of screw hold as judged by operators v pullout strength. Injury. 36(1), 55-59.

Sommers, M.B., Fitzpatrick, D.C., Madey, S.M., Vande Zanderschulp, C., Bottlang, M., 2007. A surrogate long-bone model with osteoporotic material properties for biomechanical testing of fracture implants. J Biomech. 40(15), 3297-3304.

Søreide, O., Alho, A., Rietti, D., 1980. Internal fixation versus endoprosthesis in the treatment of femoral neck fractures in the elderly: a prospective analysis of the comparative costs and the consumption of hospital resources. Acta Orthop Scand. 51(5), 827-831.

Starr, C., McMillan, B., 2013. The biology of skeletal tissue, Human Biology. Cengage Learning, pp. 87-160.

Steele, D.G., Bramblett, C.A., 1988. Bone Biology, The Anatomy and Biology of the Human Skeleton. Texas A&M University Press, pp. 10-19.

Steeves, M., Stone, C., Mogaard, J., Byrne, S., 2005. How pilot-hole size affects bone-screw pullout strength in human cadaveric cancellous bone. Can J Surg. 48(3), 207.

Stoesz, M.J., Gustafson, P.A., Patel, B.V., Jastifer, J.R., Chess, J.L., 2014. Surgeon perception of cancellous screw fixation. J Orthop Trauma. 28(1), e1-7.

Suhm, N.,Hengg,C.,Schwyn,R.,Windolf, M., Quarz, V., Hänni, M., 2007.Mechanical torque measurement predicts load to implant cut-out: a biomechanical study investigating DHS$^{®}$ anchorage in femoral heads.Arch Orthop Trauma Surg. 127 (6), 469–474

Szabó, M., Taylor, M., Thurner, P., 2011. Mechanical properties of single bovine trabeculae are unaffected by strain rate. J Biomech. 44(5), 962-967.

Tabor, Z., 2011. A novel method of estimating structure model index from gray-level images. Med Eng Phys. 33(2), 218-225.

Taniwaki, Y., Takemasa, R., Tani, T., Mizobuchi, H., Yamamoto, H., 2003. Enhancement of pedicle screw stability using calcium phosphate cement in osteoporotic vertebrae: in vivo biomechanical study. J Orthop Sci. 8(3), 408-414.

Tankard, S.E., Mears, S.C., Marsland, D., Langdale, E.R., Belkoff, S.M., 2013. Does maximum torque mean optimal pullout strength of screws? J Orthop Trauma. 27(4), 232-235.

Taylor, R., 1990. Interpretation of the Correlation Coefficient: A Basic Review. J Diagn Med Sonogr. 6(1), 35-39.

Thomas, R.L., Bouazza-Marouf, K., Taylor, G.J., 2008. Automated surgical screwdriver: automated screw placement. Proc Inst Mech Eng H. 222(5), 817-827.

Thompson, J.D., Benjamin, J.B., Szivek, J.A., 1997. Pullout strengths of cannulated and noncannulated cancellous bone screws. Clin Orthop Rel Res. (341), 241-249.

Thienpont, E., 2013. Failure of tibial polyethylene insert locking mechanism in posterior stabilized arthroplasty. Knee Surg Sports Traumatol. Arthrosc. 21(12), 2685–2688.

Tingart, M.J., Lehtinen, J., Zurakowski, D., Warner, J.J., Apreleva, M., 2006. Proximal humeral fractures: regional differences in bone mineral density of the humeral head affect the fixation strength of cancellous screws. J Shoulder Elbow Surg. 15(5), 620-624.

Turner, C.H., 1989. Yield behavior of bovine cancellous bone. J Biomech Eng. 111(3), 256-260.

Turner, C.H., 2006. Bone strength: current concepts. Ann N Y Acad Sci. 1068, 429-446.

Turner, C.H., Rho, J., Takano, Y., Tsui, T.Y., Pharr, G.M., 1999. The elastic properties of trabecular and cortical bone tissues are similar: results from two microscopic measurement techniques. J Biomech. 32(4), 437-441.

van der Meulen, M.C., Jepsen, K.J., Mikic, B., 2001. Understanding bone strength: size isn't everything. Bone. 29(2), 101-104.

van Rietbergen, B., Majumdar, S., Newitt, D., MacDonald, B., 2002. High-resolution MRI and micro-FE for the evaluation of changes in bone mechanical properties during longitudinal clinical trials: application to calcaneal bone in postmenopausal women after one year of idoxifene treatment. Clin Biomech (Bristol, Avon). 17(2), 81-88.

Watts, J.W., Abimanyi-Ochom, J., Sanders, K., 2014. Osteoporosis costing all Australians. A new burden of disease analysis – 2012–2022. Osteoporosis Australia, Sydney; 2013:80

Wegrzyn, J., Roux, J.P., Arlot, M.E., Boutroy, S., Vilayphiou, N., Guyen, O., Delmas, P.D., Chapurlat, R., Bouxsein, M.L., 2010. Role of trabecular

microarchitecture and its heterogeneity parameters in the mechanical behavior of ex vivo human L3 vertebrae. J Bone Miner Res. 25(11), 2324-2331.

White, T.O., Mackenzie, S.P., Gray, A.J., 2016. McRae's orthopaedic trauma and emergency fracture management. 3rd edition. Elsevier Health Sciences UK. pp. 86.

WHO, 2003. The burden of musculoskeletal conditions at the start of the new millennium. World Health Organ Tech Rep Ser. 919:i-x, 1-218, back cover.

Windolf, M., Perren, S.M., 2012. Basic Mechanobiology of bone healing, in: Babst, R., Bavonratanavech, S., Pesantez, R. (Eds.), Minimally Invasive Plate Osteosynthesis (MIPO), 2nd ed. Thieme, pp. 18.

Wirth, A., Mueller, T., Vereecken, W., Flaig, C., Arbenz, P., Müller, R., Lenthe, G.H., 2010. Mechanical competence of bone-implant systems can accurately be determined by image-based micro-finite element analyses. Arch Appl Mech. 80(5), 513-525.

Wirth, A.J., Goldhahn, J., Flaig, C., Arbenz, P., Muller, R., van Lenthe, G.H., 2011. Implant stability is affected by local bone microstructural quality. Bone. 49(3), 473-478.

Yakacki, C.M., Poukalova, M., Guldberg, R.E., Lin, A., Gillogly, S., Gall, K., 2010. The effect of the trabecular microstructure on the pullout strength of suture anchors. J Biomech. 43(10), 1953-1959.